EAST ENGINEERING
LIBRARY

OCT 1 1947

TEXTILE RESEARCH JOURNAL

VOLUME XVII | September, 1947 | NUMBER 9

PUBLICATION OF

TEXTILE RESEARCH INSTITUTE, INC.

AND

THE TEXTILE FOUNDATION

Editorial Office: 10 East 40th Street, New York 16, N. Y.

TEXTILE RESEARCH JOURNAL

VOL. XVII, No. 9 September, 1947

In This Issue

A New Theory of Non-Linear Viscous Elasticity
Harris Burte and George Halsey 465

Application of Microscopy to the Textile Industry
G. L. Royer and C. Maresh 477

Measurement of Friction Between Single Fibers
Nils Gralén and Bertil Olofsson 488

A Dynamic Absorption Method for Determining Water-Repellency
J. E. Simpson and Ruth M. Howorth 497

Absorption Spectra in the Detection of Chemical Changes in Cellulose and Cellulose Derivatives
J. W. Rowen, C. M. Hunt, and E. K. Plyler 504

Diffraction of Light by Cellulose Acetate Yarn
E. V. Martin 512

Abstracts 515

Editor: Julian S. Jacobs

Managing Editor: Julia M. Crisp *Abstracts Editor:* Albert R. Martin *Business Manager:* W. B. Walker

Associate Editors

H. J. Ball, Earl E. Berkley, Henry Eyring, Gustavus J. Esselen, Earl K. Fischer, Milton Harris, K. L. Hertel, H. Mark, E. R. Schwarz, Kyle Ward, Jr.

TEXTILE RESEARCH JOURNAL, published monthly at Prince and Lemon Streets, Lancaster, Pa., is devoted to the interest of research in textile and allied industries. It is the official publication of Textile Research Institute, Inc., and the Textile Foundation.

Manuscripts and communications should be sent to the editorial offices, 10 East 40th Street, New York 16, N. Y.

Subscription rates: General—$10.00 per annum; additional for postage, 50 cents to Canada, $1.00 to all other countries. Special—$5.00 per annum for United States and Canadian students, teachers, educational institutions, public libraries, governmental libraries and departments, plus 50 cents for postage to Canada. Single copies, $1.00 each.

Entered as second-class matter, April 27, 1945, at the postoffice at Lancaster, Pa., under the Act of August 24, 1912.

Contents copyrighted 1947 by Textile Research Institute, Inc.

Advertising rates supplied on request.

TEXTILE RESEARCH JOURNAL

VOL. XVII, No. 9 September, 1947

A New Theory of Non-Linear Viscous Elasticity*

Harris Burte† and George Halsey†

Contribution of the Textile Foundation and the Frick Chemical Laboratory, Princeton University, Princeton, New Jersey

Abstract

The stress-strain curve of a material is calculated on the hypothesis that when flow occurs a section of the molecular chain constituting the material changes from a configuration A to a configuration B and thereby becomes unable to elongate again. Except for a small elastic deformation of both structures, the elongation is proportional to the fraction of the material in the B configuration. The two components are assumed to be in solution with one another, and the rates of transformation are then proportional to the relative abundance of the transformed species. These rates are written in the manner of the Eyring theory of reaction rates. Systems of more than two components are discussed and several examples are calculated. The calculated curves show good qualitative agreement with stress-strain curves of the nylon-wool-rubber type.

TWO extreme types of visco-elastic behavior can be recognized. If elongation of a material is accompanied by an increase in potential energy because the molecules are strained uniformly into new positions, and this transformation is accompanied by the "exchange of old neighbors for new ones" [1], one picture of viscous action is valid. Essentially, because flow from the new position of the molecule involves the breaking of bonds quite similar to those in the old position, the situation is that of a fluid in shear, coupled in parallel with a reversible spring representing the bonds that are never broken but which absorb potential energy by being strained and distorted. This type of viscous elasticity has been discussed thoroughly elsewhere [2, 3]. It is encountered when the range of distortion is under 10 or 20 percent. Figure 1 shows schematically a molecular system of this type [4]. If force is applied to the bundle of molecules, in this case two molecular chains, the elastic component will be supplied by the deformation of the unbroken chain, while the secondary forces restraining the junction of ends in the other chain will gradually break and reform in new positions of less stress. If the total deformation is small in comparison with the length of the molecular segments in contact, these new secondary bonds will exist at what is effectively the same number of locations as before flow took place. These new bonds may be weaker (thixotropy), stronger (strain hardening, rheopexy), or essentially of the same strength.

The extreme opposite case, which is the subject of this paper, is encountered when, by flow, a sec-

* The work reported in this communication was sponsored by the Office of The Quartermaster General, Research and Development Branch, Contract W44-109-QM-1177.

† Fellows of the Textile Research Institute.

tion of the molecular segment originally with a configuration A assumes an entirely new configuration B and thereby becomes unable to move again. Except for a small elastic deformation of both structures, which will be neglected for the present, the elongation is proportional to the fraction of the segment which is in the B configuration. If l'_∞ is the elongation when all of the molecular segment is in the B state, and b is the proportion in that state at elongation l' (see table of nomenclature*), then

$$b = \frac{l'}{l'_\infty}. \tag{1}$$

The specific rate of reaction B → A at zero force and unit concentration will be written as K, where

$$K = \frac{kT}{h} e^{-\Delta F/RT}$$

(see Figure 2), where ΔF is the height of the potential energy barrier between states B and A. Then the rate of reaction as influenced by the quantity b is

$$k'_{BA} = bK. \tag{2}$$

Since bonds are broken in going from state A to state B, state A must be at a lower energy level than state B. The rate in the forward direction (A → B) will then be

$$k'_{AB} = (1 - b)KD, \tag{3}$$

where

$$D = e^{-\Delta F^*/RT} \tag{3a}$$

is a small number in keeping with the thermodynamic stability of state A, and ΔF^* is the free energy difference between state A and state B. At equilibrium under no force, $l' = l'_0$ and

$$k'_{AB} = k'_{BA}. \tag{4}$$

Therefore

$$b_0 = \frac{l'_0}{l'_\infty} = \frac{D}{1 + D}, \tag{5}$$

which leads to the observation that, at zero force, l' is not zero. This situation is resolved when it is remembered that the B state must exist in some finite concentration at zero force, but that in actuality this concentration will be negligible. In other words, D is almost zero, corresponding to the great thermodynamic stability of the A state.

* *Table of Nomenclature*

l'_∞	the elongation due to the A → B transformation, when all of the population is in the B state
a, b, c	populations in A, B, C states, respectively
l'	elongation due to the A → B transformation
K	specific rate of reaction at zero force and unit concentration
k	Boltzmann constant
T	absolute temperature
h	Planck constant
ΔF	free-energy difference
R	gas constant
k'	rate of reaction
D	defined by equation (3a)
l'_0	the elongation due to the A → B transformation, at equilibrium under no force
F	applied force
μ	coefficient of symmetry of the potential energy barrier separating two states
V_h	volume of the flow hole
α	defined by equation (8)
ρ	constant rate of elongation
t	time
β	defined by equation (13b)
F_{out}	force during an extension
F_{in}	force during a contraction
F_0	spring line force
l	total elongation
k_a, k_b	spring constants for the A and B configurations, respectively
l''	elongation due to elasticity of A and B configurations
n	ratio of rapid rate of elongation (or loading) to slower rate of elongation (or loading)
l'_t	elongation due to A → B transformation at time t
P	constant rate of loading

Fig. 1

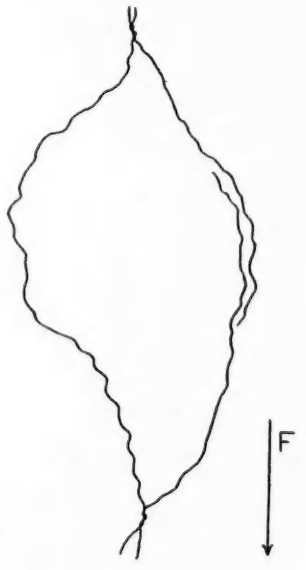

FIG. 1. *Molecular system exhibiting the "exchange of old neighbors for new ones" picture of viscous elasticity.*

It has been shown [1] that the applied force, F, affects the rate of transformation, k'_{AB}, by an amount $e^{\mu V_h F/kT}$ and the rate of transformation in the opposite direction, k'_{BA}, by an amount $e^{-(1-\mu)V_h F/kT}$, where μ is the symmetry coefficient of the potential energy barrier separating states A and B, and represents the fraction of the total work done in crossing the barrier which helps in activation. V_h is the volume of the flow hole. Thus

$$k'_{AB} = (1 - b)KDe^{\mu V_h F/kt}, \tag{6}$$

and

$$k'_{BA} = bKe^{-(1-\mu)V_h F/kT}. \tag{7}$$

For simplicity in the presentation, assume that the barrier is symmetrical ($\mu = \frac{1}{2}$) and define a quantity

$$\alpha = \frac{V_h}{2kT}. \tag{8}$$

Then

$$k'_{AB} = \left(\frac{db}{dt}\right)_{\text{from } A} = (1 - b)KDe^{\alpha F}, \tag{9}$$

$$k'_{BA} = -\left(\frac{db}{dt}\right)_{\text{from } B} = bKe^{-\alpha F}. \tag{10}$$

Fig. 2

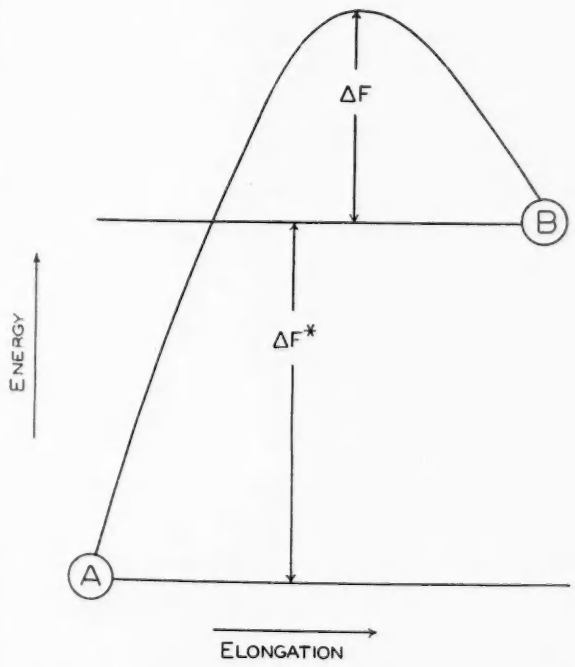

FIG. 2. *Diagrammatic representation of the potential energy barrier separating states* A *and* B.

Thus, the net rate of reaction can be written

$$\left(\frac{db}{dt}\right)_{\text{net}} = k'_{AB} - k'_{BA}$$

$$= (1 - b)KDe^{\alpha F} - bKe^{-\alpha F}, \tag{11}$$

since, by differentiating equation (1),

$$\left(\frac{db}{dt}\right)_{\text{net}} = \frac{1}{l'_\infty}\left(\frac{dl'}{dt}\right), \tag{12}$$

the rate of elongation under an applied force F is

$$\frac{dl'}{dt} = (1 - b)l'_\infty KDe^{\alpha F} - bl'_\infty Ke^{-\alpha F}. \tag{13}$$

Equation (13) is the basic differential equation for the two-position model of Figure 2 (assuming symmetry of the potential barrier). Its application to specific cases will now be considered.

At a constant rate of elongation $\rho = dl'/dt$,

$$\rho = \left(1 - \frac{l'}{l'_\infty}\right) l'_\infty KDe^{\alpha F} - \frac{l'}{l'_\infty} Kl'_\infty e^{-\alpha F}; \tag{13a}$$

or if

$$\frac{\rho}{Kl'_\infty} = \beta, \tag{13b}$$

and β is large enough to assure that the forward reaction is by far the predominant one during extension (since a large β is synonymous with a large ρ, therefore requiring a high value of F, the preceding condition will make the $e^{-\alpha F}$ term negligible when compared to the $e^{\alpha F}$ term),

$$\beta = \left(1 - \frac{l'}{l'_\infty}\right) De^{\alpha F_{\text{out}}} \tag{14}$$

where F_{out} is used to refer to the force during an extension. Equation (14) is the approximate equation for extension at a constant rate of elongation.

Upon reaching an elongation l', if the force be released, the rate of contraction (from 13a) is

$$\beta = \frac{\rho}{Kl'_\infty} = \left(1 - \frac{l'}{l'_\infty}\right) D - \frac{l'}{l'_\infty} \approx -\frac{l'}{l'_\infty}. \tag{15}$$

This rate of contraction can never be exceeded except where a compressive force can be applied. For smaller rates of contraction the force will quickly diminish to the value necessary to satisfy equation (13a). At this low force, if $-\beta/D$ is large, the term $(1 - l'/l'_\infty)KDe^{\alpha F}$ (because a large value of $-\beta$ requiring a very low force or a small value of D both tend to make the $De^{\alpha F}$ term neg-

Fig. 3

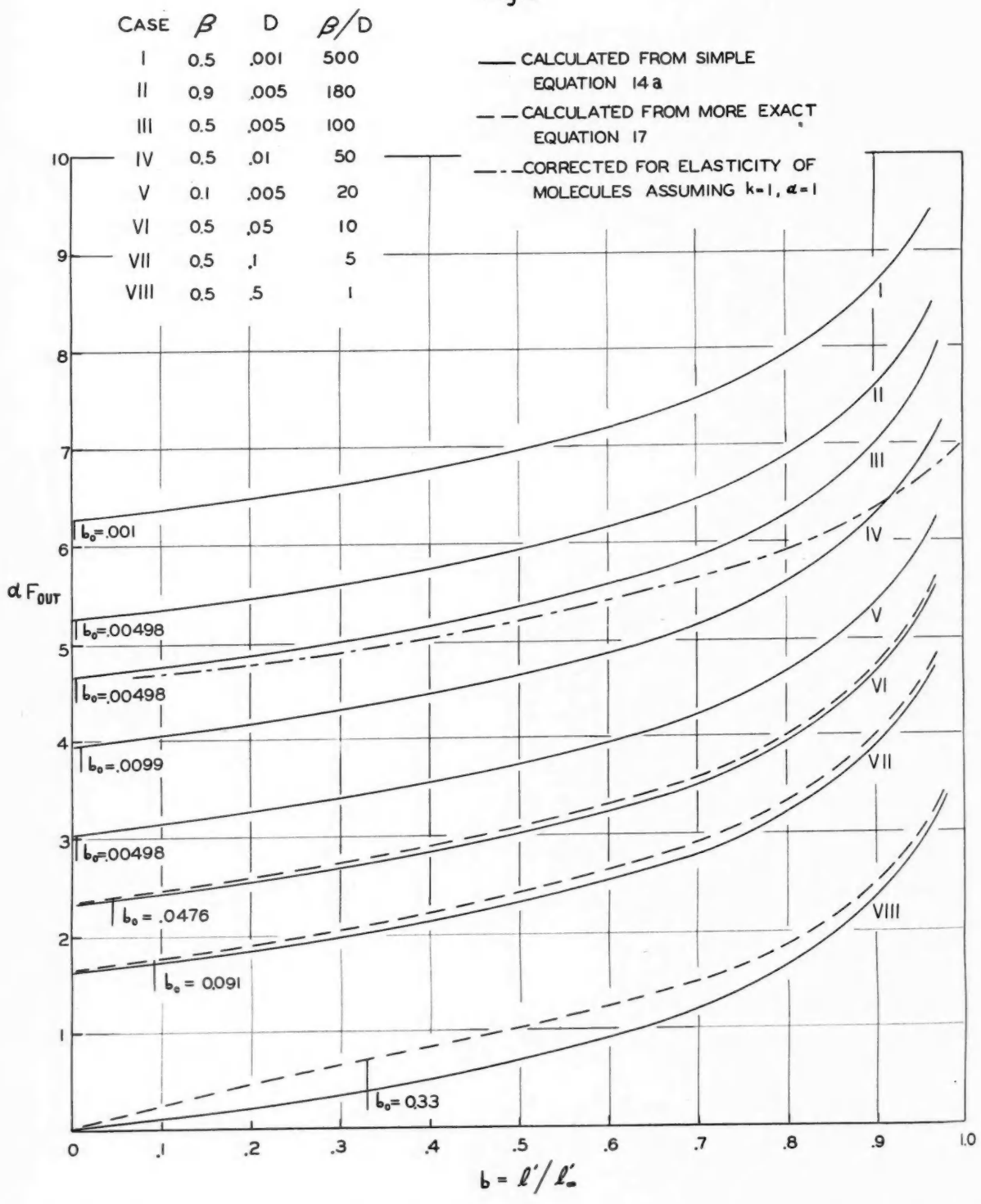

FIG. 3. *Plot of αF_{out} vs. l'/l'_∞ for various values of β and D. Deviations from the rigorous equation are shown and, in one case, the correction for elasticity of the molecules is applied.*

Fig. 4

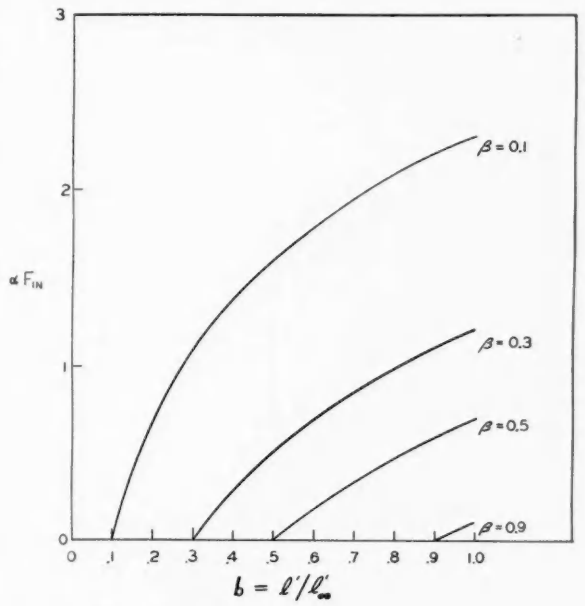

FIG. 4. *Plot of equation* (16a), αF_{in} *vs. b.* (*Lower envelope curves uncorrected for elasticity of molecules.*)

ligible compared to the $e^{-\alpha F}$ term) of equation (13a) becomes negligible and a simplified equation for contraction at a constant rate $-\rho$ can be written:

$$\beta = -\frac{l'}{l'_\infty} e^{-\alpha F_{\text{in}}}, \tag{16}$$

where F_{in} is used to refer to the force during a contraction.

These simplified equations (14, 16) will be compared with the more rigorous equation (13a). Solving equation (13a) for $e^{\alpha F}$ gives

$$e^{\alpha F} = \frac{\left(\frac{\beta}{D}\right) + \sqrt{\left(\frac{\beta}{D}\right)^2 + \frac{4}{D}\left(1 - \frac{l'}{l'_\infty}\right)\frac{l'}{l'_\infty}}}{2\left(1 - \frac{l'}{l'_\infty}\right)}. \tag{17}$$

Similarly, equations (14) and (16) give

$$e^{\alpha F_{\text{out}}} = \left(\frac{\beta}{D}\right) \frac{1}{\left(1 - \frac{l'}{l'_\infty}\right)}, \tag{14a}$$

$$e^{\alpha F_{\text{in}}} = -\frac{\left(\frac{l'}{l'_\infty}\right)}{\beta}. \tag{16a}$$

Therefore, values of αF_{out} vs. (l'/l'_∞) can be plotted

Fig. 5

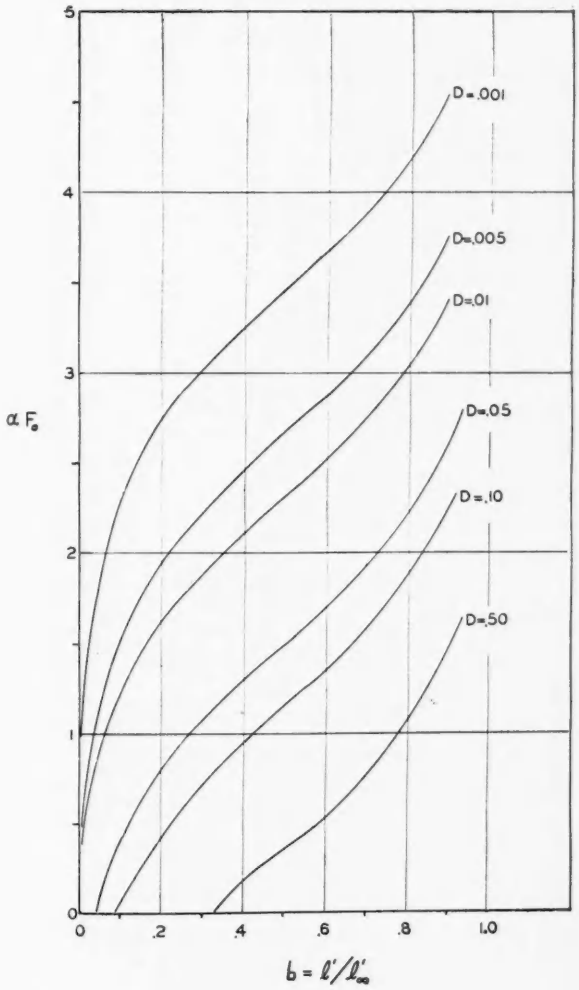

FIG. 5. *Plot of* αF_0 *vs.* $b = l'/l'_\infty$. *Spring lines uncorrected for elasticity of molecules.*

for various values of (β/D) and similarly for αF_{in} at various values of $(1/\beta)$. This is done for αF_{out} in Figure 3 and for αF_{in} in Figure 4. The extension curves (αF_{out}) and the contraction curves (αF_{in}) are often referred to as the upper and lower envelopes, respectively. Note that to plot each curve using the simplified equations, only one constant is necessary: for the upper envelope, the quotient (β/D); for the lower envelope, $(1/\beta)$. The rigorous equation (17), however, requires the knowledge of two separate constants β and D. This equation is plotted for comparison in Figure 3 at various values of β and D, and it is evident that for $\beta/D > 5$, which is the usual case, the simplified equations are quite adequate.

Fig. 6

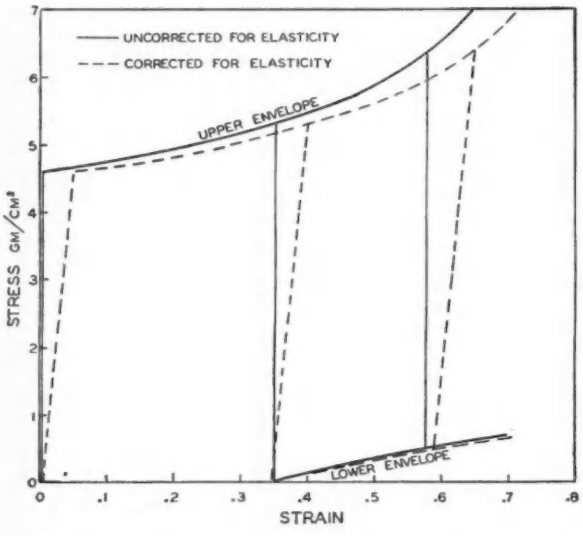

FIG. 6. *Stress-strain curves by simplified method* $\alpha = 1$, $k = 1$, $\beta = 0.5$, $D = 0.005$.

Fig. 7

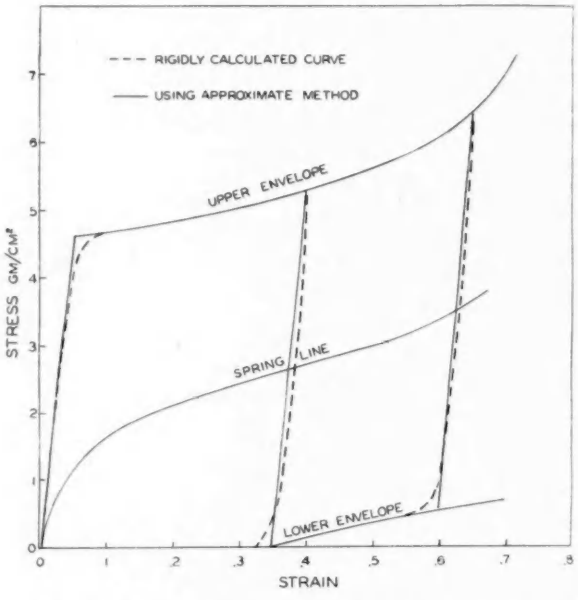

FIG. 7. *Curve showing comparison of rigorous method of constructing stress-strain curve with approximate method.*

Equations (14a) and (16a) can be written in the following form:

$$F_{out} = \frac{1}{\alpha} \ln \left(\frac{\beta}{D} \right) - \frac{1}{\alpha} \ln \left(1 - \frac{l'}{l'_\infty} \right), \quad (14b)$$

$$F_{in} = \frac{1}{\alpha} \ln \frac{l'}{l'_\infty} - \frac{1}{\alpha} \ln \beta, \quad (16b)$$

where β is now always taken to be positive.

In a previous paper [2] a point of no relaxation has been defined as the force at a given constant elongation, towards which the fiber will initially relax. If the rate of elongation is very slow (that is, if $\frac{dl'}{dt} \to 0$ is substituted in equation (13a)), the equation for the locus of points of no relaxation (commonly called the spring line [2]) is deduced:

$$0 = \left(1 - \frac{l'}{l'_\infty} \right) De^{\alpha F_0} - \frac{l'}{l'_\infty} e^{-\alpha F_0}, \quad (18)$$

where F_0 represents the spring line force. This spring line equation can be written in the two alternate forms:

$$De^{2\alpha F_0} = e^{(V_A F_0 - \Delta F^*)/kT}$$

$$= \frac{\frac{l'}{l'_\infty}}{\left(1 - \frac{l'}{l'_\infty} \right)} = \frac{b}{1 - b}, \quad (18a)$$

and

$$2F_0 = \frac{1}{\alpha} \ln \frac{l'}{l'_\infty} - \frac{1}{\alpha} \ln \left(1 - \frac{l'}{l'_\infty} \right) - \frac{1}{\alpha} \ln D. \quad (18b)$$

Comparison of equations (18b), (14b), and (16b) shows that, for the above case of a two-position model with a symmetrical potential barrier, the spring line lies halfway between the upper and lower envelopes (see Figure 7). Differentiation of these equations reveals that the slope of the spring line is the arithmetic mean average of the slopes of the upper and lower envelopes. These characteristics are similar to the properties of a simple spring-dashpot mechanical model [2].

Using equation (18a), a plot of αF_0 vs. $\frac{l'}{l'_\infty}$ at various values of D can be prepared (Figure 5). As shown in equation (5), when $F = 0$, $b_0 = l'_0/l'_\infty = \frac{D}{1 + D}$. The shape of the curves is very similar to the non-Hookean spring line previously postulated for wool [6].

Up to this point, the elasticities of the A and B configurations have been neglected. Before describing the calculation of the constants for the above equations from experimental data, it would be well to investigate the effects of this elasticity.

Fig. 8

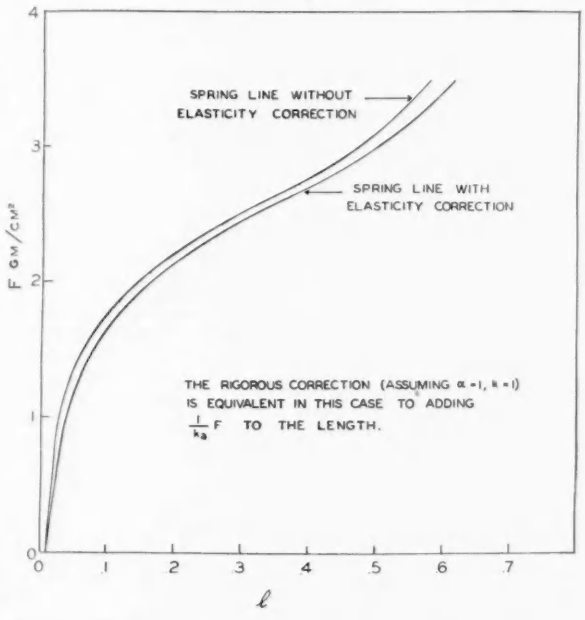
SPRING LINE WITHOUT ELASTICITY CORRECTION
SPRING LINE WITH ELASTICITY CORRECTION
THE RIGOROUS CORRECTION (ASSUMING α = 1, k = 1) IS EQUIVALENT IN THIS CASE TO ADDING 1/k_a F TO THE LENGTH.
F GM/CM²
l

FIG. 8. *Curves showing comparison between spring lines both with and without elasticity corrections.*

The total elongation l will be equal to the sum of l', the elongation due to the A → B transformation, and l'', the elongation due to the elasticity of the molecules:

$$l = l' + l''. \tag{19}$$

If the molecular chains are assumed to act as Hookean springs, we can define two spring constants k_a and k_b for each configuration; then

$$l'' = \left(\frac{1}{(1-b)k_a + bk_b}\right) F. \tag{20}$$

For simplicity in the presentation, assume that $k_a = k_b$; then

$$l'' = \frac{1}{k_a} F. \tag{21}$$

As will be shown later, this assumption can be corrected easily. The constant total rate of elongation ρ will now be dl/dt and can be written (still assuming a symmetrical barrier):

$$\rho = \frac{dl}{dt} = \frac{dl'}{dt} + \frac{dl''}{dt} = \left(1 - \frac{l'}{l'_\infty}\right) Kl'_\infty De^{\alpha F} - \left(\frac{l'}{l'_\infty}\right) Kl'_\infty e^{-\alpha F} + \frac{1}{k_a}\frac{dF}{dt}, \tag{22}$$

where

$$l' = \rho t - \frac{1}{k_a} F. \tag{23}$$

Equations (21), (22), and (23) can be solved, for a given set of constants, by a point-to-point method to give the "rigidly calculated curve" of Figure 7. The constants chosen were:

$\rho = 0.001$ sec^{-1},
$l'_\infty = 0.70$ (always expressed as a fraction of initial length),
$D = 0.005$ ($\therefore l_0 = 0.00348$),
$k_a = k_b = 1$ gm/cm^2,
$\alpha = 1$ cm^2/gm,
$Kl'_\infty = 0.002$ sec^{-1}.

The essence of the method is to assume a small value of Δt, substitute it in equation (22), and, knowing the initial conditions of F and l', calculate the increment ΔF. Whereupon the new l' is calculated from equation (23). The new values of F and l' are substituted in equation (22) and the calculation is continued. The similarity in shape between the calculated curve and the experimental curves of the nylon-rubber-wool type of material is immediately apparent. The analysis of experimental curves, using the preceding equations, is, however, unduly complex and a simplified approximate analysis will be described.

The simplified equations (14b) and (16b) are plotted for the above constants and the stress-strain curve is shown in Figure 6. If at every value of the elongation an elasticity correction equal to $\frac{1}{k_a} F$, where F is the force at that elongation, is added, the resulting curves are those shown in both Figures 6 and 7. It is evident that the rigidly calculated curve differs significantly from the approximate curve only by a rounding-off effect at the yield points. One of the curves in Figure 3 also shows the effect of the approximate elasticity correction. To calculate the constants using the approximate equations, it is therefore necessary merely to neglect the yield region and extrapolate the steep and flat portions of the experimental curve until they intersect. The stress-strain plane is then ruled with lines parallel to the initial straight position of the curve (that is, with lines of slope k_a, since until the yield point is reached the molecules are acting essentially as springs). By following these diagonal lines from the experimental curve to the

elongation axis, the value of $(l' - l'_0)$ at any value of the force can be determined; $(l'_\infty - l'_0)$ will be the elongation towards which the stress-strain curve is asymptotically approaching. Since D is usually quite small, $l_0 \sim 0$ and the preceding values can be taken as l' and l'_∞ directly. If D is found to be rather large, it is necessary to perform a trial-and-error calculation, assuming a value of D and checking it by the procedure outlined below. Reference to equation (14b) will show that if F_{out} is plotted vs. $\ln (1 - l'/l'_\infty)$ the result is a straight line of slope $-1/\alpha$ and intercept (at $l'/l'_\infty = 0$) of $\frac{1}{\alpha} \ln \frac{\beta}{D}$. Similarly, from equation (16b) a plot of F_{in} vs. l'/l'_∞ will yield a straight line of slope $\frac{1}{\alpha}$ and intercept $-\frac{1}{\alpha} \ln \beta$ when extrapolated to $l' = l'_\infty$. It is thus possible to determine experimentally all three constants.

If as in Figure 9, or as for the first contraction of Figure 7, no lower envelope is obtained, it is necessary to determine the spring line. The experimental determination of this by the process of bracketing is described elsewhere [2]. Referring to equation (18b), a plot of

$$2F_0 \text{ vs. } \ln \frac{l'/l'_\infty}{1 - l'/l'_\infty}$$

will give a line of slope $1/\alpha$ and intercept at $l'/l'_\infty = \frac{1}{2}$ of $-\frac{1}{\alpha} \ln D$.

The spring line both with and without the elasticity correction is shown in Figure 8. For the case of the spring line the approximate method of correcting for the elasticity is equivalent to the more rigorous method.

At the point where the experimental curve crosses the spring line during a return loop such as that in Figure 9, the slope is $((1 - b)k_a + bk_b)$, corresponding to the elasticity of the molecules. The slope of the final steep portion of the curve will be k_b. It is thus possible to vary the slope of the diagonal lines, drawn to effect the elasticity correction, and the assumption that $k_a = k_b$ need not be made.

If α_{out} for extension does not equal α_{in} for contraction, the barrier is not symmetrical and the following relations can be used to obtain α and μ:

$$\alpha_{out} = 2\mu\alpha, \tag{23}$$

$$\alpha_{in} = 2(1 - \mu)\alpha, \tag{24}$$

$$\alpha_{\text{spring line}} = \alpha. \tag{25}$$

In order for the above analysis to apply, the following two conditions must be met:

1. The locus of points of no relaxation must be a single-value function of the elongation—that is, the criterion for three-element model action [2] must apply.

2. The envelopes must be reproducible after each return loop—that is, thixotropic effects must be absent.

These conditions are the two main criteria for the use of the simple two-position model described above. However, the most rudimentary considerations of the molecular structure of an amorphous substance make it seem likely that there will be a "distribution of relaxation times" [2]. Nevertheless the above model does reproduce many properties of substances of the wool-nylon-rubber type quite well. The application of the present theory to such a system will be presented when experimental data necessitate it. The effects of thixotropy are discussed on page 474.

Further useful relations can be derived. For an unsymmetrical potential barrier the relationship between F_{out}, F_0, and F_{in} becomes

$$F_0 = \mu F_{out} + (1 - \mu)F_{in}. \tag{26}$$

If two constant rates of elongation β and $n\beta$ are

Fig. 9

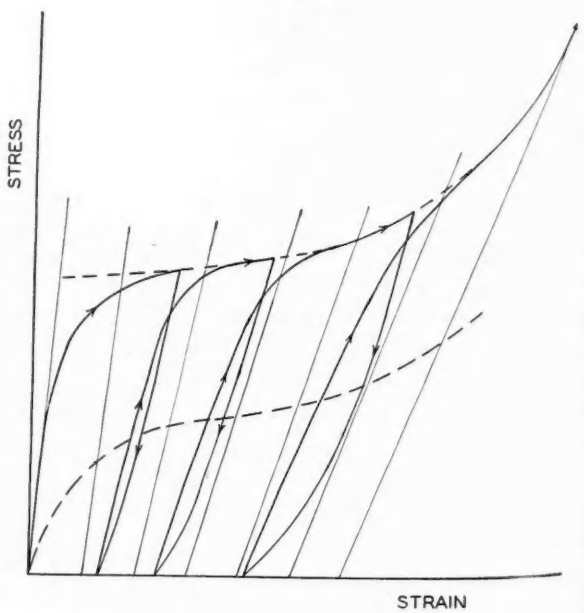

FIG. 9. *Example of stress-strain curve to which the two-position model could be applied.*

considered, for extension, then

$$2\mu\alpha F_{\text{out}_1} = \ln\left(\frac{\beta}{D}\right) - \ln\left(1 - \frac{l'}{l'_\infty}\right), \quad (27)$$

$$2\mu\alpha F_{\text{out}_n} = \ln\left(\frac{n\beta}{D}\right) - \ln\left(1 - \frac{l'}{l'_\infty}\right). \quad (28)$$

Thus if the curves are compared at the same value of elongation,

$$2\mu\alpha(\Delta F_{\text{out}}) = \ln n, \quad (29)$$

and for contraction

$$2(1 - \mu)\alpha F_{\text{in}_1} = \ln\frac{l'}{l'_\infty} - \ln\beta, \quad (30)$$

$$2(1 - \mu)\alpha F_{\text{in}_n} = \ln\frac{l'}{l'_\infty} - \ln n\beta. \quad (31)$$

Once more comparing the curves at the same value of elongation,

$$2(1 - \mu)\alpha(\Delta F_{\text{in}}) = -\ln n. \quad (32)$$

Thus

$$\frac{\mu}{1 - \mu} = -\frac{\Delta F_{\text{in}}}{\Delta F_{\text{out}}}, \quad (33)$$

which gives a method for determining μ and α from experiments at different constant rates of elongation. Equation (33) is identical with the similar equation derived for force differences on the basis of the spring-dashpot model [2].

For small values of elongation

$$\alpha F_{\text{out}} = \ln\frac{\beta}{D} + \frac{l'}{l_\infty'}, \quad (34)$$

a linear relationship. For large values, of course, $F \to \infty$. For small values of (β/D), equation (17) can be written

$$\alpha F = \tfrac{1}{2}\ln\frac{b}{D\left(1 - \frac{l'}{l'_\infty}\right)} + \frac{\beta}{2D\left(1 - \frac{l'}{l'_\infty}\right)\sqrt{\frac{\frac{l'}{l'_\infty}}{D\left(1 - \frac{l'}{l'_\infty}\right)}}}; \quad (35)$$

the force becomes linear in β and therefore shows Newtonian viscosity.

It is of interest to derive the creep law for the case of the symmetrical barrier. From equation (13) (and once more neglecting elasticity):

$$\int_0^t l'_\infty K dt = \int_{l'_0}^{l'_t} \frac{dl'}{De^{\alpha F} - \frac{l'}{l'_\infty}(De^{\alpha F} + e^{-\alpha F})}. \quad (36)$$

Since F is constant for creep,

$$l'_\infty Kt = -\frac{l'_\infty}{(De^{\alpha F} + e^{-\alpha F})} \times \ln\frac{De^{\alpha F} - (De^{\alpha F} + e^{-\alpha F})\frac{l'_t}{l'_\infty}}{De^{\alpha F} - (De^{\alpha F} + e^{-\alpha F})\frac{l'_0}{l'_\infty}}, \quad (37)$$

where l'_t is the elongation at time t. This equation represents a simple unimolecular decay law but with a relaxation time that depends on F.

At a constant rate of loading P, if the rate P is sufficiently rapid,

$$\frac{dl'}{dt} = \left(1 - \frac{l'}{l'_\infty}\right) l'_\infty KDe^{\alpha Pt}. \quad (38)$$

Integrating between 0 and l', 0 and t, yields:

$$-\ln\left(1 - \frac{l'}{l'_\infty}\right) = \frac{KD}{\alpha P}(e^{\alpha Pt} - 1). \quad (39)$$

Considering rates P and nP at a given value of l',

$$\frac{1}{n}(e^{\alpha F_n} - 1) = (e^{\alpha F_1} - 1). \quad (40)$$

If αF_n is large,

$$F_n - F_1 = \frac{\ln n}{\alpha}, \quad (41)$$

which is consistent with equation (29) for a symmetrical barrier. At a given value of F,

$$\ln\left(1 - \frac{l'}{l'_\infty}\right) = n\ln\left(1 - \frac{l'_n}{l'_\infty}\right), \quad (42)$$

in which the constant α does not appear.

The problem of the A $\to$ B transformation has been treated on the basis of the single-phase nature of the mixture of the two components A and B. If because of cooperative phenomena there is a phase boundary between the A and the B modifications, then the factors $(1 - b)$ and b will not appear in the expressions for k'_{AB} and k'_{BA}, respectively. Under such a hypothesis, the force necessary to elongate the fiber would be a constant until the end of the elongation, l_∞, is reached, at which point the force would rise suddenly to infinity (neglecting the elasticity of the molecules). In actuality, the equi-

librium problem would not be expected to be of this nature over the whole range of elongation. Rather, as is typical of critical phenomena, the two phases would coexist during the middle range of l, causing a flat portion of the equilibrium stress-strain curve in the middle range. This is actually observed in some cases. The solution of the finite rate problem involving two coexisting phases is very difficult; but, essentially, the more rapid the rate, the more nearly the experiment would be expected to conform to the mixed crystal model.

Although the model described here could be essentially duplicated by a model with the proper non-linear elements in the Eyring shear model, the naturalness of the present model for dealing with the nylon-rubber-wool type of stress-strain curve is apparent. These curves consist of an initial steep portion, composed apparently of the sum of both a stiff spring and the yield force of the viscous component of the elongation, followed by a very flat portion, and ending in a steep section that represents the exhaustion of the chain lengths [5]. The model presents an incidental derivation of a rubber-like elasticity law quite different from the current ones.

Often, experiments show that the model must be more complex than the simple two-configuration system described above. Suppose, for example, that the B structure contracts to an intermediate state C, which, while it occupies the same elongation as A, is at a higher energy level because all of the secondary bonds in the A structure have not reformed. These bonds will be considered to re-form at a rate that is undisturbed by the force.

Then, if a, b, and c are the concentrations, and

$$a + b + c = 1, \tag{43}$$

as before,

$$b = \frac{l'}{l'_\infty}. \tag{43a}$$

Then (see Figure 10)

$$k'_{AB} = (1 - b - c)D_1D_2K_1e^{\alpha F}, \tag{44}$$

$$k'_{BA} = bK_1e^{-\alpha F}, \tag{45}$$

$$k'_{CB} = cD_1K_2e^{\alpha F}, \tag{46}$$

$$k'_{BC} = bK_2e^{-\alpha F}, \tag{47}$$

$$k'_{AC} = (1 - b - c)K_3D_2, \tag{48}$$

$$k'_{CA} = cK_3, \tag{49}$$

where, for the illustrative model, it has been assumed that all barriers are symmetrical, and that α is a constant. The K and D factors are defined as for the two-state model and refer to the free-energy differences with the same subscripts. These free-energy differences are defined in Figure 10. Differentiating equation (43a) and substituting for $\left(\frac{db}{dt}\right)_{net}$,

$$\frac{1}{l'_\infty}\left(\frac{dl'}{dt}\right) = (k'_{AB} - k'_{BA}) + (k'_{CB} - k'_{BC})$$
$$= [(1 - b - c)D_1D_2K_1e^{\alpha F} - bK_1e^{-\alpha F}]$$
$$+ [cD_1K_2e^{\alpha F} - bK_2e^{-\alpha F}]. \tag{50}$$

The equation for $\left(\frac{dc}{dt}\right)_{net}$ can also be written:

$$\left(\frac{dc}{dt}\right)_{net} = (k'_{BC} - k'_{CB}) + (k'_{AC} - k'_{CA})$$
$$= [bK_2e^{-\alpha F} - cD_1K_2e^{\alpha F}]$$
$$+ [(1 - b - c)K_3D_2 - cK_3]. \tag{51}$$

Equations (43), (50), and (51) are simultaneous, so that it is possible to eliminate a and c and find l as a function of F.

The curves for such a model can be constructed in a manner entirely analogous to the method used

Fig. 10

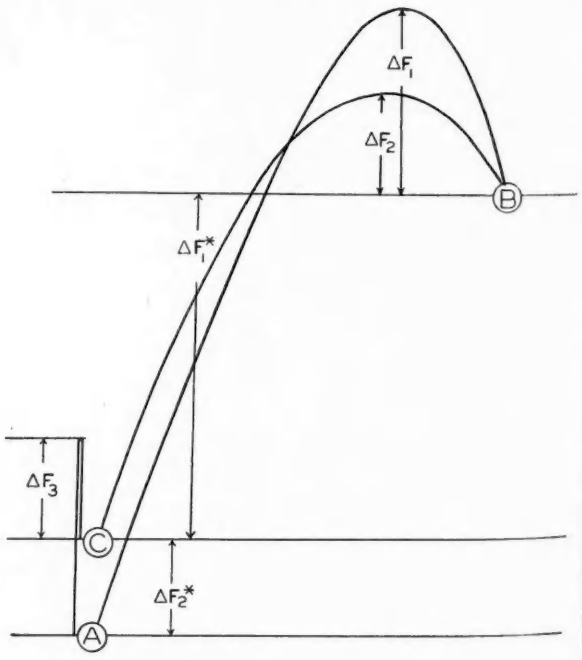

FIG. 10. *Potential-energy diagram of a simple, three-position model which exhibits thixotropy.*

Fig. 11

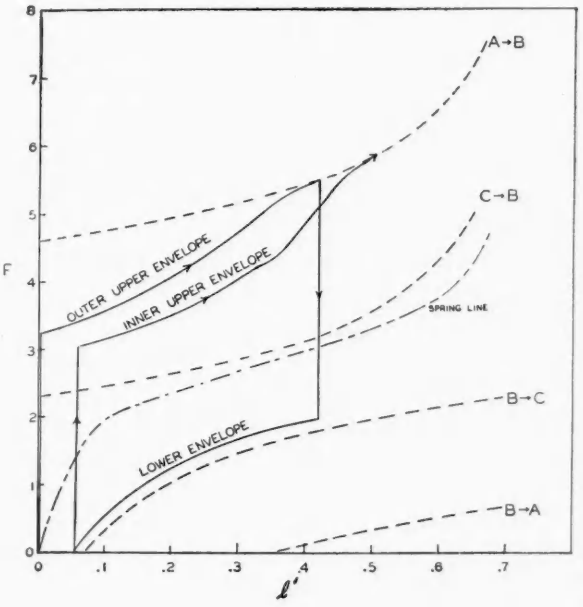

FIG. 11. *Stress-strain curves for three-position model of Figure 10. These curves are without the elasticity correction.*

— — — *Assuming transformations go entirely by one of the two paths.*

——— *Stress-strain curve calculated using simplified equations. Elasticity correction not included.*

— - — *Ultimate spring line.*

for the simple model. The constants chosen were:

$$K_1 l_\infty = 0.002 \text{ sec}^{-1} \qquad l_\infty = 0.7$$
$$K_2 l_\infty = 0.01 \qquad \rho = 0.001 \text{ sec}^{-1}$$
$$D_2 = 0.50 \qquad \alpha = 1 \text{ cm}^2/\text{gm}$$
$$D_1 = 0.01$$

Setting

$$k'_{AB} = k'_{BA},$$
$$k'_{CA} = k'_{AC},$$
$$k'_{BC} = k'_{CB},$$

at zero force and equilibrium conditions gives

$$a_0 = 0.664,$$
$$b_0 = 0.0033,$$
$$c_0 = 0.333.$$

By neglecting the $e^{-\alpha F}$ term for extension and the $e^{\alpha F}$ term for contraction, the curves in Figure 11 were constructed. These are shown before the approximate elasticity corrections have been applied. K_3 was assumed to be small enough to make the $C \rightarrow A$ transformation negligible during the time it takes to perform the elongation and contraction cycles. The spring line is derived by setting $\frac{dl'}{dt} = 0$ and $\frac{dc}{dt} = 0$ in equations (50) and (51). This represents the final spring line to which a substance following this model will ultimately relax. However, if points of no relaxation are determined by the bracketing technique [2], the present model will exhibit what has been previously known as five-element action [2]. This will be discussed more fully in a future paper. The curves for $A \rightarrow B$, $C \rightarrow B$, $B \rightarrow C$, and $B \rightarrow A$ transformations (assuming that the forward or reverse reaction goes entirely by one of the two paths) are shown in order to highlight the effect of the thixotropy.

If the factors D_1, D_2, K_1, K_2, and K_3 separate the processes because of their great differences in magnitude, the model yields quite simple and useful relationships. In other words, the flow in the forward direction will be solely from C when C is populated, and then from A when C is empty. The flow in the backward direction is all $B \rightarrow C$ and no $B \rightarrow A$. Then, at rest a much slower process, $C \rightarrow A$, can be observed.

With such a system recycling produces a lowering of F_{out} without changing F_{in}. It is characteristic of a system of this type that, if a second elongation be continued past the highest value previously reached, the extension curve will return to the higher level associated with the $A \rightarrow B$ transformation. During the second contraction the same path as before is followed. There is thus no thixotropy in the contraction for this particular model.

Experimental work may justify a more complex model. Discussion of most particular cases will await the application of these cases to specific experimental data. Essentially, if the various equilibrium positions are arranged so that the application of a force in a single direction with no reversals can cause only one jump or transformation for a given molecule, the model will show a distinct limiting elongation l_∞, the essential characteristic of the simple model of this paper. Equilibrium positions can be arranged so that, under any normal loading history, the value of F_{out} at a given value of elongation is continually and irreversibly decreasing, and irreversible thixotropic effects can thus be explained. As more and more elements are added in series with one another in the direction of

the applied force, the approach to l_∞ becomes more remote, and, ultimately, as these positions extend indefinitely in both directions against and with the direction of application of the force, the situation becomes very much that of the Eyring shear model. The exact relationship is discussed elsewhere [7].

The application of the above theory to the mechanical properties of wool fibers is now in process, and the results will be reported in due course.

Acknowledgment

The authors wish to thank Dr. J. H. Dillon, under whose direction the work described in this paper was done, for reading the manuscript and clarifying the presentation; Mr. Sidney M. Katz for a critical examination of the derivations; and Miss Corneil Messler for preparing the figures and the typescript.

Literature Cited

1. Halsey, G., White, H. J., Jr., and Eyring H., TEXTILE RESEARCH JOURNAL **15**, 295 (1945).
2. Halsey, G., *J. Applied Phys.* In press.
3. Eyring, H., and Halsey, G., *J. Colloid Sci.* **2**, 17 (1947).
4. Eyring, H. Classroom lectures at Princeton University (unpublished).
5. Meredith, R., *Shirley Institute Memoirs* **19**, 5 (1944).
6. Halsey, G., and Eyring, H., TEXTILE RESEARCH JOURNAL **16**, 329 (1946).
7. Dunell, B., and Halsey, G. Paper in preparation.

Application of Microscopy to the Textile Industry*

G. L. Royer and C. Maresh

Microscopical Laboratory, Calco Chemical Division, American Cyanamid Company, Bound Brook, New Jersey

THE use of microscopy in the textile field is not new, since it is well known to the textile technologist. It has been used extensively for the study of the structure of fibers and fabrics and to some extent in a study of dyeing, printing, and finishing. It is possible to identify the fibers to be colored, examine the damaging effect of treatments, study the penetration of dyes, investigate causes of color defects, study methods for improved color application, observe the effects of fiber finishes, etc. In these studies, the microscope, if operated by qualified personnel, can be a useful tool in the evaluation of quality of the textile and thus make it possible to produce a satisfactory product at the lowest possible cost.

Fiber Morphology

In modern dyeing the colorist is confronted with the application of color to fabrics containing many different fibers. Since no class of dyes has been discovered which is applicable to all fibers, it is necessary to know the fiber or fibers which make up the material to be dyed so that the dyes having the most satisfactory properties can be chosen. Dye identification stains, and such tests as burning to detect characteristic odor, are often useful. However, in many cases use of the microscope is desirable for definite confirmation and quantitative estimation of fibers in mixtures. In addition to identification, microscopical examination can be employed to determine the fiber size, fineness, or denier, and the quality of the fibers under inspection. For example, the amount of mature and immature cotton can be determined by viewing in polarized light [41], the presence or absence of a skin on rayon may be ascertained [21], and the presence of pulled and mechanically damaged wools can be detected [47].

Longitudinal examination has been the most common method, since it is easy to place a few fibers on a slide and look at them. When a fiber is mounted properly in a liquid of a different refractive index from its own, it is possible to study the fiber surface. If the fiber is mounted in a liquid of similar index of refraction, its surface will disappear and the body color, internal structure, and foreign material will be more apparent. Tests for the identification of the synthetic protein fibers have been developed [31] which are based upon their swelling characteristics in concentrated sulfuric acid.

Many important observations can be made by cross-sectional studies. Color Plate Figures 4–24 (opposite page 480) are photomicrographs of cross sections of representative textile fibers at a magnification of about 300 times. Although it is not always possible to identify a fiber by its cross-sectional pattern alone, this is a definite aid. The method of cross-sectioning using the histological technique of mounting in paraffin and cutting on the large biological microtomes is time-consuming, expensive, and somewhat difficult to execute. By the so-called Hardy [14] method, cross sections can be made in a few minutes. The Calco Modified Hardy microtome [34], shown in Figure 1, incorporates many of the original features, but includes a heavier base and a smoother cutting surface. Figure 2 is a diagrammatic sketch showing its operation. The fibers to be cross-sectioned are inserted into the slot (A, B, C) and cut off evenly on both sides of the plate (D). A plunger at the bottom pushes the fibers out of the top of the slot (F). Cellulose acetate dissolved in acetone or a colloidion solution is brushed over the top of the fibers (G). After this has dried, the fibers are cut as shown in (H). Because the first section contains fibers of varying lengths, it is discarded and the operation is repeated (I, J), but this time the fibers are pushed up a known amount by a definite turn of the plunger screw. When a satisfactory section is obtained, it

*This paper was presented by G. L. Royer before the Scottish and London Sections of the Society of Dyers and Colourists in England in April, 1947, and published in the September, 1947, issue of the *Journal* of that Society.

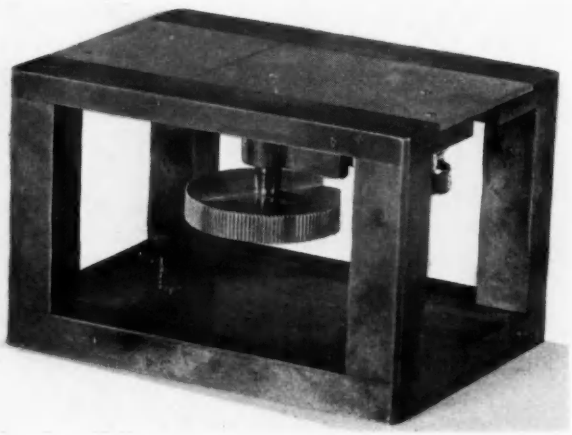

FIG. 1. *Calco Modified Hardy Microtome.*

is mounted on a microscope slide in a permanent mounting medium (K, L, M). A small press (N) is useful in obtaining flat sections. The section is then ready for examination under the microscope at low or high magnification.

In addition to the physical appearance of longitudinal or cross section, it is possible under the microscope to follow also the effect of color stains. Stains are available [8] which will aid in the identification of the various textile fibers. Microchemical tests [7] can be used to identify various chemical constituents in or on the fibers. Both of these are also useful in a study of the fundamental physical and chemical structure of natural and synthetic fibers.

In addition to using these techniques for the identification of fibers, it is possible to study the penetration of dyes and finishing agents into the fibers and correlate this factor with others such as colorfastness, color strength, creaseproofing, shrinkage control, etc. Since many of these properties are not dependent solely upon the single fiber but upon the relationship of one fiber to another, it may be desirable to examine the entire fabric. The surface may be examined at low power with a binocular type of microscope which gives a good conception of the third dimension. For a higher-power magnification of surface phenomena, the Epi illuminator of Zeiss or the Ultrapak of Leitz is very useful. Cross-sectional studies of fabrics can be made to determine the extent of penetration of dye or of other textile treatments into the cloth and to study the structure and fiber composition of union materials. See Color Plate Figures 1–3 for examples. These sections can be made in the Hardy-type microtome if the fabric is thin enough to fit into the slot. If the fabric is too thin, the free space can be filled by packing the fabric in with paper or cellophane. The biological type of microtome is preferred when the fabric is too thick to fit into the slot.

Fiber Pretreatments

In textile processing, the various treatments which are carried out previous to dyeing often modify the fiber so as to change its physical and chemical characteristics and also influence the subsequent treatments such as dyeing and finishing. In the processing of bast fibers such as linen, jute, hemp, ramie, etc., it is necessary to separate fibers by a process called "retting." The efficiency of this separation can be determined microscopically. The physical characteristics of the finished fabric and the dye penetration depend upon the removal of the ligneous portions and the breaking up of the fiber bundles so as to produce a finer fiber. For special purposes, coarser fiber bundles are desirable and the microscope is useful in controlling this.

The microscope has been of use in determining the degree of degumming and also to detect the presence of weighting in silk. The amount of damage which silk encounters during processing can also be studied by cross-sectional examination of the rate of dye penetration, in much the same way as it can for wool (see page 479).

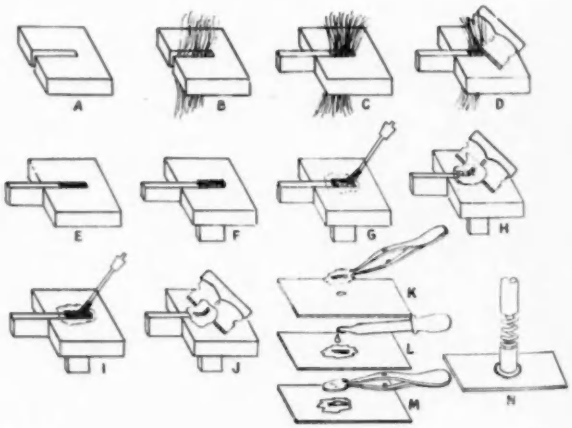

FIG. 2. *Diagrammatic sketch showing use of microtome.*

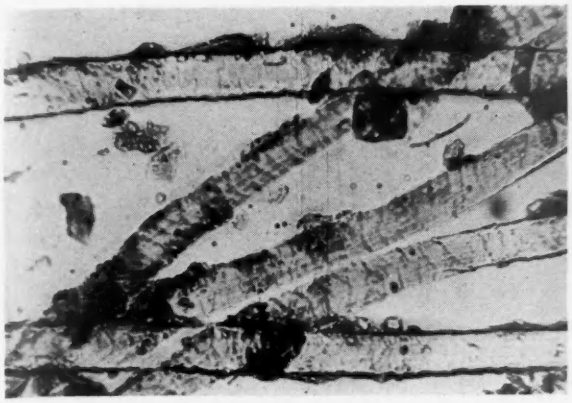

FIG. 3. *Dye-stain test applied to raw wool.*

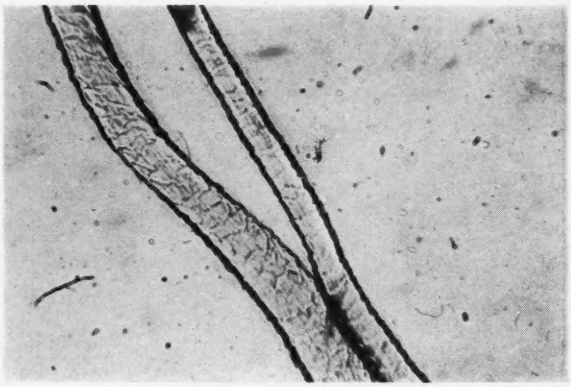

FIG. 4. *Dye-stain test applied to oiled top.*

The efficient removal of the natural grease from wool fiber is the first step in wool processing. This is usually done with a solvent or the more customary soap-and-soda scour. It is believed that the solvent method has the least "damaging" effect upon the wool and that the amount of "damage" [17] caused by the other processes depends upon their control. In order to investigate this process, a microscopical staining procedure was developed which shows the location of the wool grease and gives some estimation of the amount that is present.

This test is made with a saturated solution of Calcogas Red 0–5078. (This oil-soluble dye is similar to C.I. 258.) The solution is prepared by suspending an excess of this dye in 67-percent 3–A alcohol. The alcohol solution is heated, then cooled to room temperature, and allowed to stand for a short time before filtering. After filtration, the solution is ready for use. The sample to be examined for oil or wool grease is immersed for 1½ hours in this dye solution. It is then removed, rinsed twice in 67-percent alcohol, and dried, after which it is ready for examination. The sample may be examined by visual comparison with samples of known oil content or it may be mounted on a slide and examined microscopically. For the microscopical examination, we have found that mounting in glycerin jelly is quite satisfactory. Regular water mounts can be made but these are of course not permanent and the examination must be made shortly after preparation. Mounting in oil or Canada balsam is unsatisfactory.

The 67-percent concentration of 3–A alcohol was used because it does not readily dissolve oil or wool grease and it contains a small enough quantity of water so that the oil-soluble dye has sufficient solubility. This method is similar to that used by the histologist for the determination of fats in tissue. Although we do not believe that quantitative results can be obtained by its use, we do believe that it is quite useful in locating the oil fats in wool. Figure 3 shows grease on raw wool and Figure 4 shows the location of spinning oil on oiled top.

For a number of years the Calco laboratory has employed microscopical techniques to investigate changes in physical appearance of wool fibers, and dye or stain penetration to study "damage" or alterations which occur during processing prior to dyeing. Since most of these affect dyeing in one way or another, they will be discussed in the following section on fiber dyeing, but the examinations can be reversed and the penetration of the dye can be related to the changes which take place in the fiber. These observations then can be related to the physical properties of the fibers rather than to dyeing. Many acid milling dyes and some of the chrome complexes of chromable dyes have been used to detect a mechanical break in the epidermis or the scale layer of the wool fiber [20]. Thus, it is possible to confirm that wool has been damaged by a mechanical treatment such as carding or abrasion due to wear. This test has been used to identify reworked wool. Whewell, with Austerlitz [49], has presented an excellent review of the measurement of damage in wool and, with Woods [50], has described a microscopical test which has proved useful in our laboratory for studying the condition of natural and chemically treated wools. Whereas their test detects and estimates mechanical damage, we have adapted a similar staining and counting technique to the study of modifications in the wool caused by chemical treatments. More recently Carter and Consden [6] and Phillips [23] have

described similar methods for examining chlorinated wool after staining with Kiton Red G, and Semple [42] has developed a photoelectric method of estimating this wool damage.

Wool fibers which have received chemical treatments such as chlorination and alcoholic potash [10] have been studied by staining and examination in cross section [17]. The penetration of different types of dyes can be easily seen. In the case of chlorinated wool Calcocid Phloxine 2G (C.I. 31) left the outer chlorinated layer colorless, whereas Calcozine Blue ZF (C.I. 922) dyed this layer very heavily. The alcoholic potash treatment also modifies wool so as to give more or less equal dye diffusion into all wool fibers, including those which showed poor dye penetration before treatment.

Saponification of acetate rayon can be followed by cross-sectioning and staining with cellulose and cellulose-acetate-type dyes. The original acetate can be stained one color and the parts which have been converted to cellulose can be stained a contrasting color. This technique was first called to our attention by Burns [5]. Since the saponification reagent diffuses in from the outside, in the cross section of early samples there will appear to be a ring of dye, and in later samples the dye will show further penetration into the center as the conversion becomes more complete.

The mercerization of cotton can be similarly studied. An examination of Color Plate Figure 13, which is a cross section of cotton, and Color Plate Figure 14, which is one of mercerized cotton, reveals a difference in structure. The mercerized cotton has swollen and has lost the kidney shape of the regular cotton. Some idea of the extent of mercerization can be estimated from the fibers which have not been changed. The mercerized sample shown in the cross section contains some still unreacted cotton. This examination is of importance in the dyeing of mercerized cotton, which dyes differently from regular cotton. This microscopical test has been used often to show that the cause of uneven dyeing is the result of uneven mercerization, which obviously does not appear until the material is dyed. The test can also be used to determine the penetration of the mercerization when the process is applied to piece goods.

Dyeing

Microscopy is a useful tool for investigating dyeing. It is possible by means of it to determine the penetration of dye into the fabric and into the individual fibers, as well as the distribution of dye from fiber to fiber. This distribution can be related to properties such as color value, solidness of shade, fastness to crocking, fastness to washing, fastness to light, and levelness of dyeing. The Calco laboratories have published several papers [19, 20, 32, 36–38, 48] discussing microscopical observations of wool dyeing in which the importance of unlevel fiber dyeing or fiber selectivity has been emphasized. This phenomenon has been shown to be caused by variations from fiber to fiber in wool materials due to natural causes such as weathering, type of wool, and chemical "damage." The rate of dye penetration into the various wool fibers has been shown to vary over wide limits, particularly with the faster-to-washing types of dyes such as milling and chrome dyes. Level-dyeing colors may diffuse unequally into different fibers at low temperatures or in the early stages of dyeing, but at higher temperatures and on continued dyeing usually they will redistribute themselves so as to deposit uniformly in all the fibers. This uniform distribution of dye is desirable in order to obtain the maximum color value and also to eliminate skitteriness which results from poor fiber levelness. In certain cases, an increase of 50 percent in color value can be obtained with the same amount of dye if it is properly distributed. The fastness properties are also improved. Cross-sectioning of the textile and the use of high magnification make the dye penetration more evident than it appears in a regular longitudinal examination. The use of this technique will help to determine the cause of poor dyeing and aid in improving dyeing results.

The same microscopical techniques have been applied to union dyeing [18]. By a study of the cross sections, it is possible to determine which of the fibers in a mixture have taken up certain dyes, and if examination is made at various stages of the dyeing process, the transfer of the various dyes from one type of fiber to another can be observed. The examination of so-called union dyes which dye more than one type of fiber, and of dye mixtures made up of selected dyes which dye specific types of fibers, makes it possible to clarify and to correct some of the factors which enter into union dyeing.

In rayon dyeing, the microscope and cross-sectioning techniques have been used to study the initial take-up of vat and direct dyes, with removal of

CROSS-SECTIONS OF TEXTILE FIBERS

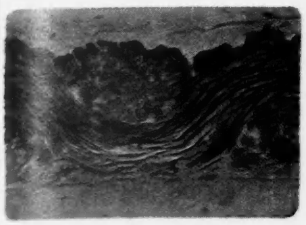

Fig. 1. Cotton Fabric

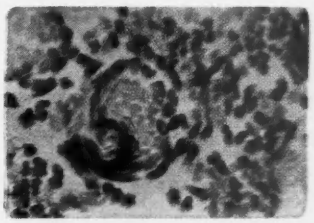

Fig. 2. Acetate-Viscose Fabric

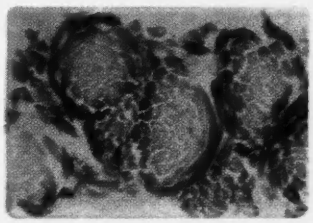

Fig. 3. Same Acetate Removed

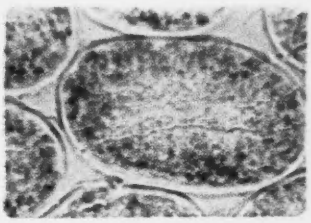

Fig. 4. Human Hair

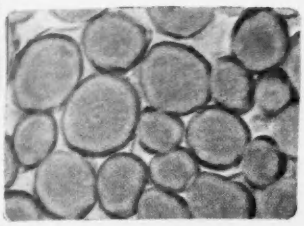

Fig. 5. Wool

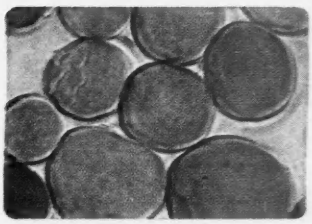

Fig. 6. Mohair

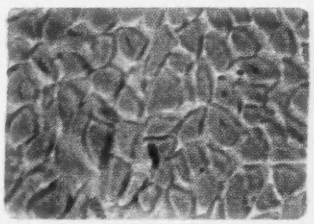

Fig. 7. Silk

Fig. 8. Tussah Silk

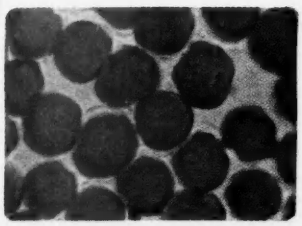

Fig. 9. Lanital

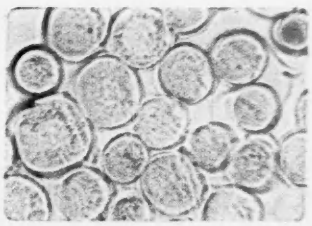

Fig. 10. Aralac

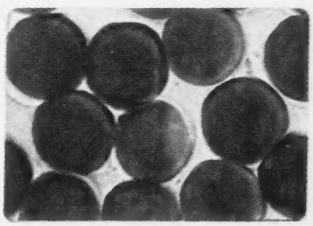

Fig. 11. Soya Bean

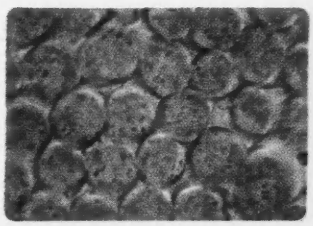

Fig. 12. Nylon

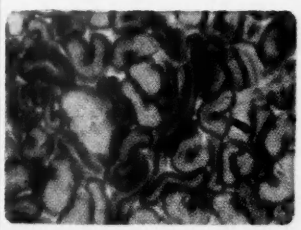

Fig. 13. Cotton

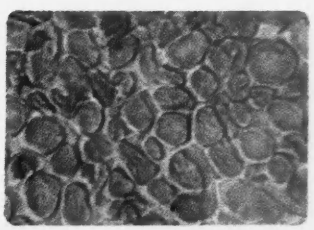

Fig. 14. Mercerized Cotton

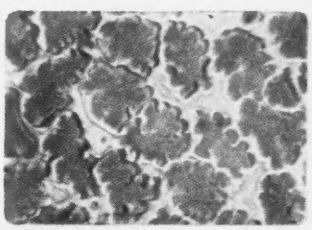

Fig. 15. Viscose Rayon

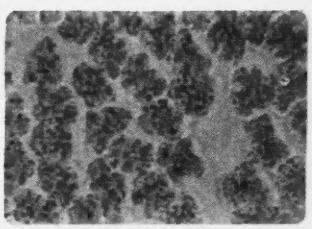

Fig. 16. Pigmented Viscose Rayon

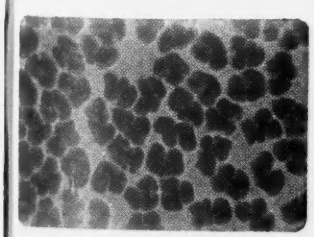

Fig. 17. Acetate Rayon

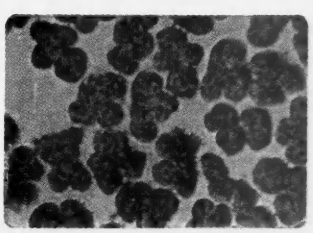

Fig. 18. Pigmented Acetate Rayon

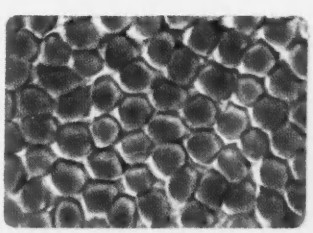

Fig. 19. Bemberg Rayon*

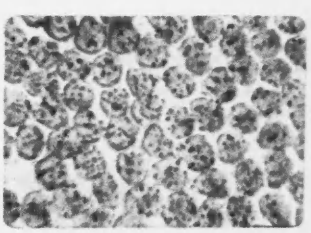

Fig. 20. Pigmented Bemberg Rayon*

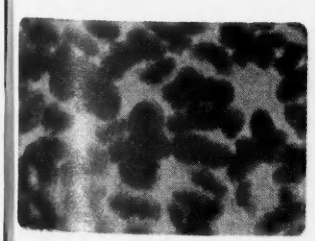

Fig. 21. "Rug" Bemberg Rayon*

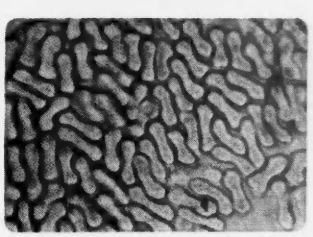

Fig. 22. Vinyon

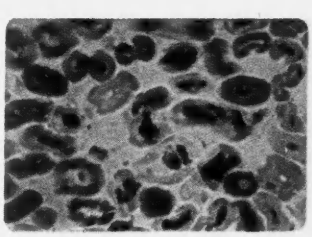

Fig. 23. Fur Felt

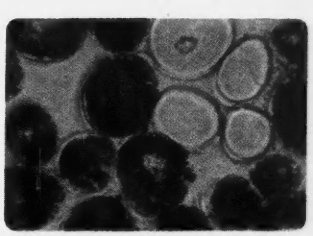

Fig. 24. Llama

Photomicrographs made in laboratories of Calco Chemical Division, American Cyanamid Company, Bound Brook, N. J.

*"Bemberg", registered trade mark of American Bemberg Corporation, for cuprammonium cellulose yarns made by that corporation.

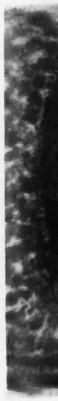

sampl
deter
have
tures,
qualit
variou
posse
the s
penet
Rate
manu
ing,
penet

Na
cause
the n
not c
tratio
Imma
of co
Unite
there
great
obtai

Pr
micr
and
tion
tions
ing.
the
in th
secti

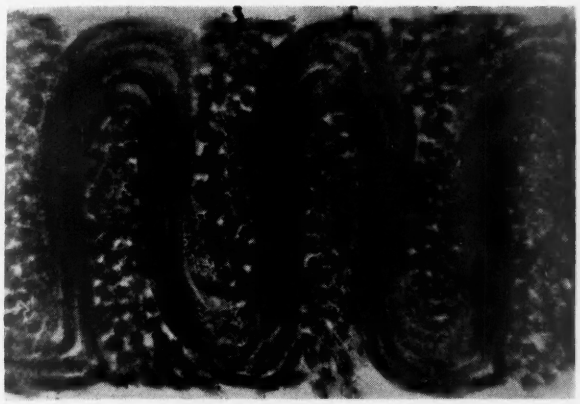

FIG. 5. *Cross section of rayon vat print.*

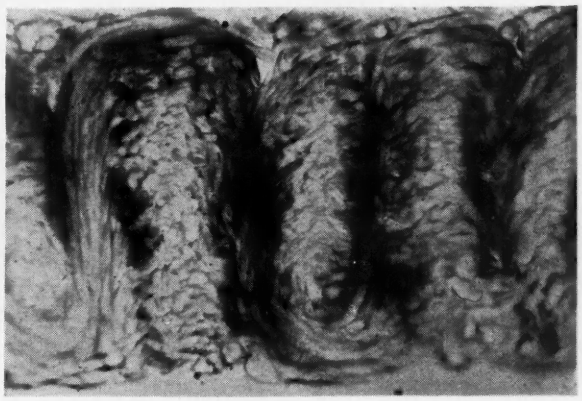

FIG. 6. *Cross section of cotton vat print.*

samples during the early stages of dyeing so as to determine how quickly the dyes penetrate. Studies have also been made of the penetration of dye mixtures, since the cross-sectional method will reveal qualitative differences in the rate of diffusion of the various dyes in a mixture. Cross sections of rayons possessing a so-called skin show that in some cases the skin portion is undyed, but that the dye has penetrated through the skin and dyed the center. Rate of dye penetration into rayon reveals such manufacturing variations as stretch, extent of ageing, etc., which must be controlled if uniform dye penetration is to be attained [39].

Natural variations exist in the cotton fiber which cause differences in dye diffusion. However, with the normal cotton dyes, the variations in cotton do not cause such extreme differences in rate of penetration into the individual fibers as those of wool. Immature cotton and nearly two hundred samples of cotton of various types grown throughout the United States have been used in this study. While there are differences in dyeing, they are not so great as was expected. The data on cotton dyeing obtained in this study will be published later.

Printing

Printing can be defined as localized dyeing. The microscope has been used to study the particle size and state of dispersion of vat dyes and the condition of the starch in the printing gum. Cross sections of the printed cloth after printing, after ageing, after oxidation, and after soaping have shown the distribution and penetration of the dye on and in the cloth. Color Plate Figure 1 shows the cross section of a finished print. A correlation of these many observations can be related to the color value and shade of the final print so that vat dyes of the proper form can be manufactured. A comparison of the cross sections of a vat-dyed rayon print and a vat-dyed cotton print (Figures 5 and 6, respectively) reveals a different distribution of the color in the two cloths. The structure of the threads in the cotton cloth prevents the dye from penetrating directly through. The color thickener flows more or less along the path of least resistance—namely, the threads—and dyes only the outside fibers of the threads. In the case of rayon, the paste flows uniformly down among all the fibers. This is probably due to the fact that the uneven kidney shape of cotton forms a tighter thread than the uniform serrated rayon. These observations are useful in formulating different color pastes for cotton and rayon.

Fabric Finishing

Fabric finishing as discussed here will cover the application of starch, resins, and some chemical treatments. The cooking of the starch is one factor which can be investigated with the aid of the microscope. The breakdown of the starch grains can be followed with the regular microscope or, still better, with the polarizing or phase microscopes [30]. Under the polarizing microscope the cross-like structure is clearly evident until the grain swells and bursts. The condition of the starch is important with respect to the viscosity, which, in turn, influences the application of the finish on, and the properties of, the finished cloth. The distribution of the starch can be determined by making cross sections and then staining them with iodine. The type of starch film

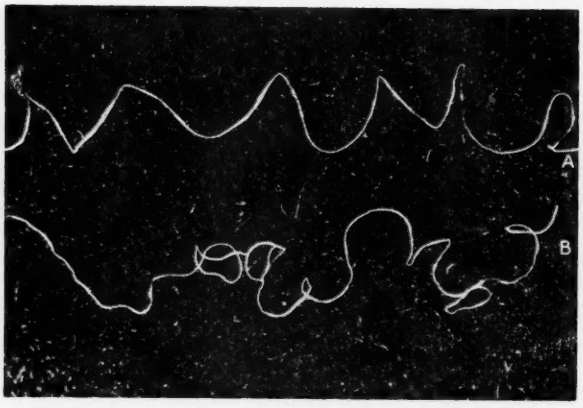

FIG. 7. *Single wool fibers. A (top)—Lanaset-treated. B (bottom)—untreated.*

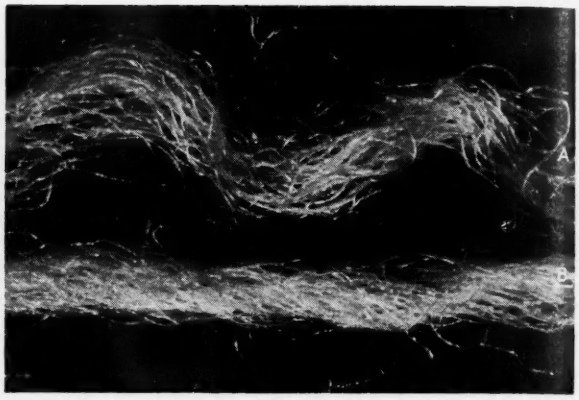

FIG. 8. *Threads from fabric. A (top)—Lanaset-treated. B (bottom)—untreated.*

—that is, whether it is continuous or discontinous—will affect the stiffness of the finish.

For permanent finishes, resins of many types are used. Microscopical examination of cross sections, together with staining techniques, can be used for the identification of many types of resins and also for their location in the fabric and individual fibers. Norwick [22], Stafford, *et al.* [46], Graff [12], Dixon *et al.* [9], and Wilcock [51] have published reports on their work using macro dye and chemical tests for the identification of resins and also for detecting the extent of cure. We have used these tests and have gone further in applying such tests to cross sections and to individual fibers. Thus, it is possible to study the resins within the fabric and within the fiber so as to have a better understanding of the mechanism of their function. It can be shown that the resins such as the water-soluble urea-formaldehyde and melamine-formaldehyde types go into the rayon and cotton fibers, whereas the polymerized vinyl and acrylate types go only into the fabric and surround or coat individual fibers. The former resins can be identified with acid dyes such as Calcocid Alizarine Blue SAPG (C.I. 1054) in acid solution. This solution does not dye cellulose. The latter resins are best stained with oil-soluble dyes. These tests are applied to the cross sections after they have been cut, wherein the dye will have complete access to the portion under investigation.

"Extent of cure" tests for urea and melamine resins have been used to determine whether or not full benefit has been made of the applied resin. One method is to apply the acid dye-resin identification test on samples before and after washing in water. Washing will remove any uncured resin, and the difference in dye pick-up between the samples before and after washing determines the effectiveness of the cure. Cross sections show whether the resin in the fabric has been insufficiently cured or whether there was a general improper cure throughout the thickness of the fabric. Another method for determining the extent of cure is to use a direct dye such as Calcodur Blue SL (Pr 71) which normally dyes cellulosic fibers quite well. It has been found that with melamine and urea resins uncured resin does not limit the dye take-up; but properly cured resin-treated rayon or cotton dyes slowly, if at all, in a solution which consists of 0.125 gram of dye and 0.625 gram of sodium chloride in 500 milliliters of water. This test, besides determining the extent of cure, will indicate the proper quantity and location of resin deposition when correlated with satisfactory samples.

Dye-staining techniques and low-power examinations have been useful in studying the application of Lanaset resin.* Cross sections and longitudinal views [17] show that the treatment slowed down the penetration of dye both through the epidermal layer and into the core itself. When applied to a single wool fiber (Figure 7) it sets the hair in the form it had during the cure and the fiber will retain this set even when wet-out. A similar phenomenon occurs when fabric is treated and cured, as is shown by threads removed from treated fabrics (Figure 8). Low-power examinations of the treated and untreated fabrics, after drastic washing, showed the untreated to be badly felted and the structure to be generally disrupted. The treated fabric showed little change

*U. S. Trade Mark (American Cyanamid Co.), applied to a melamine resin for use in wool shrinkage control.

TABLE I

Fiber	References	Refractive indices N_ϵ	Refractive indices N_ω	Birefringence $N_\epsilon - N_\omega$
Ramie and flax, native	[26]	1.596	1.528	0.068
Cotton, native	[26]	1.578	1.532	0.046
Cotton mercerized under tension	[26]	1.586	1.522	0.044
Cotton mercerized without tension	[26]	1.554	1.524	0.030
Cuprammonium	[26]	1.552	1.525	0.027
Viscose (no-skin)		1.549	1.523	0.026
Viscose (thick-skin)		1.541	1.516	0.025
Lilienfeld rayon		1.564	1.522	0.042
Viscose (no-skin)	50% godet stretch	1.554	1.526	0.028
	30% godet stretch	1.552	1.526	0.026
	0% godet stretch	1.548	1.526	0.018

during washing. The phase microscope, to be discussed later, has aided in showing the proper distribution of resin at the scale interstices (see Figure 13). Thus the microscope has played a part in the study of the mechanism of shrinkage control of wool with resins, and it is thought that fiber control gained by proper resin impregnation and distribution is an important factor in obtaining wool fabrics which show excellent shrinkage control.

Physical Properties of Fibers

In addition to the usefulness of the regular microscope to the textile technologist as a tool for visual examination of fibers and fabrics and for observing the effects of pretreatments, dyeing, and finishing operations, the polarizing microscope can be used to study, at least in a qualitative manner, the degree of orderly structure within a fiber.

The refractive indices of the various textile fibers, one of the properties which can be determined with this instrument, are useful not only for quick identification of the fiber under examination but also for differentiation of the various types of rayon and protein fibers. The manufacture of rayon has become so diversified that the microscopist is called upon to determine whether a rayon is of a highly oriented type such as Durafil and Fortisan, or a less oriented type. Moisture pick-up, dyeing rate, extensibility, and tenacity can be correlated with crystallinity, which is reflected in the refractive indices of the fiber.

The double-refraction or birefringence is progressively lower for native cellulose, cotton mercerized under tension, cotton mercerized under no tension [26], and regenerated cellulose. It is related to the degree of orientation of the micelles with respect to the fiber axis, at least on the outer surface. Lilienfeld rayon shows a considerably higher birefringence than ordinary types of rayon, and this checks with the high degree of crystalline order of this type of rayon as shown by x-ray. The birefringence of rayon also increases with increase in stretch applied to the fiber during manufacture [15]. Table I summarizes the indices of refraction and calculated birefringence for a set of experimental yarns. Fiber anisotropy or birefringence can be determined also by a study of resultant dichroism of dyed fibers, as shown by Preston and Tsien [27].

Cross sections of no-skin viscose rayon show it to be homogeneous throughout, and examination between crossed Nicol prisms shows a "uniaxial" character or a high axial orientation. Thick-skin rayon in cross section shows a progressive change from high axial orientation on the outer periphery to areas of high lateral orientation (crystallization). The nonhomogeneity visible in the outer portion or skin of the fiber is very likely due to the disruption which results from the change from the high lateral orientation to the high axial orientation of the micelles which takes place in the layer known as the skin of the fiber. As shown by Figure 9, the crystallization of the core of the thick-skin fiber appears to be spherulitic. The different lobes of the serrated cross-sectional structure extinguish alternately between crossed Nicol prisms as the section is rotated. The difference in structural order of core and skin of rayon fiber has been investigated by other techniques such as swelling and staining [21, 25, 40, 44, 45, 52] and confirms the picture described above.

A similar study has also been made of synthetic protein and mixed protein-cellulose fibers. The data are shown in Table II. Insufficient denaturation of the globular proteins during the production of protein fiber is reflected in the low birefringence of many of these fibers. The low tensile strength, both

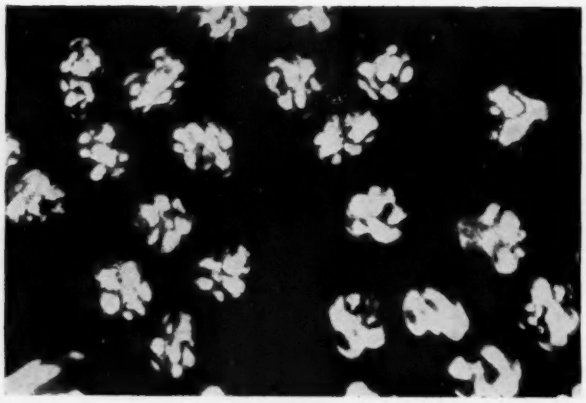

FIG. 9. *Cross section of thick-skin viscose rayon between crossed Nicol prisms.*

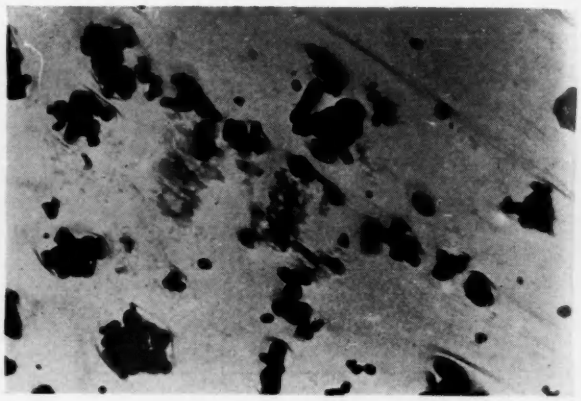

FIG. 10. *TiO_2—electron micrograph.*

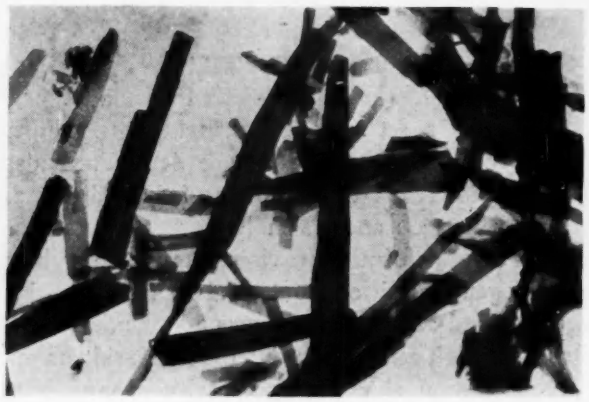

FIG. 11. *Vat brown—electron micrograph.*

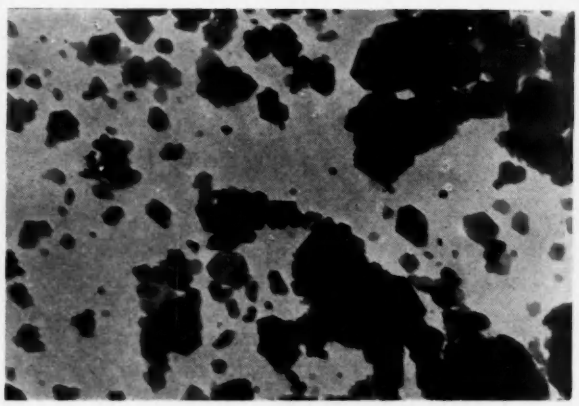

FIG. 12. *Clay—electron micrograph.*

wet and dry, rapid dye diffusion, and swelling behavior are of course related to the low degree of crystalline order found for the protein fibers. Cisalfa, which is a mixed polymer system of protein and cellulose, exhibits refractive indices (and birefringence) intermediate between those of regenerated protein and cellulose fibers.

New Instruments

Proof of benefits reaped by the use of the microscope are reflected in the rapidity with which the textile and related industries are using the electron microscope and, more recently still, the phase microscope.

The electron microscope remedies the old problem of the optical microscope—namely, that of limited resolution. This instrument has made it possible to determine the shape and size distribution of various materials such as delustering agents and vat dyes, the shape and size of which seriously affect the nature of the finished fabric to which they are applied. Figures 10, 11, and 12 are electron micrographs of three representative materials used by the textile industry. The actual fiber may be studied by the use of replica [2], disintegration [1], or thin-section ultra-microtome [11] techniques.

The phase microscope solves another of the problems of the optical microscopist—namely, that of not being able to resolve fine structure which varies only slightly in thickness or density toward light. With the new phase microscope [3], such discontinuity in a textile or other material can be shown in good contrast without the need for staining, altering, or otherwise damaging the sample.

The practical application of the optical principles underlying the phase microscope was first realized about 1932 in Germany. Independent development in the United States was begun about 1941 by the American Optical Company. Although, admittedly, much research remains to be done, the phase microscope is already finding useful application in dyeing,

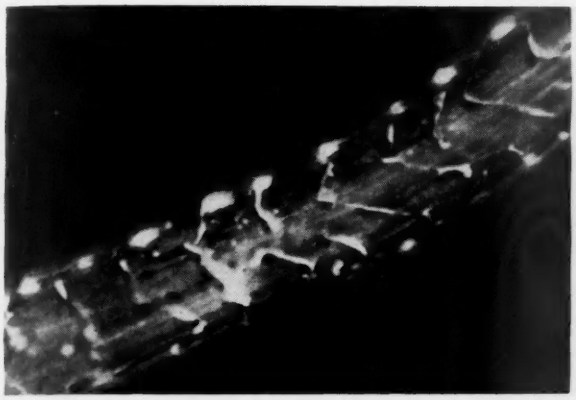

FIG. 13. *Lanaset-treated wool fiber—phase microscope.*

FIG. 14. *Untreated wool fiber—phase microscope.*

finishing, and pigment problems. H. Reumuth [30] in his paper "Application of Phase Microscopy to Textile Fiber Research" has described the application of the instrument to textile problems in Germany.

The optical principle underlying the phase microscope has been adequately described in the literature [3]. Light rays directed by an annular plate in the condenser are affected slightly by minute discontinuities of the specimen under examination and are changed further in their amplitude and phase relationships with respect to the undeviated rays by a specially constructed plate called the phase plate, which is located at the back focal plane of the objective to produce a final image of enhanced clarity.

Figure 13 shows a wool fiber treated with Lanaset resin mounted in a medium of refractive index approximately that of wool and photographed with the phase microscope, using a $0.07A + 0.25\ \lambda$ phase plate. The white areas show clearly the location of the resin on the wool fiber. Figure 14 shows an untreated wool fiber similarly mounted. The degree to which such discontinuities are brought out may be varied by changing the absorption and phase retardation of the various sectors of the phase plate. Much can be done to improve visibility by choice of immersion media of the correct refractive index relationships to the material under examination.

TABLE II

Fiber	Refractive indices N_ϵ	N_ω	Birefringence $N_\epsilon - N_\omega$
Lanital	1.542+	1.542	0.000+
Aralac	1.537+	1.537	0.000+
Soy bean	1.545+	1.545	0.000+
Ardil (peanut)	1.545+	1.545	0.000+
Zealon	1.539	1.532	0.007
Zein	1.536	1.532	0.004
Cisalfa	1.546	1.533	0.013

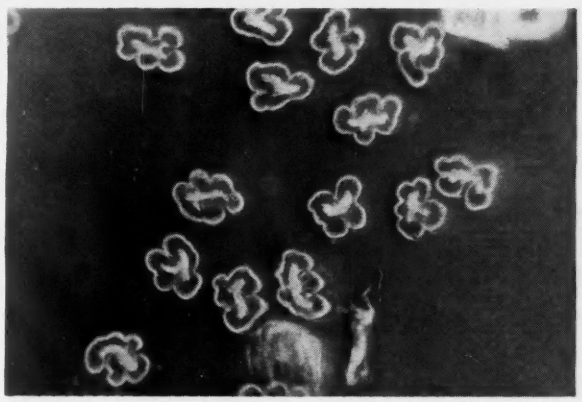

FIG. 15. *Cross section of thick-skin rayon fiber—phase microscope.*

Figure 15 shows a cross section of thick-skin rayon under the phase microscope. The difference in structure of the core and skin portions is as clearly brought out with this instrument as with staining techniques.

Thin, colorless crystalline materials stand out boldly, making determination of their shape and size an easy matter. The nature of thin coatings of finishing agents on textiles, paper fibers, leather, and pigments can be more accurately determined. The phase microscope has also been found beneficial in the examination of emulsions and dispersions of fine particle size.

Fluorescence Microscopy

Fluorescence microscopy has found some use in the textile field [13, 28, 29, 33]. Many studies of dye penetration can be followed at low dye concentrations using fluorescent dyes. Early stages of dye penetration [18] are more evident and combination dyeings [36] are often more easily studied. Dyes which are quite transparent to visible light, such as

leuco vat dyes, can easily be traced in both printing and dyeing studies. Spots of oil on fabrics can often be detected by their fluorescence; thus the cause of dyeing resists may be revealed. Likewise, active mildew on wool can be distinguished by its bright fluorescence. Fluorescent dyes can be used as tracers and indicators in chemical analysis and often for the identification of specific chemicals.

Optical Staining

"Optical staining" by the use of the Rheinberg color-contrast method has been of interest as a special technique of microscopical illumination. The Zeiss Mikropolychromar has been useful in carrying out this technique. An article by Royer, Maresh, and Harding [35] describes the principles and use of this apparatus. Briefly, it makes it possible to color with two different hues the indirect and the direct beams of illumination from a microscope condenser, and, hence, to differentiate between the reflected and the transmitted parts of a microscopical image.

Photography

In addition to providing permanent records of what is seen through the microscope or what is seen with the unaided eye, photography has the advantage, as pointed out by Bradley [4], of being able to record weak fluorescent and phosphorescent effects, utilize spectral wave lengths outside the range of human vision, and to record motion.

The penetration of dye into textile fibers can be followed by the time-lapse exposure technique [16] to give fast-motion pictures (as opposed to slow-motion ones). This speeding-up makes it possible to observe motion which is too slow to be observed at its natural rate.

By use of color film and prints, such as Ansco color and Kodachrome, the sample can be photographed and recorded in color. With the use of 35-mm. film the cost of this method is very reasonable and the color transparencies obtained can readily be projected for study or exhibition.

When 35-mm. film is used for photomicrographic work, there are various types of cameras and attachments which can be connected to the microscope so that focusing and exposure are attained. These attachments have been described in detail in a bulletin by Royer, Maresh, and Harding [34]. By either a sliding, rotating, or prism arrangement, the image of the material under examination is shifted from the ground glass, where visual examination and focusing adjustments are made, to the camera proper. To standardize the exposure, a photoelectric exposure meter with a sensitivity suitable for use in photomicrography and macro color photography has been developed which makes it possible to obtain satisfactory color photomicrographs on the first exposure of practically all subjects which have been examined. For photomicrographs by ordinary transmitted light, a light value is taken from the sample directly on the ground glass. To establish the correct exposure level for photomicrographs in polarized light, it has been found desirable to take the exposure reading with a $\frac{1}{4}\lambda$ mica retardation plate inserted between the crossed Nicol prisms at an angle of 45 degrees with respect to the vibration directions of the polarizer and analyzer. The sensitive galvanometer described above can be used on some fluorescent specimens which give rather bright fluorescence. It is thus possible to establish the exposures on a standard fluorescent material which completely fills the field and then use this standard in setting up the apparatus for future exposures.

For photography of small objects or at low magnifications, a microscope is not necessary. Photographic lenses of suitable focal length can be used, and Micro Tessar and Micro Teleplat lenses are available for magnifications of 1 to 40. The same type of camera equipment used with the microscope may be employed since the lenses may be attached by connecting tubes directly to the copying and focusing attachments. To establish the proper level of exposure, a piece of gray cloth or paper having a reflectance of about 30 percent is used as a standard. A similar technique, using a fluorescent cloth instead of the standard gray cloth, has been employed for establishing light levels for fluorescent low-power or macro photography.

The subject of photomicrography in black and white is capably covered by Shillaber [43] and by a booklet on photomicrography by the Eastman Kodak Co. [24]. The careful adjustment of the color of the illumination and the necessity for accurate determination of exposure are two factors which are important in color photography but of less importance in black and white. However, the use of exposure meters for black and white prevents the wasteful use of film and produces negatives with correct exposure.

Acknowledgment

The authors wish to acknowledge the help which they have received from their associates, both in

carrying out the experimental work and for encouraging the development of microscopical techniques. Thanks are due to the Chemical Research Laboratory of the American Viscose Corporation for supplying some of the rayon samples studied in this investigation.

Literature Cited

1. Barnes, R. B., and Burton, C. J., *Ind. Eng. Chem.* **35**, 120 (1943).
2. Barnes, R. B., Burton, C. J., and Scott, R. G., *J. Applied Phys.* **16**, 730 (1945).
3. Bennett, A. H., Jupnik, H., Osterberg, H., and Richards, O. W., *Trans. Am. Microscopical Soc.* **65**, 99 (1946).
4. Bradley, C. W., *J. Soc. Dyers and Colourists* **61**, 61 (1945).
5. Burns, C. Private communication.
6. Carter, E. G. H., and Consden, R., *J. Text. Inst.* **37**, T227 (1946).
7. Chamot, E. M., and Mason, C. W., "Handbook of Chemical Microscopy," 2nd Ed., New York, John Wiley & Sons, 1938.
8. Davis, H. L., and Rynkiewicz, H. J., *Ind. Eng. Chem., Anal. Ed.* **14**, 472 (1942).
9. Dixon, J. K., *et al., Am. Dyestuff Reptr.* **35**, 215 (1946).
10. Freney, M. R., and Lipson, M. J., *J. Council Sci. Ind. Research* **14**, 25 (1941).
11. Fullam, E. F., and Gessler, A. E., *Rev. Scientific Instruments* **17**, 23 (1946).
12. Graff, J. H., *Paper Trade J.* **122**, 41 (1946).
13. Haitinger, Max, "Die Fluoresgenzanalyse in der Mikrochemie," Vienna and Leipzig, Emil Haim & Co., 1937.
14. Hardy, J. I., U.S.D.A. Circular No. 378, Supt. of Documents, Washington, D. C. Price, 5 cents.
15. Hermans, P. H., Hermans, J. J., and Vermaas, D., *J. Polymer Sci.* **1**, 156 (1946).
16. Kienle, R. H., and Royer, G. L., *Am. Dyestuff Reptr.* **28**, 638 (1939).
17. Kienle, R. H., Royer, G. L., and McCleary, H. R., *Am. Dyestuff Reptr.* **34**, 42 (1945).
18. Millson, H. E., and Royer, G. L., *Am. Dyestuff Reptr.* **31**, 280 (1942).
19. Millson, H. E., Watkins, W. H., and Royer, G. L., *Am. Dyestuff Reptr.* **36**, 45 (1947).
20. Millson, H. E., Royer, G. L., and Wissemann, M. E., *Am. Dyestuff Reptr.* **28**, 632 (1939).
21. Morehead, F. F., and Sisson, W. A., TEXTILE RESEARCH JOURNAL **15**, 443 (1945).
22. Norwick, B., *Ind. Eng. Chem., Anal. Ed.* **16**, 274 (1944).
23. Phillips, H., *Dyer* **96**, 299 (1946).
24. "Photomicrography, An Introduction to Photomicrography with the Microscope," 14th Ed., Rochester, New York, Eastman Kodak Co., 1944.
25. Preston, J. M., *J. Soc. Chem. Ind.* **50**, 199T (1931).
26. Preston, J. M., *Trans. Faraday Soc.* **29**, 65 (1933).
27. Preston, J. M., and Tsien, P. C., *J. Soc. Dyers and Colourists* **62**, 368 (1946).
28. Radley, J. A., *J. Soc. Dyers and Colourists* **53**, 376 (1937).
29. Radley, J. A., and Grant, J., "Fluorescence Analysis in Ultra-Violet Light," New York, D. Van Nostrand Co., 1935.
30. Reumuth, H., TEXTILE RESEARCH JOURNAL **17**, 69 (1947).
31. Royer, G. L., *Am. Dyestuff Reptr.* **32**, 165 (1943).
32. Royer, G. L., and Maresh, C., *Am. Dyestuff Reptr.* **32**, 181 (1943).
33. Royer, G. L., and Maresh, C., *J. Biol. Phot. Assoc.* **15**, 107 (1947).
34. Royer, G. L., Maresh, C., and Harding, A. M., "Microscopical Techniques for the Study of Dyeing," Calco Technical Bulletin No. 770, Bound Brook, N. J., 1945.
35. Royer, G. L., Maresh, C., and Harding, A. M., *J. Biol. Phot. Assoc.* **13**, 123 (1945); *see also* Calco Technical Bulletin No. 770 [34].
36. Royer, G. L., and Millson, H. E., *Am. Dyestuff Reptr.* **29**, 697 (1940).
37. Royer, G. L., Millson, H. E., and Amick, C. A. Paper presented April 2, 1947, to the Midlands Section of the Society of Dyers and Colourists.
38. Royer, G. L., Millson, H. E., and Stearns, E. I., *Am. Dyestuff Reptr.* **32**, 285 (1943).
39. Royer, G. L., McCleary, H. R., and de Bruyne, J. M. A., *J. Soc. Dyers and Colourists*, August, 1947; TEXTILE RESEARCH JOURNAL **17**, 438 (1947).
40. Schramek, W., and Helm, J., *Kolloid-Z.* **85**, 291 (1938).
41. Schwarz, E. R., and Shapiro, L., *Rayon Text. Mo.* **19**, 371 (1938).
42. Semple, W. L., *J. Text. Inst.* **37**, T260 (1946).
43. Shillaber, C. P., "Photomicrography in Theory and Practice," New York, John Wiley & Sons, 1944.
44. Sisson, W. A., *J. Phys. Chem.* **44**, 513 (1940).
45. Sisson, W. A., TEXTILE RESEARCH JOURNAL **15**, 443 (1945).
46. Stafford, R. W., *et al., Paper Trade J.* **120**, 51 (Apr. 19, 1945).
47. von Bergen, W., and Krauss, W., "Textile Atlas," New York, American Wool Handbook Co., 1942.
48. Watkins, W. H., Royer, G. L., and Millson, H. E., *Am. Dyestuff Reptr.* **33**, 52 (1944).
49. Whewell, C. S., and Austerlitz, F. J., *J. Soc. Dyers and Colourists* **59**, 45 (1943).
50. Whewell, C. S., and Woods, H. J., *J. Soc. Dyers and Colourists* **60**, 148 (1944).
51. Wilcock, C. C., *Papers of the American Association of Textile Technologists* **1**, 35 (1945).
52. Wuhrmann, K., *Helv. Chim. Acta* **28**, 666 (1945).

Measurement of Friction Between Single Fibers

Nils Gralén and Bertil Olofsson

Swedish Institute for Textile Research, Gothenburg, Sweden *

Introduction

The frictional forces acting between the fibers in a fiber mixture, a top, or a yarn have been the object of several scientific studies. One of the practical aspects has been the felting properties of wool, which are assumed to be due to the difference in frictional coefficients of the wool fiber when it is moved in different directions (towards root or tip). Another operation in the textile industry where the friction between the fibers should be of essential importance is the drawing and spinning of short fibers into yarn.

One method frequently used for friction measurements consists in arranging a great number of fibers parallel to form a mat of fibers over a plate or between two rods. The friction is measured by applying the mat on an inclined plane and increasing the angle until slipping occurs. The best-known application of this principle is Speakman's "violin bow" method for measurement of the scaliness of wool [8]. The pulling force can also be obtained by loads on a balance pan [1]. A special instrument for measuring wool scaliness is the lepidometer [7], which simulates the one-way movement of an animal fiber when it is rubbed between one's finger and thumb. The movement is balanced and the force is measured by means of a torsional arrangement. A third method is to curl the fiber over a wheel or a circular rod, place a load (P_1) at one end of the fiber, and measure the force (P_2) which is necessary at the other end for slipping. The frictional coefficient is given by the equation: $P_2/P_1 = e^{\mu\Phi}$, where Φ = the angle of the arc of contact and μ = the frictional coefficient. This principle has been used by Lipson and Howard [3] and by Martin and Mittelman [4] for measuring the friction of wool fibers. Morrow [6] has used several different methods for determining the friction of fibers, and also of yarns and fabrics. He has used the principles mentioned, but has also measured the force necessary to draw a fiber out from between two plates which are pressed together.

In some of the investigations mentioned only the force necessary to start the slippage has been measured; in other cases the surfaces of the fibers where friction occurs have been in movement relative to each other during the measurement, and the forces necessary to sustain this motion were measured. In the first case we refer to static friction (indicated by subscript "*s*") and in the second case to dynamic friction (indicated by subscript "*d*").

Design of Apparatus and Performance of Measurements

In the methods of most of the authors mentioned above measurement has been made of the friction between one or several fibers and some other material, such as glass, rubber, leather, or horn. It is obvious that a very essential part of the friction present during the fiber movements in milling and spinning acts between the single fibers. Thus we considered it to be of the greatest interest to measure the frictional forces that appear on the rubbing of one fiber against another, and we have designed an apparatus for that purpose. As the forces are quite small, we have used a torsional thread for the measurements. The apparatus is similar to that of Bowden and Leben [2], which is used for measuring friction between metallic surfaces and has been adapted for fibers by Mercer [5].†

Figure 1 shows the essential part of the instrument. *A* is a piano wire, about 60 cm. long, fixed to a steady stand at its upper and lower ends. *B* is a small aluminum balance suspended on a steel needle bearing with horizontal axis. The bearing frame (*C*) is fixed to the midpoint of the piano wire and has a vertical plane mirror (*D*). One end of the balance has a fork (*E*) with clamping

* Dr. Gralén is Director of the Institute.

† Since this paper was submitted for publication, Mercer and Makinson (*J. Text. Inst.* **38**, T227 (1947)) have published further details of their friction measurements.

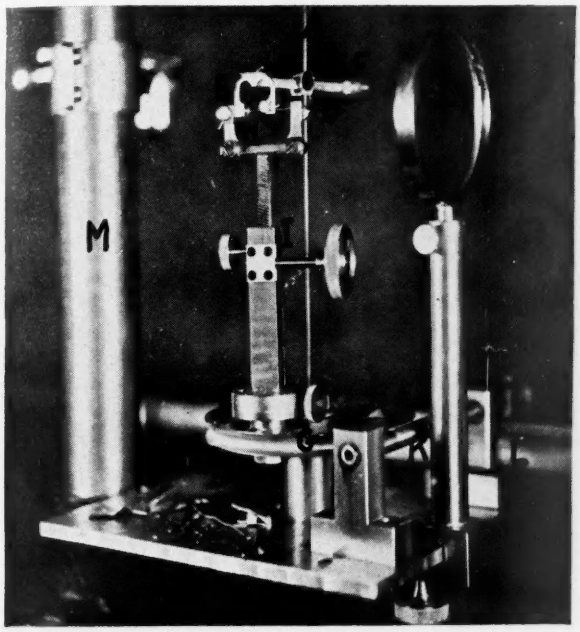

FIG. 1. *Detailed photograph of the fiber friction meter.*

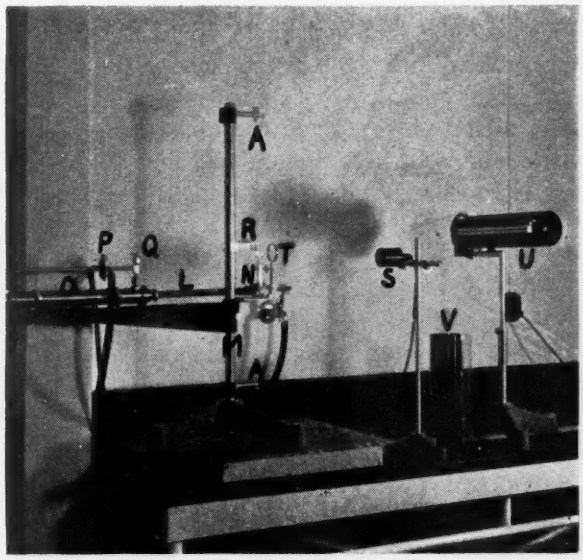

FIG. 2. *Full view of the fiber friction meter.*

screws for fastening a fiber. A load may be applied by weights on a little pan at the same end of the balance. In order to insure a constant moment of the load, the pan has a notch perpendicular to the balance arm, and the weight (a piece of metal wire) is placed in the notch. At the other end of the balance there is a screw for adjusting it to equilibrium (*F*). The wire goes through a central hole in the bearing of a horizontal toothed wheel (*G*). The second fiber holder (*H*) is fixed to this wheel and can be raised and lowered by means of the rack and pinion (*I*). By a horizontal revolving of the holder the angle between the fibers can be changed, and the distance from the center (of the piano wire) may be adjusted by a radial movement of the holder on the horizontal wheel. The wheel can be revolved slowly by the screw (*K*), moved by the rack (*L*) which is driven hydraulically.

A full view of the apparatus may be seen in Figure 2. *M* is the stand with the parts described for Figure 1 (at *N*). *O* is a metal cylinder with a piston fixed to the rack *L*. The direction of the piston movement is changed by turning the cock (*P*) and the speed is regulated by the needle valve (*Q*). The balance arm can be supported by the arrangement shown at *R*. The torsion of the wire is determined optically: the filament of an incandescent lamp (*S*) is focused by the lens (*T*) and reflected in the mirror (*D*) to the slit of a revolving cylinder camera (*U*) which has a horizontal axis. The camera rotation is synchronized with that of the toothed wheel (*G*) by a transmission from a wheel on the screw (*K*) to the camera wheel. *V* is a holder for the light tracing paper, which is put into the camera.

On starting a measurement the two fibers are fixed in the clamps with suitable stretching, which can be obtained by applying a stretching load during the fastening. The balance is adjusted to horizontal equilibrium by means of the screw *F*. After adjusting the lower fiber holder to the correct distance from the center and at the desired angle to the upper fiber, the same holder is raised to bring the fibers into contact. The balance is supported while the load is placed on the pan, and then released. Water pressure is applied to the piston and the speed is adjusted. The upper fiber will follow the lower fiber in its horizontal movement until the torsional moment of the piano wire is great enough to counterbalance the frictional force between the fibers. The frictional force at this point is F_s, the static frictional force. When the movement of the lower fiber passes this point, slipping occurs. During the slipping motion, the dynamic frictional force, F_d, will counteract the slippage and brake the motion until it stops. When the upper fiber has come to rest on the lower fiber, the same movement will start again. The force F_d is always smaller than F_s. Thus the

tracing on the photographic paper will show a slow increase of the torsional angle up to the point of slippage, and a rapid decrease back to the braking point—that is, a saw-tooth curve.

Occasional vibrations in the apparatus must be avoided since they can cause the fiber slippage to start before the maximum frictional force has been attained. The use of hydraulic power instead of electric power is very essential because an electric motor always causes vibrations. The stand is placed on a heavy metal plate which rests on a thick fiber plate on a steady table. The room is located on the ground floor of the building, which is founded on bedrock, and no disturbances have been observed. Banging of doors in the immediate vicinity and other shocks must, of course, be avoided.

There is a slight friction in the balance bearings and therefore a small load (about 3 mg.) is necessary to start a motion of the balance in the vertical direction. This fact makes it necessary to apply a correction of 3 mg. of the load to get the value of the normal pressure (N) between the fibers. The figures given later in this paper are all corrected in this way.

The total length of the cylinder with the hydraulic piston, which drives the apparatus, corresponds to a movement of about 3 mm. of the lower fiber. This causes a small change in the angle between the fibers, which means a change of the moment of the frictional force, corresponding to about 0.5 mgf.* in the frictional force. The measured forces are always taken as averages over the whole movement, and therefore this variation is of practically no importance.

The load must be kept so low that no noticeable extension of the fibers occurs, since this causes a bending of the fibers at the point of contact. A suitable range of load is 20–100 mg.

The angle between the fibers can be varied down to a value of about 10°, but not less. A variation of the angle does not cause any measurable change of the friction for even fibers. The frictional coefficient for two nylon fibers was 0.42 for an angle of 10°, 0.40 for one of 45°, and 0.42 for one of 90°. The last figure is probably a little too high, because there might have been an elastic tension and a vibration, just as the bow acts on a string on a violin. The measurements reported here were performed at an angle of 20°.

* Milligrams force.

Theory

Symbols used:

N = load = normal pressure between the fibers

F = frictional force

μ = frictional coefficient = $\dfrac{F}{N}$

θ = torsional angle of the piano wire

I = moment of inertia of the torsional system (balance)

D = moment of torsion of the torsional system

T = time of a free oscillation of the torsional system

$\omega = \sqrt{\dfrac{D}{I}}$

r = distance from center of rotation (the piano wire) to the point of friction (moment arm of the frictional force)

A = distance from mirror to camera in cm.

$n - n_0$ = deflection in cm. of the light beam on the camera scale.

k_A = sensitivity of the apparatus = frictional force (in mgf.) necessary for a deflection $n - n_0$ of 1 cm. at the distance A

The general moment equation for the torsional movement when the frictional force acts against the torsional force is

$$I\frac{d^2\theta}{dt^2} = -D\theta + Fr. \tag{1}$$

No damping elements are taken into consideration, because their influence is very small.

A. Static Friction

When the torsional system turns synchronously to the lower fiber, which moves with a constant velocity, we have

$$\frac{d^2\theta}{dt^2} = 0, \quad \text{which gives} \quad F = \frac{D\theta}{r}, \tag{2a}$$

and, in the moment of slippage,

$$F_s = \frac{D\theta_s}{r}. \tag{2b}$$

From the definition of k_A we have

$$F_s = k_A(n_s - n_0). \tag{3}$$

$n_s - n_0$ is measured, and k_A can be determined (see "Experimental Data," below).

The deflection is also given by the equation

$$2\theta_s A = n_s - n_0. \tag{4}$$

From equations (2b), (3), and (4) we obtain

$$D = 2Ark_A. \tag{5}$$

D is thus easily determined from known quantities. On the other hand, D can be calculated from the dimensions of the wire:

$$D = \frac{2\pi p a^4}{l}, \tag{6}$$

where p is the torsional modulus, a the radius, and l the length of the wire.

It should be mentioned that T can be determined rather accurately by oscillation experiments, and I can be calculated from the equation

$$T = 2\pi\sqrt{\frac{I}{D}}. \tag{7}$$

B. Dynamic Friction

If the dynamic frictional force were equal to the static, there would be no slippage back from the point of maximum torsional angle, but the torsional balance would stay constant at this deflection during the continued motion of the lower fiber. This, however, never occurs experimentally. A very pronounced and rapid back slippage appears, also for the most even fibers, as described earlier. This means that the dynamic frictional forces are smaller than the static; however, they are not zero. If they were zero, the balance would swing back to a deflection θ_s on the other side of its position of equilibrium; since they are not, the slippage always stops at an earlier stage. The point where the movement stops is called the brake point (indicated by subscript "b").

We suppose the dynamic frictional force to be constant, independent of the relative velocity of the fibers:

$$F = F_d = \text{constant } (0 < F_d < F_s). \tag{8}$$

The general equation (1) then takes the form

$$I\frac{d^2\theta}{dt^2} = -D\theta + F_d r, \tag{9}$$

and its general solution is

$$\theta = \frac{r}{D}F_d + c\sin(\omega t + \delta). \tag{10}$$

The arbitrary constants c and δ are determined from the values for the point of maximum deflection, where the slippage starts. At this point we have

$$\theta = \theta_s; \quad t = 0; \quad \text{and} \quad \frac{d\theta}{dt} = 0, \tag{11}$$

which gives

$$\delta = \frac{\pi}{2} \quad \text{and} \quad c = \theta_s - \frac{r}{D}F_d. \tag{12}$$

From equations (12) and (10) we then get

$$\theta = \frac{r}{D}F_d + \left(\theta_s - \frac{r}{D}F_d\right)\cos\omega t. \tag{13}$$

For the brake point we have

$$\theta = \theta_b; \quad \frac{d\theta}{dt} = 0, \tag{14}$$

which gives $\sin\omega t = 0$ and $\cos\omega t = -1$, and

$$\theta_b = \frac{r}{D}F_d - \left(\theta_s - \frac{r}{D}F_d\right)$$

or

$$F_d = \frac{D}{r}\frac{\theta_s + \theta_b}{2} = \frac{D}{r}\theta_d \tag{15}$$

if

$$\theta_d = \frac{\theta_s + \theta_b}{2}. \tag{16}$$

Thus F_d can be calculated from the arithmetical mean of θ_s and θ_b in the same way as F_s is calculated from θ_s (equation (2b)).

Experimental Data

A. Apparatus Constants

The sensitivity k_A is determined by means of balancing the torsional moment of the wire by a steel plate spring which is fixed vertically with its upper end in a special holder. The lower end of the spring has a hook that is connected to the balance of the apparatus by a horizontal string (a straight and flexible fiber). On stretching of the string perpendicularly to the balance arm the holder of the spring is adjusted, so that the spring and balance are in their equilibrium positions. A force P applied in the direction of the string gives a deflec-

TABLE I. COMPARISON OF BALANCE DEFLECTION AND SPRING DEFLECTION

$n-n_0$	Spring deflection
0.92	0.31
1.52	0.48
2.58	0.87
3.60	1.22
4.15	1.39
4.95	1.67
5.95	2.00
6.85	2.30
7.88	2.63
8.90	2.95
9.90	3.26
10.90	3.59

TABLE II. CALIBRATION OF THE SPRING WITH DIFFERENT LOADS

Load (mgf.)	Spring deflection
0.0	0.00
4.0	0.30
6.5	0.33
9.0	0.53
11.4	0.61
13.6	0.71
17.5	0.94
21.2	1.12
25.1	1.32
27.8	1.49

tion α of the spring; the equation $P = \text{const.} \times \text{tg}\ \alpha$ is valid. P is proportional to the deflection of the light beam on the camera scale, and tg α is determined by readings of the spring deflection on a millimeter scale placed behind the spring. The spring is calibrated by turning it to a horizontal position and applying loads at its free end. Tables I and II show the results obtained.

From these values, which show the validity of the equation applied, we get $k_A = 6.26$ mgf. for $A = 76.7$ cm., and $k_{100} = \dfrac{k_A A}{100} = 4.8$ mgf. It was found that a considerable change in the tension of the piano wire had no influence on the value of k_A.

The value of r is 2.0 cm. From equation (5) we get $D = 1{,}920$ mgf. $\times$ cm. $= 1{,}890$ erg. For the piano wire, $p = 8.2 \times 10^{11}$ dynes/cm^2 (from tables), $a = 0.0125$ cm., and $l = 65.6$ cm., which gives $D = 1{,}920$ erg from equation (6) in good agreement. The time of oscillation, T, was determined to be 0.328 sec., and from equation (7), $I = 5.15$ g. $\times$ cm^2.

TABLE III. FRICTION BETWEEN TWO WOOL FIBERS

μ_s = static frictional coefficient; σ = the standard deviation of μ_s. Load = 47 mg.

	Fibers untreated		Fibers halogenated
	μ_s	σ	μ_s
Fibers placed in opposite directions			
Movement against scales	0.73	0.25	0.41
Movement with scales	0.15	0.04	0.27
Fibers placed in the same direction			
Movement against scales for the lower fiber	0.26	0.07	0.32
Movement with scales for the lower fiber	0.24	0.05	0.31

B. Measurements on Wool

Some experiments on the friction of wool fibers have been performed. The wool used was a sample of 58s South American Crossbred. For each experiment two fibers of about the same thickness and observable scaliness were chosen.

Figure 3 and Table III show some of the registration curves and figures obtained.

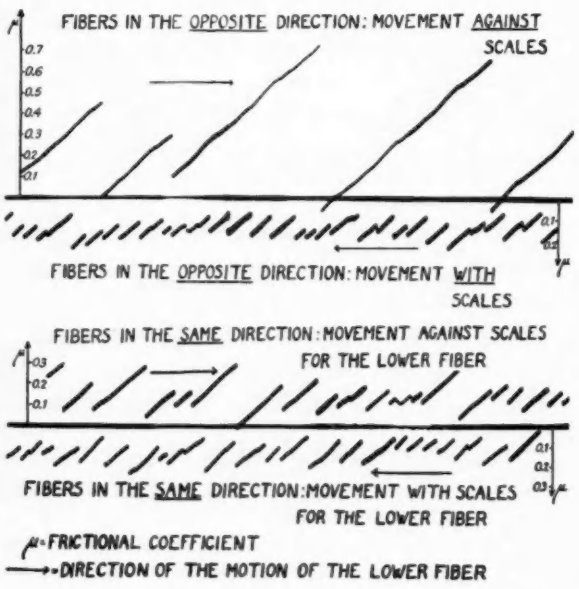
FIBERS IN THE OPPOSITE DIRECTION: MOVEMENT AGAINST SCALES
FIBERS IN THE OPPOSITE DIRECTION: MOVEMENT WITH SCALES
FIBERS IN THE SAME DIRECTION: MOVEMENT AGAINST SCALES FOR THE LOWER FIBER
FIBERS IN THE SAME DIRECTION: MOVEMENT WITH SCALES FOR THE LOWER FIBER
μ-FRICTIONAL COEFFICIENT
DIRECTION OF THE MOTION OF THE LOWER FIBER

FIG. 3. *Photograms of the movement between two wool fibers in the friction meter.*

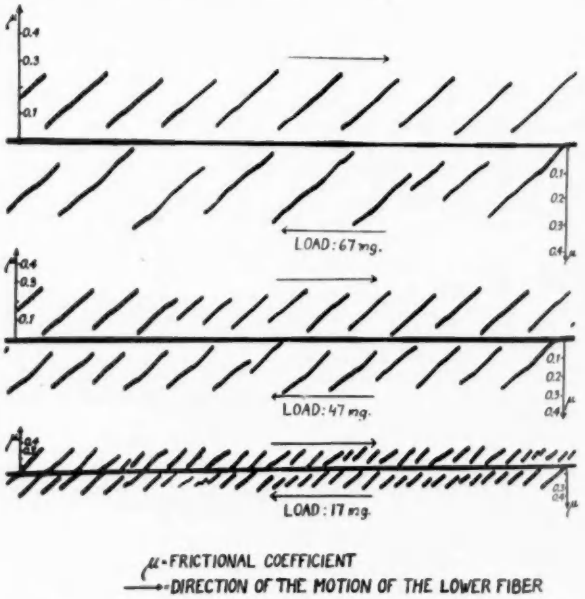

FIG. 4. *Photograms of the movement between two viscose rayon fibers in the friction meter.*

TABLE IV. FRICTION BETWEEN TWO VISCOSE RAYON FIBERS

μ = frictional coefficient; σ = standard deviation of μ; ϵ = the probable statistical error of $\mu = \pm \frac{\sigma}{\sqrt{m}}$; m = number of measurements.

Static friction

N	μ_s	σ	ϵ	m
17	0.302	0.035	±0.004	82
47	0.282	0.018	±0.002	62
67	0.276	0.018	±0.002	67
97	0.271	0.019	±0.002	75

Dynamic friction

N	μ_d	σ	ϵ	m
17	0.180	0.026	±0.003	82
47	0.156	0.011	±0.002	62
67	0.144	0.010	±0.001	67
97	0.140	0.006	±0.001	75

If the fibers are placed in opposite directions and the lower one is moved in the tip direction, the tips of the fiber scales will hook onto each other, and the frictional forces will be very high. Static frictional coefficients about unity are found. There is a great dispersion of the values due to the unevenness of the scales and variations in the distances between them. If the lower fiber is moved in the root direction, no hooking can occur and we obtain the real friction between the surfaces of the scales, which is very much smaller. If the fibers are put in the same direction, the direction of movement is of no importance, and the friction is only a little greater than in the second case.

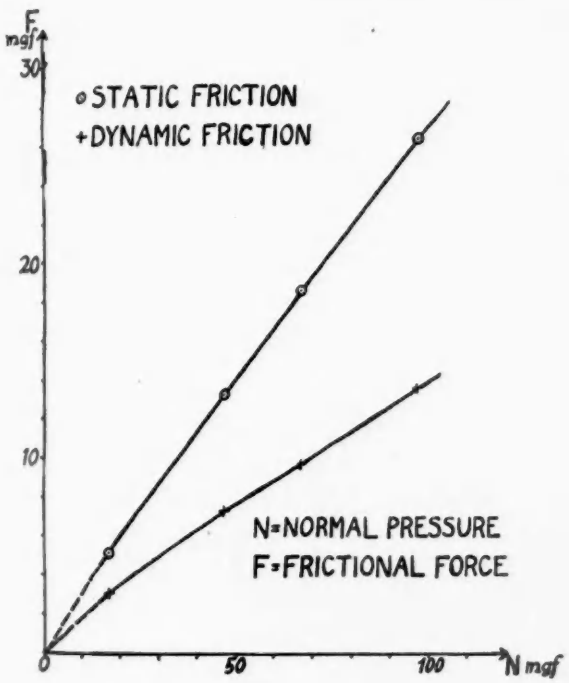

FIG. 5. *The relationship between frictional force and normal pressure for viscose rayon fibers.*

A strong halogenation of the fibers (by treatment with a saturated solution of bromine in distilled water at room temperature for 15 minutes) does diminish the anti-scale friction and increase the with-scale friction, but there is still a pronounced difference. It is obvious that the decrease of the felting properties on halogenation cannot be explained only by friction measurements in the dry state. The friction must be measured in the liquid used for milling, if any significant relationship is to be found. It is possible to place a bowl around the fiber holders in the apparatus for measurements in liquids. Such an arrangement requires special consideration of buoyancy and probably surface tension. We have not made any such measurements so far.

C. Measurements on Smooth Fibers

In order to study the mechanism of friction between fibers without any disturbances such as those caused by the scales of the wool, we have made some measurements on smooth synthetic fibers, such as nylon, acetate, and viscose rayon. A glossy viscose rayon from I.G. (Agfa Kunstseide Nm. 60/30) was found to be very smooth and especially suitable for these studies. The dispersion (standard deviation) of the dynamic frictional coefficients is considerably lower than that of the static ones.

Figure 4 shows some photograms for these fibers at different loads and Table IV gives the values of the frictional coefficients.

Dependence of the Frictional Forces on the Area of Contact

Figure 5 shows the dependence of the frictional force of the same viscose fiber on pressure. As a first approximation we have $\mu = \frac{F}{N}$ = constant for both static and dynamic friction. However, there is a small increase of μ with decreasing N. This can be interpreted by assuming that small adhesion forces act between the fibers and give $F > 0$ even

for $N = 0$. If this adhesion force is considered to be proportional to the area of contact, then

$$F = \mu_0 N + \alpha S, \tag{17}$$

where μ_0 = the real frictional coefficient, independent of N; S = the area of contact; and α is a measure of the force of adhesion per unit area between the fibers. This equation has already been given by Morrow [6] to explain some of his results. Equation (17) can also be written

$$\mu = \frac{F}{N} = \mu_0 + \alpha \frac{S}{N}. \tag{18}$$

In Figure 6 μ is plotted against $\frac{1}{N}$, which gives an almost straight line. Its intersection with the μ-axis gives μ_0 and its slope gives αS. The curvature might be interpreted as a small change in S, because

$$\frac{d\mu}{d\left(\frac{1}{N}\right)} = \alpha S. \tag{19}$$

The area of contact, S, is very small in the case of two fibers. The influence of the second term in equation (18) would be greater for greater values of $\frac{S}{N}$. In order to give an idea of the dependence on the area S, two polished plates of perspex* were fixed at the positions of the two fibers in the apparatus. The upper plate had an area of 1×2 cm^2 and the lower 2×5 cm^2. The upper one was always kept within the borders of the lower one. With a load of 20–50 mg. we obtained frictional coefficients of approximately 0.6, which is a very high value. But with an inclined-plane experiment the frictional coefficient at a load of 20 g. was determined to be 0.3. A decrease of the area gave a small decrease of the frictional coefficient, but experimental difficulties made it impossible to obtain any quantitative measurements. The fact that the real area of contact cannot be directly determined from the geometrical area must be taken into consideration. If the real area of contact were the same as the geometrical area in the measurements on the perspex plates, the experimental values obtained would give $\alpha \sim 7.5$ mgf./cm^2 ($\mu_0 \sim 0.3$). We did not try to measure the frictional forces between polished metallic plates, although these can be made smoother than perspex plates. The adhesion forces between metallic plates are certainly different in nature from those between plates of a high polymer (perspex), which is chemically more like the fibers.

* Polymerized methyl methacrylate.

Influence of the Relative Velocity on the Dynamic Friction

We have supposed that the dynamic frictional force F_d is independent of the relative velocity of the fibers. This assumption can be made probable by a simple calculation.

Equation (13) gives the angular velocity of the slippage:

$$\frac{d\theta}{dt} = -\omega(\theta_s - \theta_d) \sin \omega t, \tag{20}$$

where θ_d is given by equation (15).

The average velocity between the points of slippage and brake is given by (compare with equations (11) and (14)):

$$\left|\frac{d\theta}{dt}\right|_{av.} = \frac{\int \left|\frac{d\theta}{dt}\right| dt}{\int dt} = \frac{\left|\int_0^{\frac{\pi}{\omega}} \omega(\theta_s - \theta_d) \sin \omega t dt\right|}{\int_0^{\frac{\pi}{\omega}} dt}$$

$$= \frac{2\omega}{\pi}(\theta_s - \theta_d). \tag{21}$$

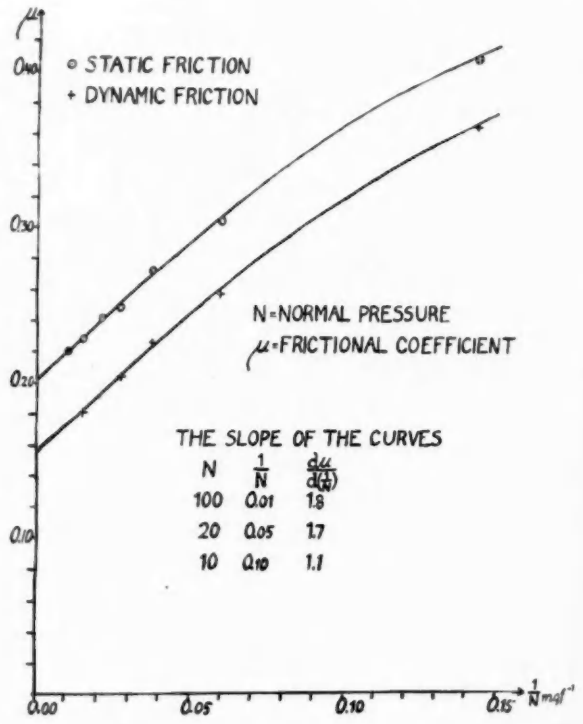

FIG. 6. *The dependence of the frictional coefficients on the normal pressure for viscose rayon fibers.*

Substituting θ_s and θ_d according to equations (2b) and (15) gives

$$\left|\frac{d\theta}{dt}\right|_{av.} = \frac{2\omega r}{\pi D}(F_s - F_d). \qquad (22)$$

We have further

$$F_s - F_d = N(\mu_s - \mu_d). \qquad (23)$$

Figure 6 shows the dependence of both μ_s and μ_d on N, or, rather, $\frac{1}{N}$, for the viscose fibers investigated. It is seen that $\mu_s - \mu_d$ is almost constant, or $\frac{d\mu_s}{d\left(\frac{1}{N}\right)} = \frac{d\mu_d}{d\left(\frac{1}{N}\right)}$, and thus $\left(\frac{d\theta}{dt}\right)_{av.}$ is proportional to N, according to equations (22) and (23). From the values obtained, $\mu_s - \mu_d$ is found to be 0.047 ± 0.003, when N varies between 7 and 67 mg. As the variation of μ_d is the same as the variation of μ_s with N, it is very probable that μ_d is independent of $\frac{d\theta}{dt}$; a dependence on $\frac{d\theta}{dt}$ would very likely give $\frac{d\mu_s}{d\left(\frac{1}{N}\right)} \gtrless \frac{d\mu_d}{d\left(\frac{1}{N}\right)}$ for a certain value of N from the curves obtained in Figure 6. A calculation according to equation (22) gives values of $\left|\frac{d\theta}{dt}\right|_{av.}$ from 0.04 to 0.40 sec^{-1}, which corresponds to velocities of 0.08–0.80 cm./sec. The maximum velocity is $\pi/2$ times the average velocity, and thus the frictional coefficient is probably constant for velocities up to 1.5 cm./sec.

Uses of the Apparatus

It is our intention to extend our measurements of the scaliness of wool and also to make them in suitable liquids in order to study the relationship of scaliness to milling properties. This problem was studied earlier, but it is our hope that the measurement of friction between single fibers, which was not used earlier, would give more information about the movement of the fibers in a fabric during the milling process. It is necessary to measure a relatively large number of fibers, and also to consider the dispersion of the values obtained. The dispersion gives a measure of the unevenness of the fiber surface, which is obvious especially in the anti-scale movement.

The apparatus is suitable also for studies of the friction forces acting in the drawing of fibers in the process of spinning. It will be possible to study the effect of different auxiliaries for decreasing or increasing the friction between fibers, such as spinning oils, matting agents, finishing agents for rayon staple, and so on. Following are some figures on the friction between viscose fibers treated with the silica dispersion substance "Syton," which is recommended as a friction-increasing agent:

% Syton	μ_s
0	0.22
25	0.33
50	0.36

In the drawing of the fiber bundle before spinning, it is probably essential that there should be a minimum of frictional forces when the fibers move in the drawing frame or in the drawing system on a spinning frame. This should facilitate the movement of the fibers and improve the evenness of the bundle and thus of the yarn. This means that the dynamic frictional coefficient should be low. On the other hand, the cohesion of the fiber bundle should be high, which means that the forces necessary for starting a movement of any fiber should be high—that is, the static frictional coefficient should be high. However, too great a disparity between static and dynamic friction would probably result in uneven drafting, with a tendency to concentrate the draft in the parts which have started to move, and leave other parts thick. We plan to investigate these problems.

Summary

1. An apparatus for measurement of the frictional forces between two single fibers has been designed and constructed.

2. It is shown that it is possible to measure both static and dynamic friction with the apparatus described and the theory for these measurements is developed.

3. Some measurements on wool and artificial fibers are reported. The anti-scale frictional coefficient of wool has values up to unity but with a great dispersion, whereas the with-scale frictional coefficient is much lower and has a small dispersion. Treatment with bromine water decreases the difference considerably.

4. It is shown that the frictional coefficient is approximately linearly dependent on the inverse value of the normal pressure (load) between the fibers. The slope of the line is assumed to be due

to adhesion forces which are proportional to the area of contact.

5. The dynamic frictional coefficient is independent of the velocity of the fibers, at least for velocities up to 1.5 cm./sec.

6. The intended uses of the apparatus are discussed. It can be used for studying the influence of wool scaliness on milling properties and the importance and influence of static and dynamic frictional forces between fibers in the drawing of fibers for spinning.

Acknowledgment

The authors wish to thank Mr. L. Mattsson of the Laboratory Machine Shop for building the apparatus and for helpful suggestions in its construction.

Mr. J. Lindberg of this laboratory drew our attention to the application of equation (17), and we are indebted to him for valuable discussions.

Literature Cited

1. Bohm, L., *J. Soc. Dyers and Colourists* **61**, 278 (1945).
2. Bowden, F. P., and Leben, L., *Proc. Roy. Soc.* **169A**, 371 (1938–9).
3. Lipson, M., and Howard, P., *J. Soc. Dyers and Colourists* **62**, 29 (1946).
4. Martin, A. J. P., and Mittelman, R., *J. Text. Inst.* **37**, T269 (1946).
5. Mercer, E. H., *Nature* **155**, 573 (1945).
6. Morrow, J. A., *J. Text. Inst.* **22**, T425 (1931).
7. Speakman, J. B., Chamberlain, N. H., and Menkart, J., *J. Text. Inst.* **36**, T91 (1945).
8. Speakman, J. B., and Stott, E., *J. Text. Inst.* 22, T339 (1931).

A Dynamic Absorption Method for Determining Water-Repellency*

J. E. Simpson† and Ruth M. Howorth‡

I. Introduction

The merits of water-repellent clothing to prevent passage of water during limited rainfalls and to afford greater body comfort by permitting evaporation of perspiration through the fabric were indicated in the civilian rainwear items during the late 1930's. The possible military value of water-repellent clothing was recognized before this country was drawn into World War II. However, the performance requirements for military usage far exceeded those for civilian garments, and the need for additional improvement was obvious.

It is emphasized that keeping a soldier dry is the summation of a great many factors. The principal points concerned, in addition to the individual physiology and weather conditions, are (*a*) finish, (*b*) fabric construction, and (*c*) garment design. The huge program that the Quartermaster Corps undertook in order to give the Allied soldiers the best water-repellent clothing, based upon these factors, has been presented in a previous paper [6]. That paper has emphasized the great need which existed at the beginning of this development period for adequate methods of measuring pertinent characteristics of water-resistance of fabrics and garments.

In a broader sense, there are two general classes of water-resistance test methods. A review of the most commonly known ones follows.

1. *Methods which evaluate both the finish and the fabric construction (such as hydrostatic pressure, water-permeability, drop penetration, and air-permeability).*

The Bundesmann Tester [2], employing falling drops impinging on the fabric specimen, was one of the earliest recognized methods. It still finds considerable favor on the Continent although its design is very intricate and the results can be replicated only in the hands of the most skilled technologists. In this country, the du Pont Rain Tester developed by Slowinske [7] which makes use of small water streams of different pressures has had wide application. At the request of the Quartermaster Corps, the Textile Foundation in 1943 initiated the development of a drop-penetration device which makes more practical application of the Bundesmann principle. This work was continued by the Milton Harris Associates, and the resulting method [8] has been adopted as one of the means of evaluating Army fabric constructions and finishes [6]. The Research and Development Division, Philadelphia Quartermaster Depot, in 1944 developed devices for producing artificial rainfall which closely simulates natural rainfall of chosen intensities between 0.1 and 3.0 inches per hour [4]. This has been of inestimable value in measuring water penetration of fabric swatches and for testing garments under realistic conditions. Air-permeability measurements [3] give valuable information concerning the porosity of fabrics. This method may be used to show the extent to which a finish may have "plugged" the interstices, thus decreasing its ability to transmit water vapor.

2. *Methods which principally evaluate the finish or hydrophobic state of the filaments and yarns (surface tension, absorption, and contact angles).*

The surface-spray test developed by the American Association of Textile Colorists and Chemists has been used for a number of years as a rapid qualitative means of controlling mill application of repellents [3]. Attempts to consider these as quantitative

---

* This article is one of a series of technical papers dealing with the principal phases of the research, development, and production problems on the Army's water-repellent clothing. These publications have appeared, or will appear, in various scientific journals interested in particular phases of the program.

† Surface-active materials technologist, Research and Development Branch, Military Planning Division, Office of The Quartermaster General. Present position: Director, Chemical Development Division, Orr and Sembower, Inc., Reading, Pennsylvania.

‡ Research technologist at National Association of Dyers and Cleaners on Quartermaster problems. Present position: Research Technologist at The Harris Research Laboratories, Washington, D. C.

measurements have been oftentimes severely criticized. The shortness of time (25 to 30 seconds) and the static condition of holding the fabric while making the test put a definite limitation on its value. One of the oldest methods for measuring wetting phenomena is the Draves test applicable to yarns [3]. Another test which has enjoyed long usage is the static immersion water-absorption test [3]. Bartell and coworkers have derived an empirical formula claimed to be a means of quantitatively evaluating the degree of repellency of a treated fabric [1]. This method relies principally upon determination of the advancing and receding contact angles in a water drop rolling over a static surface. Wakeham and Skau [9] have developed a method for measuring the contact angle on a fabric surface when it is statically suspended in water.

II. Need for a More Realistic Water-Repellency Test

It is noteworthy that all of the above methods determine repellency of the treated fabric in an immobile position, a situation which does not simulate what occurs to a garment that is actually worn in the rain. Not only has the improvement of finishes been severely handicapped by the limitations of existing methods, but the inability to distinguish between the role played by the finish and that played by the fabric construction under dynamic usage conditions has made extremely difficult the development of appropriate fabrics for all-weather outer garments. Maximum advantage could not be taken of yarn-swelling to close interstices,* although research in this country [5] had further demonstrated that optimum water-resistance of a fabric is governed by the combination of the degree of hydrophobicity of the yarns plus the rate of change in original dimensions of the yarns caused by wetting [5, 6]. Although it is possible, for many kinds of fibers thus to close eventually the interstices to the extent that no water will pass through the fabric, there is a definite time lag from the initial exposure to water before sufficient swelling occurs. It has been shown, in addition, that maximum resistance is attained by applying sufficient water-repellent finish so that the force of the falling water droplets will not drive them through the interstices. As the fibers gradually become wet, there is enough fiber distortion to keep the pore size less than the critical penetration value, thus offsetting the lowered hydrophobicity [5]. The important point, of course, is to know accurately the degree of hydrophobicity required to accomplish the purpose. Measurements of the amounts of hydrophobic materials applied can be obtained best under dynamic conditions of exposure to water and under conditions which would be independent of the fabric construction.

Nearly all of the water-repellents utilized in textile mills are applied in the form of emulsions. Even at best, under these conditions it is extremely doubtful that the repellent finish can be uniformly applied throughout a fabric. The usual tendency is for the repellent material to be deposited on the outer fabric surfaces. Static conditions of testing this "shingle" covering of repellent may indicate such a finish to have ample durability to wear factors and to offer good resistance to wetting such as when the garment is worn in the rain. However, ample evidence has been obtained to show that these poorly adhering outer coverings of repellents will be shifted or ruptured during wear, and the finish will offer little repellency to water [6]. On the other hand, dynamic conditions of testing (such as those involving mechanical action) would also overcome the repellent films and thus indicate the temporary value of such a finish.

Another question which static methods largely leave unanswered is whether the poor protective value of a given treated fabric is due largely to the low innate hydrophobic value of the finish or to the fabric construction characteristics. Much laborious trial-and-error testing could be eliminated if the finish could be quickly and accurately evaluated with respect to its real ability to retard absorption of water. A dynamic method would appear advantageous for this purpose.

In the case of thick fabrics it has been found that static repellency tests give erroneous indications of the total water absorbed by a garment worn in the rain. The same criticism can be made of static methods when they are used to evaluate relatively impervious materials such as webbing and plastic-coated items.

It became apparent from these considerations that a method was needed which would measure the percentage of water absorbed per unit time—that is, the rate of absorption, while the item was flexed and

* A development originated by the Shirley Institute of England over a period of several years.

rubbed in a manner simulating conditions to be expected when a garment is in use.

III. Development of a Dynamic Water-Absorption Method

A number of ideas were exploited in an effort to establish a dynamic water-absorption method which would meet the needs outlined above. Devices which were considered in the study included (*a*) a large beaker equipped with stirrer, (*b*) water and fabric suitably contained in a sealed jar which was subjected to the action of a vertical sample shaker, (*c*) launder-o-meter with various means of increasing action within the jars, and (*d*) a 19-by-24-inch horizontal power-laundry machine. All of these methods were abandoned for various reasons such as insufficient mechanical action, action localized in spots on the fabric specimens, results not reproducible, method too slow and cumbersome, or action which obviously did not simulate the flexing and rubbing sustained by a garment while being worn. From these studies it appeared desirable to use an end-over-end rotary device, as its effect could be replicated. It was believed that if a large enough container were employed the fabric pieces of a reasonable size could "float" more freely in the medium and not suffer the limited, localized actions such as oftentimes occur in the launder-o-meter. It was believed that the number and size of test specimens, the container size, and the quantity of water should be selected to afford substantial pounding, flexibility, and sliding actions. The simplest, and at the same time the most realistic, means of simulating the frictional and mechanical action that garments undergo while being worn seemed to be that produced when one fabric specimen rubs against another similar fabric specimen.

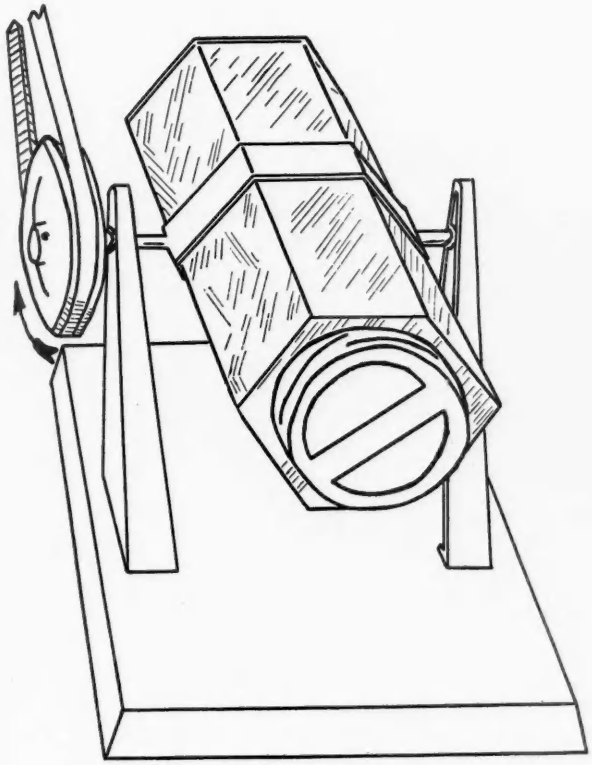

FIG. 1. *Dynamic water-absorption tumbler jar.*

The method evolved from these ideas has been adopted as one means of evaluating water-resistant finishes. It is now a part of the *Supplement* (dated October 8, 1945) to Federal Specification CCC-T-191a [3]. For clarity of this presentation, the method is outlined below.

Dynamic Water-Absorption Method

(*a*) *Tumbler Jar.* The apparatus consists of a 6-liter, hexagonal-sided glass tumbler jar with dimensions approximately 6¾ inches in diameter by 12 inches in height (see Figure 1). It is rotated at a constant speed of 55 revolutions per minute by means of an electric motor connected through suitable reducing gears. The inner surface of the wide-mouthed lid (screw-type) is covered with a rubber gasket. The jar must be free of all extraneous matter (particularly wetting agents, detergents, soaps, etc.).

(*b*) *Wringer.* The wringer is a household laundry wringer equipped with soft rubber squeeze rolls of 2⅛ to 2¼ inches in diameter and hardness of from 70 to 80 (A scale) durometer units. It is so constructed that the pressure on the top roller is maintained by a dead weight, rather than by the customary spring tension, sufficient to exert 5 pounds per linear inch of the roller. The wringer is power-driven at a constant rate so that the sample passes through the rolls at the rate of 1 inch per second.

(*c*) *Blotting Paper.* The blotters used in this test are 10-by-10-inch squares conforming to the following requirements:

(1) They shall have an absorbency of 1 milliliter of distilled water in 8 to 14 seconds when tested in accordance with Section IV, par. 13, of Federal Specification UU-P-31, *Paper, General Specifications,* except that distilled

TABLE I

Sample No.	Laboratory	Fabric*	Dynamic absorption values (%) 10 min.	20 min.	30 min.	60 min.
1a	Harris Research Labs.	Type IV Oxford (9-oz.)	14.4	17.6	21.6	27.2
1b	Philadelphia QM Depot	Type IV Oxford (9-oz.)	16.7	18.0	21.2	25.9
2a	Harris Research Labs.	Type IV Oxford (9-oz.)	15.9	20.7	24.0	28.4
2b	Philadelphia QM Depot	Type IV Oxford (9-oz.)	15.9	22.2	24.9	29.2
3a	Harris Research Labs.	Type I Oxford (6.5-oz.)	15.9	19.6	21.3	24.2
3b	Philadelphia QM Depot	Type I Oxford (6.5-oz.)	16.3	18.8	20.1	25.3
4a	Harris Research Labs.	Type I Oxford (6.5-oz.)	16.0	19.4	20.4	23.2
4b	Philadelphia QM Depot	Type I Oxford (6.5-oz.)	16.4	18.3	19.2	21.7
5a	Harris Research Labs.	Type II poplin (5-oz.)	16.6	20.0	21.7	23.4
5b	Philadelphia QM Depot	Type II poplin (5-oz.)	18.4	20.8	21.9	23.9
6a	Harris Research Labs.	Type II poplin (5-oz.)	21.0	22.1	24.7	24.5
6b	Philadelphia QM Depot	Type II poplin (5-oz.)	21.2	21.6	22.1	23.7
7a	Harris Research Labs.	9-oz. sateen	19.4	24.8	28.2	33.7
7b	Philadelphia QM Depot	9-oz. sateen	19.5	25.9	29.1	33.2
8a	Harris Research Labs.	9-oz. sateen	17.2	20.6	22.7	27.1
8b	Philadelphia QM Depot	9-oz. sateen	17.8	20.7	23.7	27.6

* All fabrics treated with the same kind of durable repellent finish. The degree of hydrophobicity achieved, however, is the sum of a number of factors. As an example, Sample 7, taken from beginning of the mill run, clearly indicates that optimum application conditions were not being achieved. Adjustments made during the run improved this, as evidenced by Sample 8, taken later.

water at 70° (± 1°) F shall be substituted in place of standard writing ink, and the blotters, before testing, shall have been exposed for 12 hours to standard atmospheric conditions of 65 percent (± 2 percent) relative humidity at 70° (+ 10°) F.

(2) The thickness of the blotting paper shall be between 0.026 and 0.029 inch (see Section IV, par. 11, Federal Specification UU-P-31); the bursting strength shall be between 38 to 47 points (see Section IV, par. 9, of same specification); the weight of 500 sheets (24-by-38 inches) shall be 240 pounds (par. 7 of same specification).

(*d*) *Test Procedure.* A fabric sample to be evaluated for dynamic water-absorbency is cut into 8-by-8-inch squares, cut on a 45° bias with the direction of the warp (to minimize fraying). After "randomizing" of the squares, two sets of 5 specimens each are brought to moisture equilibrium with standard atmospheric conditions of 65 percent (± 2 percent) relative humidity at 70° (± 10°) F. The 5 specimens of a set are rolled together and quickly weighed to ± 0.1 gram. Each set is thus weighed; then the specimens are placed in the tumbler jar one at a time; 2 liters of freshly distilled water at 80° (± 1°) F are added to the jar; the jar is then closed and rotated at 55 r.p.m. At the end of the designated time interval one specimen at a time is removed from the water, immediately put through the wringer once without blotters, and then put through once between unused blotters. The specimens are passed individually through the wringer at the rate of 1 inch per second, with the specimen edge parallel to the rolls of the wringer. Each specimen (which has been run through the wringer without and with blotters) is left between the blotters until the 5 specimens from one set have been through the wringer. At that time the 5 specimens are again rolled together quickly and weighed as before.* The same procedure is then repeated for the 5 specimens of the second set in the tumbler jar.

TABLE II

Fabric	Dynamic water absorption (%) 10 min.	20 min.	30 min.	60 min.
6.5-oz. Type I wind-resistant Oxford (Finish A)	14.1	16.0	17.3	21.2
9.0-oz. Wind-resistant sateen (Finish A)	13.6	17.2	18.8	21.7
6.5-oz. Type I wind-resistant Oxford (Finish B)	21.5	27.5	34.1	41.8
9.0-oz. Wind-resistant sateen (Finish B)	21.3	28.1	33.0	44.0

* NOTE: The specimens must be protected as much as possible from air drying during these operations.

TABLE III

Fabric and finish	Air-permeability ($cm^3/cm^2/sec.$)	Hydrostatic pressure (cm.)	Drop-penetration value* (min.)	Spray rating	Dynamic water absorption (%) 10 min.	20 min.	30 min.	60 min.
Finish X (durable)								
5-oz. poplin (initial)	3.4	42	8.2	100	15.9	17.9	19.0	21.1
5-oz. poplin (laundered)†	3.6	25	3.2	90	29.9	36.9	38.0	39.3
5-oz. poplin (dry-cleaned)‡	3.6	39	4.4	80	17.1	19.6	21.7	23.7
Finish Y (nondurable)								
5-oz. poplin (initial)	3.2	40	19.4	100	28.1	34.8	37.1	41.2
Finish Z (nondurable)								
5-oz. poplin (initial)	3.6	41	8.5	100	36.0	39.2	44.4	45.0

* Number of minutes required for 10 ml. water to penetrate the fabric.
† Method specified in *Supplement* to Federal Specification CCC-T-191a.
‡ *Idem.*

The tumbler jar is emptied and 2 liters of freshly distilled water at 80° (± 1°) F are added. The 10 specimens of the two sets are immediately returned to the jar and another cycle is made exactly like that just described. The number of cycles and length of time for the cycles may be adjusted to meet the requirements of the particular kind of sample under consideration. It has been noted that the shorter the first time interval of dynamic exposure, the greater is the experimental error for that specific value. However, it has been found that any exposure time beyond 10 minutes gives easily reproducible results.

For routine test purposes, a single time-interval cycle is usually sufficient. A total cycle of 20 minutes is quite suitable for this purpose.

The percentage of water absorbed for any given total exposure is calculated according to the equation:

$$\% \text{ water absorbed} = \frac{W_i}{W_o} \times 100,$$

in which W_i = increase in weight from the original weight of the set and W_o = original weight of the conditioned set.

IV. Applications of the Dynamic Water-Absorption Method

This procedure was developed primarily for evaluating water-repellent finishes applied to flat cotton fabrics such as the wind-resistant poplins, sateens, twills and Oxfords, and for other flat cotton fabrics such as herringbone twill. However, it will be shown later in this paper that it is applicable to other types of materials as well.

The techniques of the test are simple but must be rigidly followed in order to obtain accurate results. The precision is considered to be ± 1.0 percent. The reproducibility of results in two different laboratories is illustrated in Table I.

The method is independent of such fabric factors as variations in yarn count and imperfections in weaving. Valid comparisons of the same quality of finish may be made although it is applied to different flat cotton fabrics (Table I). Table II gives the dynamic water-absorption values for a good finish and a poor finish each applied to 6.5-ounce type I wind-resistant Oxford and 9-ounce wind-resistant sateen. Both tables illustrate how this method will give comparable values for the same quality finish even though it is applied to cotton fabrics of different constructions and weights. Conversely, the data show how the test will distinguish between finishes of different quality whether applied to the same or to different cotton fabrics.

Table III illustrates another advantage of the dynamic absorption method. All of the results obtained by the other test methods would indicate that during initial wear periods prior to any cleaning treatment finish Y would give the greatest resistance to wetting of the fabric. Finish X and finish Z appear to be identical. Actually, however, finishes Y and Z soon lose their high initial repellency when worn and flexed, particularly under wear conditions exerting wet mechanical action [6]. On the other hand, the dynamic absorption method offers a rapid

means of subjecting a treated fabric to wet mechanical action which somewhat simulates this sort of wear condition. Examination of the dynamic water-absorption rates for these three finishes illustrates this point. It must be remembered, however, that this procedure measures the hydrophobic state of the fabric and is not to be confused with the water-penetration qualities, which are the result of a number of factors, including the hydrophobic state.

The method is applicable also to more resilient fibers such as woolens. It is true that as the thickness increases for these resilient fabrics, the absolute absorbency increases. However, the method is still capable of evaluating the finishes as long as they are applied to the same type of wool fabric. The Harris Research Laboratories * have correlated this laboratory method with water absorption and water penetration obtained under the artificial rainfall conditions perfected by the Research and Development Division of the Philadelphia Quartermaster Depot.

This new method is particularly valuable in measuring the water-repellency of items having physical dimensions not suited to the commonly used tests. Ribbons, webbings, and shoelaces are good examples. From a military standpoint, for instance, it is important to prevent equipage from absorbing moisture and thus reduce the "pay load" a soldier can carry. Figure 2 shows the water-absorbency under dynamic conditions for 1-inch webbing which has had various treatments. These absorbency curves certainly give more valid predictions of the amount of moisture which might be absorbed under actual use conditions than the spray rating of 90 for the "untreated" and of 100 for the two "treated" samples.

V. Conclusions

These studies appear to justify the following conclusions:

1. The dynamic absorption method is believed to be the most precise one that has been developed to date for:

   (*a*) Determining the maximum hydrophobic level which any particular water-repellent is capable of producing on a fabric.

   (*b*) Determining the true degree of hydrophobicity of a fabric at any time (when new, after wear, after any cleaning operation, or after any other treatment).

   (*c*) Ascertaining the efficiency of application of a repellent finish (application factors may include uniformity of penetration, distribution of a finish through the fabric, proper curing, etc.).

   (*d*) Quickly indicating the protective qualities of a finish during any given use period until the repellency may become changed by wear.

2. Although the method may be used for evaluating finishes applied to resilient fabrics, the present method of removing excess water by pressure puts limitations upon its usefulness for such fabrics.*

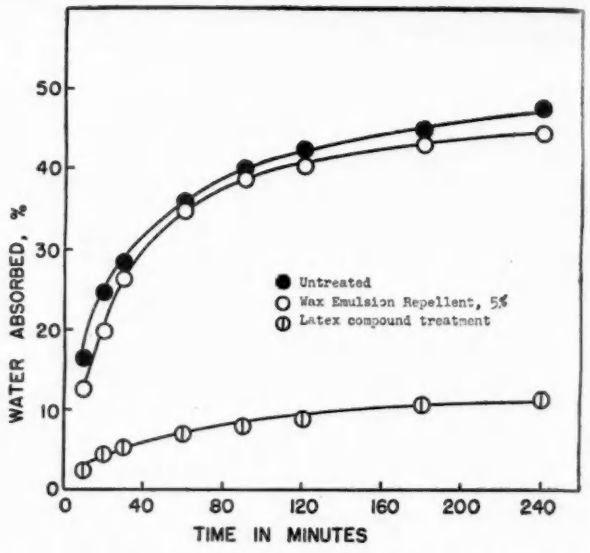

FIG. 2. *Dynamic water absorption of cotton webbing.*

VI. Acknowledgment

The suggestions made by research associates of The Harris Research Laboratories and of the Research and Development Division of the Philadelphia Quartermaster Depot have materially assisted in the development of the method described in this paper.

Literature Cited

1. Bartell, F. E., Private communications to the senior author, 1943 and 1944.
2. Bundesmann, H., *Melliand Textilber.* **16**, 128 (1935).
3. Federal Specification CCC–T–191a, Textiles: General Specifications, Test Methods ("Supplement" dated Oct. 8, 1945).

* These findings will be published in the near future.

* Some work has been done by The Harris Research Laboratories to improve this feature by substituting a definite free-drainage period in lieu of removing excess water by pressure.

4. Landsberg, M. I., and Moody, F. J., Devices for Producing Artificial Rainfall for Tests of Water-Repellent and Waterproof Materials, TEXTILE RESEARCH JOURNAL **16**, 211 (May 1946).
5. Minor, F. W., Sookne, A. M., Simpson, J. E., and Harris, M., The Use of Water-Permeability Measurements on Swelling-Type Fabrics, TEXTILE RESEARCH JOURNAL **16**, 539 (Nov. 1946).
6. Simpson, J. E., The Army's Water-Repellent Clothing, *Am. Dyestuff Reptr.* **35**, 243, 272 (1946).
7. Slowinske, G. A., Address before the American Association of Textile Technologists, New York, March, 1944.
8. Sookne, A. M., Minor, F. W., Simpson, J. E., and Harris, Milton, A Drop-Penetration Apparatus for Evaluating Water-Repellent Fabrics, *Am. Dyestuff Reptr.* **35**, 295 (1946).
9. Wakeham, H., and Skau, E. L., A Tensiometric Method for Evaluating Surface Wettability by Measurements of the Contact Angle, *J. Am. Chem. Soc.* **67**, 268 (Feb. 1945).

Absorption Spectra in the Detection of Chemical Changes in Cellulose and Cellulose Derivatives*

J. W. Rowen, C. M. Hunt, and E. K. Plyler

With the increasing availability of commercial spectrometers, particularly for the infrared, increasing application of spectrometric methods to the study of the structure of high polymeric materials is being made. The present work presents this approach to the structure of cellulose and its derivatives.

The infrared spectrograms which have been obtained for these substances show marked contrasts between the different chemically modified celluloses studied.

Abstract

The spectral absorption of thin films of cellulose acetate, regenerated cellulose, the acetate and regenerated cellulose after oxidation with nitrogen dioxide gas, and the regenerated cellulose after oxidation with periodic acid followed by chlorous acid are recorded for the infrared from 2 to 15 microns and the ultraviolet from 215 to 400 millimicrons. The regenerated cellulose absorbed ultraviolet radiant energy only at the short-wave-length end of the region studied, and there the transmittance of a film 2.8 microns thick was only slightly reduced. The acetate and oxidized celluloses absorbed in this region to a greater extent but gave no narrow absorption bands. Marked changes were observed in some of the absorption bands in the infrared region in going from cellulose acetate to regenerated cellulose and to their oxidation products. These changes were correlated with changes in the OH, CO, and COOH groups. The results indicate the possibility of estimating the amount of these groups present by spectral absorption measurements.

Present-day theories regarding the chemistry and structure of cellulose, its derivatives and degradation products have been extensively studied and reviewed by several writers [7, 8, 10, 12, 13, 18]. However, only limited use of spectrometric measurements as a means of following the modification of cellulose by various treatments has been reported [2, 6, 9, 19]. This paper contains results of the measurement of the absorption spectra of cellulose and cellulose acetate before and after chemical treatments.

The structural formula generally assigned to cellulose is:

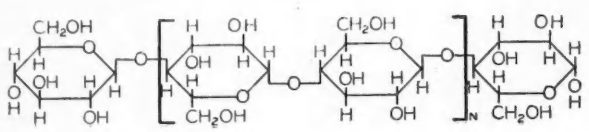

where N may take values as high as 4,500. Any sample of cellulose is considered to be made up of varying proportions of these long-chain molecules, the lengths of the individual chains depending upon the source of cellulose and its history. The greater the proportion of the shorter chains in a sample the greater the number of end groups.

Cellulose is relatively unstable and some of the linkages between atoms may be ruptured—for example, when cellulose is exposed to light, heat, or chemical agents. Shorter chains and additional end groups may be formed. When exposed to extreme conditions, cellulose may be degraded to relatively simple compounds.

The groups which are found in cellulose or which may be formed as a result of oxidation or cleavage include the ketone, aldehyde, hemiacetal, carboxyl, and hydroxyl groups. These groups are responsible for characteristic absorption bands in the spectra of simpler organic compounds. Not only would the bands be expected to be present in the absorption spectra of cellulose and cellulose derivatives but the magnitude of the absorption might be a quantitative measure of the number of the groups responsible for the band.

Chemical methods for the quantitative evaluation of the groups in cellulosic materials [16, 18] sometimes lead to erroneous results because of changes in the cellulose produced by the conditions to which it is subjected during analysis. The spectrophotometric method of analysis probably would not result in appreciable change. Another way in which the spec-

* This paper, which is from the U. S. Department of Commerce, National Bureau of Standards, appears also in the August issue of *J. Research Natl. Bur. Standards.*

trophotometric method could be useful is in investigating the preferential attack of reagents on specific parts of the cellulose molecule. For example, the oxidation of the secondary alcohol groups on carbon atoms 2 and 3 of the ring by periodic acid [11, 15] and the oxidation of the carbon atom in the 6-position to carboxyl by nitrogen dioxide gas [17, 20] could perhaps be followed spectrophotometrically.

The work reported in this paper was undertaken with these points in mind.

I. Materials and Methods

The cellulose used in this study was prepared by deacetylation, in an inert nitrogen atmosphere, of cellulose acetate. The cellulose acetate was obtained in the form of yarns; it was first extracted with ether, dried, then wet with distilled water and dried again to insure complete removal of the ether. The acetate was dissolved in redistilled acetone and cast into films on a glass plate with a Bird film applicator at room temperature. The film was then soaked from the plate with distilled water and dried.

1. Preparation of Cellulose Films

The films were deacetylated by soaking them for 24 hours in a 0.4*M* alcoholic sodium hydroxide solution under an atmosphere of nitrogen. They were then washed with alcohol, soaked for 20 minutes in a 10-percent solution of glacial acetic acid in alcohol, again soaked for a half hour in water, and then air-dried.

2. Treatment of Films with Nitrogen Dioxide ($NO_2 - N_2O_4$)

Films of cellulose acetate and/or regenerated cellulose were suspended at room temperatures in a glass chamber which was evacuated. Dry nitrogen dioxide was then passed into the chamber. The films were left in the nitrogen dioxide atmosphere for 2 hours and then soaked for another 2 hours in distilled water with three changes of water.

3. Treatment of Films with Periodic Acid and Chlorous Acid

The films were immersed for 2 hours in a 0.042*M* solution of periodic acid which was buffered with sodium acetate at a pH of 4.5. After contact with the periodic acid the films were soaked for an additional 2 hours in distilled water and then washed three times with fresh distilled water. The films were dried and subsequently transferred to a 5-percent solution of sodium chlorite buffered to a pH of 2.2 with phosphoric acid. They were allowed to remain in this solution for 2 hours. The films were then washed for 2 hours more and dried.

4. Measurement of Thickness of Films

Thickness measurements were made with a "Mikrokator" [1] which was checked against steel gage blocks calibrated by the Gage Section of the National Bureau of Standards. The standard deviation of five measurements did not exceed 0.2 micron on any spectrometer specimens. Thickness measurements obtained in this manner with cellulose acetate film averaged 0.3 micron less than thickness measurements based on weight, area, and density calculations.

5. Measurement of Spectral Absorption in the Ultraviolet Region

The ultraviolet absorption spectrum was measured with the Beckman-model DU quartz spectrophotometer [5]. The wave-length calibrations on the scale of the instrument were found to check very well against the known wave lengths of the lines of the hydrogen and mercury discharge tubes. It was observed in the region from about 310 to 400 millimicrons that when readings were made every 5 millimicrons ripples appeared in the absorption pattern of these cellulosic materials. The amplitude and position of these ripples varied with the orientation of the sample in the light beam. They were interpreted as having been caused by optical interference. However, it was possible to orient the film in the beam in such a position as to virtually eliminate them.

Figure 1 is based upon measurements made at 5-millimicron intervals.

6. Measurement of Spectral Absorption in the Infrared Region

The infrared absorption spectrum was measured with a Perkin-Elmer recording infrared spectrometer with a sodium chloride prism. This type of instrument has been previously described [4]. The instrument was equipped with specially constructed gears operated by a synchronous motor for changing the wave length, and another gear mechanism for automatically increasing the slit width in such a way as to partially compensate for the lower energy of the

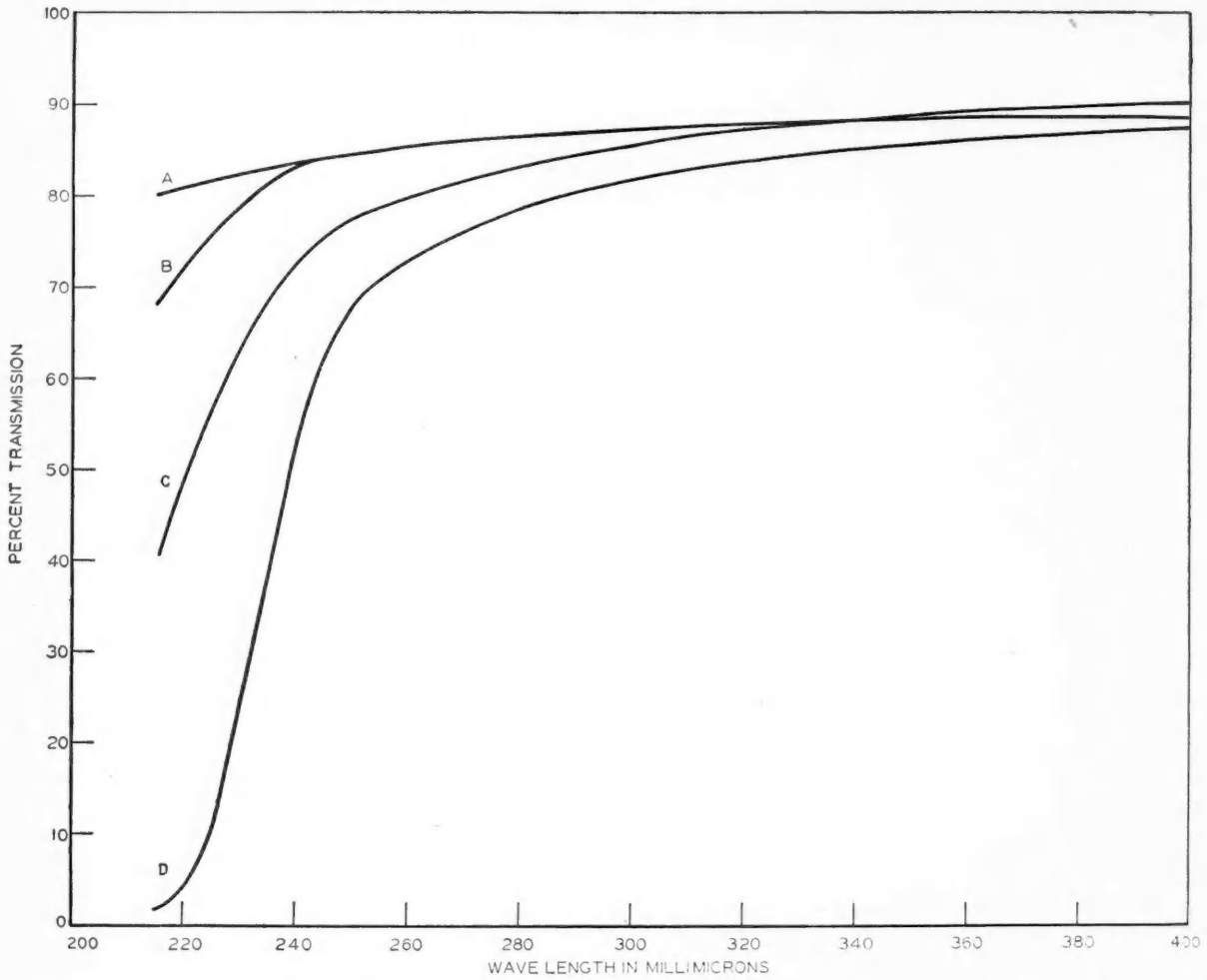

FIG. 1. *Ultraviolet absorption curves. A—Cellulose regenerated from cellulose acetate (film thickness 2.8 microns). B—Cellulose treated with periodic acid followed by chlorous acid (film thickness 3.6 microns). C—Cellulose acetate (film thickness 4.1 microns).* D—*Cellulose treated with nitrogen dioxide gas (film thickness 3.3 microns).*

radiation source in the longer wave lengths. Since the instrument is a single-beam spectrometer, the absorption bands of atmospheric water vapor are superimposed upon the absorption spectrum of the film under observation. The estimation of the extent of absorption by the film in this region is therefore less precise than in other regions. This uncertainty has been indicated in the spectra by broken lines.

II. Results and Discussion

The infrared and ultraviolet absorption spectra of cellulose in the oxidized and acetylated states are shown in Figures 1 to 6 inclusive. The infrared spectra of these materials have in general many more bands than the ultraviolet absorption spectra. The absorption of ultraviolet light by the resonance forms of the groups of the cellulose molecule appears to take place in the energy region which is mainly below 200 millimicrons and hence in the vacuum region (see Figure 1). In order to evaluate these bands in the ultraviolet region properly it appeared necessary to measure the absorption in the vacuum ultraviolet region as had been done for some aliphatic fatty acids [14]. It was noted that untreated cellulose had much less of a tendency to absorb short-wave-length radiation than the modified celluloses, as indicated in curve A of Figure 1. Exposure of such films of cellulose to light and to most of the oxidizing agents resulted in an increased absorption of the short wave lengths. In many cases the absorbing agent in the cellulose created by the

treatment was water-soluble and showed general absorption in water. In this way it was occasionally possible to check on the extent of oxidation and the contamination of the films used in this study.

The groups in the cellulose which contained oxidized carbon gave rise to bands in the infrared region. This spectrum, therefore, was more informative than the ultraviolet absorption spectrum. The striking alteration which accompanies deacetylation may be noted by contrasting the curves of Figure 2 and Figure 4. The changes in the infrared absorption spectrum of cellulose acetate which occur upon exposure to nitrogen dioxide ($NO_2 - N_2O_4$) may be seen in Figures 2 and 3. This oxidizing gas also has a marked effect on the absorption spectrum of cellulose. The effect of a somewhat arbitrary concentration of periodic acid (followed by chlorous acid) on the infrared absorption spectrum of cellulose is shown in Figure 6. The bands shown in the various figures are discussed under the appropriate titles, as follows:

1. Cellulose Acetate

As indicated previously the cellulose acetate was the starting point for the regeneration of the cellulose used in the study. The infrared absorption spectrum of the original cellulose acetate is shown in Figure 2. This spectrum is characterized by several well-defined bands. The first band of appreciable intensity occurs at 2.8 microns and is probably related to the O-H stretching vibration. The band at 3.4 microns is believed to be the familiar band attributed to the C-H stretching vibration. The intense band at 5.7 microns falls in the general region characteristic of the ester carbonyl group and it shows a strong absorption in the cellulose acetate film. The band at 7.2 microns is characteristic of the C-CH_3 group and hence appears in both Figures 2 and 3 (untreated and nitrogen-dioxide-treated cellulose acetate). The intense absorption at 8.1 microns may be noted in Figures 2 and 3. It is attributed to the ester group since a band in this general position is always observed in the spectra of esters. These last three bands also appear in polyvinyl acetate as well as in other simpler acetates [3]. The strong band at 9.5 microns is present in all the infrared absorption spectra (Figures 2–6, inclusive) and is probably due to the C-O vibration. This vibration is very intense for methyl alcohol and is also found in polyvinyl alcohol [3].

2. Oxidized Cellulose Acetate

When cellulose acetate is oxidized with nitrogen dioxide (N_2O_4—NO_2) two new bands (Figure 3) appear in the infrared spectrum. These absorptions take place at 6.1 and 7.8 microns. The band at 7.8 is evident as a bulge in the side of the broad band at 8.1 microns. It will be noted later that these two bands correspond closely with the two bands which are created when cellulose is treated with nitrogen dioxide. Most organic compounds containing carboxyl groups have two strong absorption bands at approximately 6.0 and 7.8 microns. The possibility that the two bands described above might be due to carboxyl groups which have been created by the oxidation of the unacetylated number-6 C-OH group will be discussed later.

3. Cellulose

When cellulose acetate is deacetylated the marked changes which result from this process may be noted by comparing Figure 2 with Figure 4. One notes that the O-H vibration at 2.8 microns has become much more intense and at the same time slightly shifted to longer wave lengths. The ester carbonyl group at 5.7 microns, the CH_3 group at 7.2, and the typical ester band at 8.1 microns are all absent. On the other hand, the C-O band at 9.5 microns has been considerably broadened.

4. Cellulose Oxidized with Nitrogen Dioxide

When the cellulose film is treated (as described under experimental procedure) with nitrogen dioxide, certain characteristic changes occur in the spectrum of cellulose (see Figure 5). First the O-H absorption at 2.9 microns seen in Figure 5 is somewhat decreased in intensity. In addition three other bands appear, the one at 5.7, one at 6.1, and a third at 7.8 microns. The band at 5.7 microns falls in the general region characteristic of the C=O group and the other two bands are also associated with the carboxyl group as indicated under the discussion of oxidized cellulose acetate. In our work the two strong bands at 6.1 and 7.8 microns were

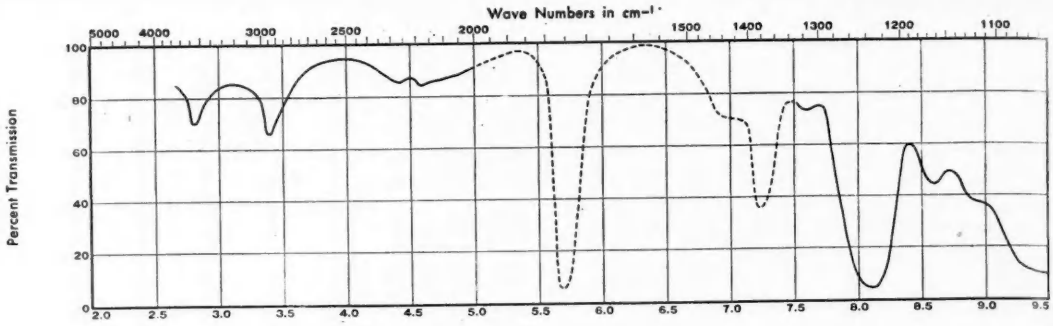

FIG. 2.

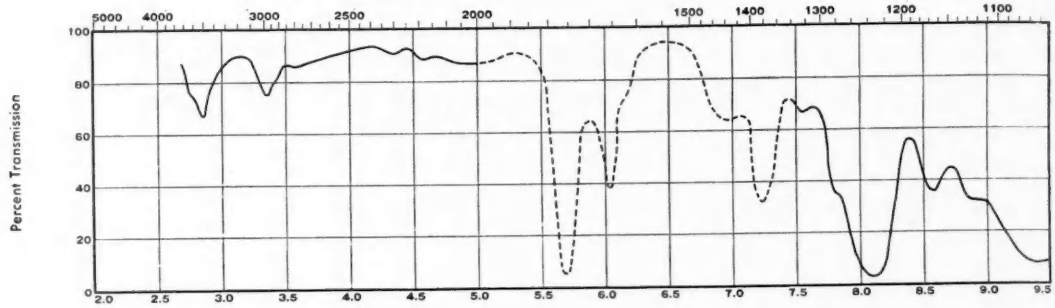

FIG. 3.

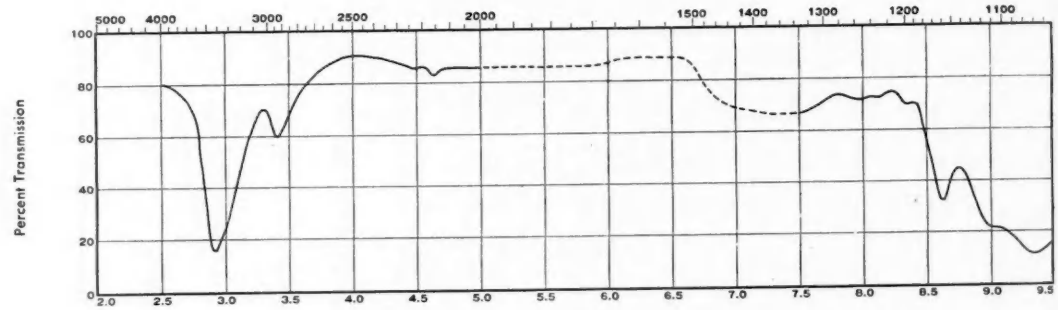

FIG. 4.

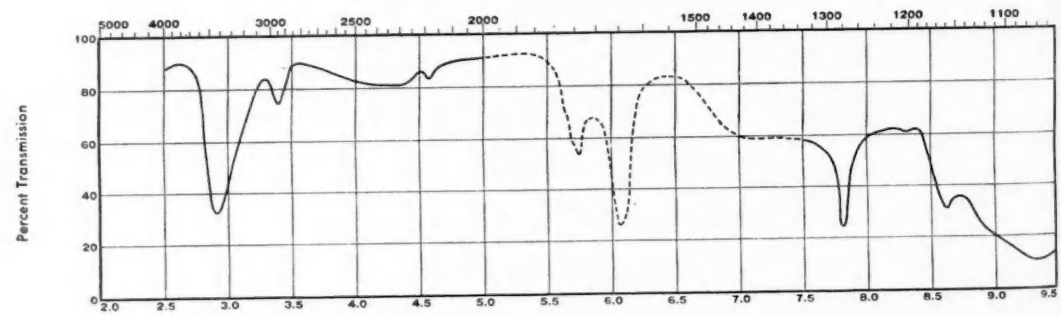

FIG. 5.

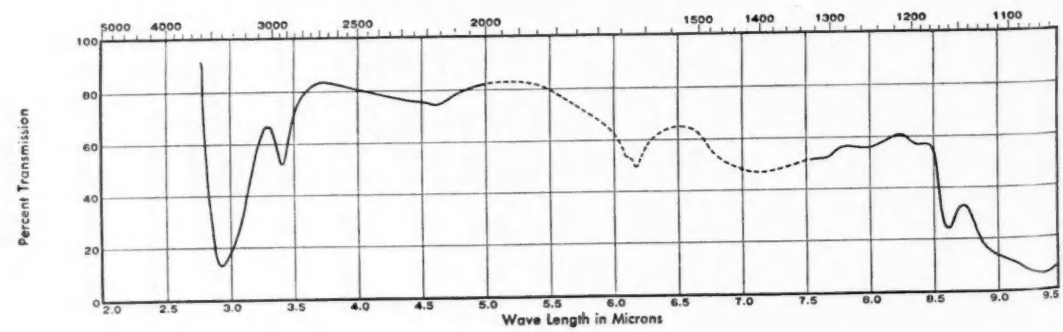

FIG. 6.

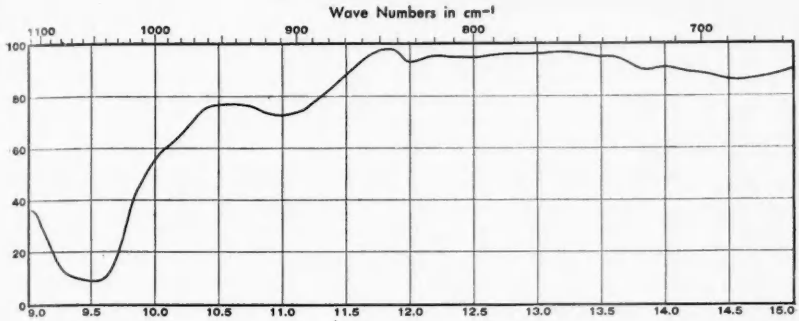

Infrared absorption curve of cellulose acetate (film thickness 4.1 microns).

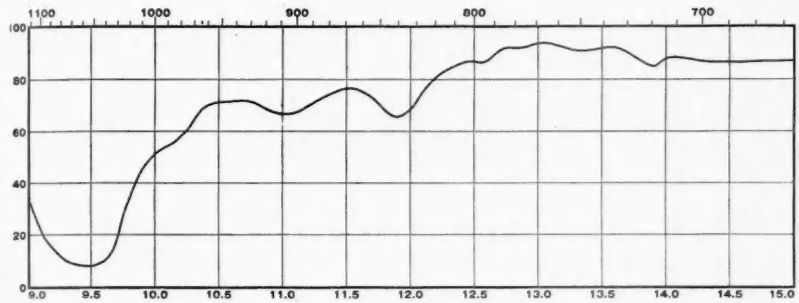

Infrared absorption curve of cellulose acetate exposed to nitrogen dioxide gas (film thickness 3.3 microns).

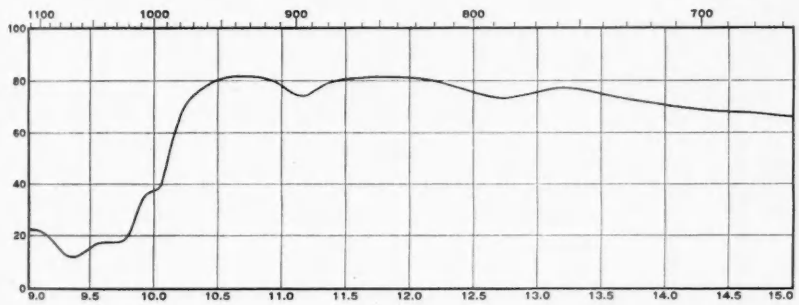

Infrared absorption curve of regenerated cellulose (film thickness 2.8 microns).

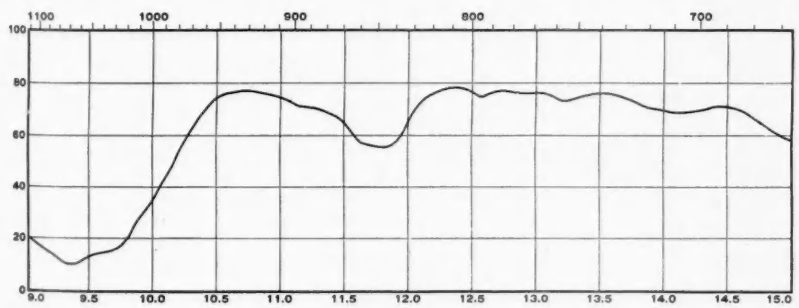

Infrared absorption curve of regenerated cellulose exposed to nitrogen dioxide gas (film thickness 3.3 microns).

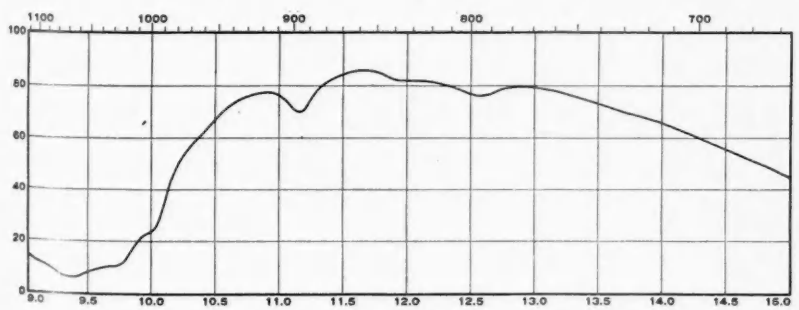

Infrared absorption curve of regenerated cellulose treated with periodic acid followed by chlorous acid (film thickness 3.6 microns).

always associated with the oxidized cellulose believed to contain carboxyl groups.

5. Cellulose Treated with Periodic and Chlorous Acids

Exploratory experiments of the effect of periodic and chlorous acids on the infrared absorption spectrum of cellulose have been performed. Neither of these acids alone or in sequence had nearly so marked an effect on the cellulose as had nitrogen dioxide. However, a small band shown in Figure 6 at 6.2 microns, not present in the spectrum of the original cellulose, was found in the treated cellulose. No definite conclusions can be drawn concerning the band until more information is available.

III. Correlation of Absorption Bands with Changes in Chemical Structure

Cellulose contains over 49 percent of oxygen, and this oxygen content may be expected to undergo a very small but definite increase throughout the life of the cellulose in the atmosphere. The oxidized cellulose would not be expected to be a homogeneous molecular species. In fact, one would expect the oxidized cellulose to consist of a mixture of many different kinds of oxidized cellulose molecules. Workers recognizing the complexity of "oxidized" cellulose have attempted to study the effect of specific oxidizing agents on the polymer. Kenyon and coworkers have studied the oxidation of cellulose by nitrogen dioxide. They presented evidence [17, 20] that the mode of attack by this agent was highly specific. Their work indicated that the primary alcohol group on carbon atom 6 was oxidized to a carboxyl group by the oxidizing gas. The work of Jackson and Hudson [11], and Harris *et al.* [15] indicated that periodic acid has a specific oxidizing effect on cellulose. These experiments indicate that this agent converts the secondary alcohol groups on carbon atoms 2 and 3 to aldehyde groups in accordance with the following scheme:

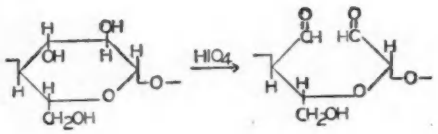

Since the conditions of the reaction of nitrogen dioxide with cellulose, described in the experimental data, are very similar to those employed by Kenyon *et al.* [17, 20], it is reasonable to suppose that carboxyl groups were the primary product of the reaction. Furthermore, since adequate steps had been taken to remove any unreacted nitrogen dioxide, and since very little if any nitrocellulose would be formed under the experimental conditions, it appears reasonable to assume that the three bands present in Figure 5 (the ones at 5.7, 6.1, and 7.8 microns) are all manifestations of the carboxyl group in the 6-position.

Whether or not the intensities of these bands lend themselves to the quantitative estimation of carboxyl groups is not known at present. The presence of the "carboxyl" bands (5.7, 6.1, and 7.8 microns) in the spectrum of the treated cellulose acetate films (Figure 3) suggests the possibility that a considerable number of the primary alcohol groups (6-position) present in this material are attacked by nitrogen dioxide and converted to carboxyl groups.

The intensification of the O-H band (2.8 microns) in Figure 4 which accompanies deacetylation is quite striking. Presumably each acetyl group (absorption at 5.7, 7.2, and 8.1 microns) is replaced by a hydroxyl group in this conversion and the difference in intensities in the two bands (2.8–2.9 microns) is some measure of the number of OH groups regenerated in the process.

The effect of periodic acid, reported by other workers, was not observed in the absorption spectra of the treated cellulose in the spectral ranges studied. However, it is pointed out that these experiments may not have provided the optimum conditions for the generation of the aldehyde groups on the second and third carbon atoms. The weak band at 6.2 microns in Figure 6 is evidence of some reaction which did take place in these preliminary attempts.

When the cellulose acetate is converted to cellulose and when the latter is oxidized to oxycellulose certain fundamental aspects of the long-chain molecular structure remain intact. For example, the skeletal ring-chain structure should not be profoundly altered during some of the above reaction steps. One might, therefore, expect to see manifestations of the unchanging portions of the molecule in the infrared spectrum. The absorption band at 8.6 appears in the spectrum of all of the cellulose derivatives examined in this study. This band may be a fundamental vibration which is associated with the ring skeleton. The absorption band at 3.4 microns also is common to all of the spectra and it is un-

doubtedly due to the C-H stretching vibration which is characteristic of all of the compounds.

This study indicates the possibility of using the infrared absorption spectrum as a means of elucidating the alterations which may be made in the cellulose molecule.

IV. Summary

1. The ultraviolet and infrared absorption spectra of cellulose, cellulose acetate, and certain oxidized samples of cellulose have been obtained.

2. Acetylation and oxidation of cellulose are reflected by profound changes in the absorption spectra of these materials.

3. This study indicates the possibility of detecting and estimating the amounts of such groups as

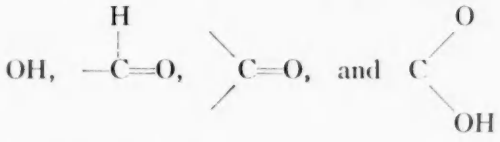

in cellulosic materials.

Acknowledgment

The authors are indebted to Lee A. Dunlap and Walter Stone of the Textile Section of the National Bureau of Standards, for assistance in making some of the measurements reported in this paper.

Literature Cited

1. Anonymous, *Machinery* (New York), **45**, 729 (June 1939); **46**, 127–9 (Feb. 1940).
2. Atsuki, Katsumoto, and Sobue, Hiroshi, *J. Soc. Chem. Ind.*, Japan, Supplemental binding **36**, 589B–595B (1933).
3. Barnes, R. B., Gore, R. C., Liddel, U., and Williams, van Zandt, "Infrared Spectroscopy," New York, Reinhold Publishing Co., 1944.
4. Barnes, R. B., McDonald, R. S., Williams, van Zandt, and Kinnaird, R. F., *J. Applied Physics* **16**, 77–86 (1945).
5. Cary, H. H., and Beckman, A. O., *J. Opt. Soc. Am.* **31**, 682–9 (1940).
6. Champetier, G., and Marton, R., *Bull. soc. chim.* **10**, 102–6 (1943).
7. Davidson, G. F., *J. Text. Inst.* **27**, 144–58 (1936).
8. Haworth, W. N., *J. Soc. Dyers and Colourists* **56**, 49–58 (1940).
9. Herzog, R. O., and Laski, G., *Z. physik Chem.* **121**, 136–42 (1926).
10. Heuser, Emil, "The Chemistry of Cellulose," New York, John Wiley & Sons, Inc., 1944.
11. Jackson, E. L., and Hudson, C. S., *J. Am. Chem. Soc.* **59**, 2049–50 (1937); **60**, 989–91 (1938).
12. Ott, Emil, "Cellulose and Cellulose Derivatives," New York, Interscience Publishers, Inc., 1943.
13. Pacsu, E., and Hiller, L. A., TEXTILE RESEARCH JOURNAL **16**, 243–8 (1946).
14. Platt, J. R., Rusoff, I., and Klevens, H. B., *J. Chem. Physics* **11**, 535–44 (1943).
15. Rutherford, H. A., Minor, F. W., Martin, A. R., and Harris, M., *J. Research Natl. Bur. Standards* **29**, 131–41 (1942).
16. Sookne, A. M., and Harris, M., in Ott, Emil, "Cellulose and Cellulose Derivatives," New York, Interscience Publishers, Inc., 1943, p. 77.
17. Unruh, C. C., and Kenyon, W. O., *J. Am. Chem. Soc.* **64**, 127–31 (1942).
18. Unruh, C. C., and Kenyon, W. O., TEXTILE RESEARCH JOURNAL **16**, 1–12 (1946).
19. Wells, A. J., *J. Applied Phys.* **11**, 137–40 (1940).
20. Yackel, E. C., and Kenyon, W. O., *J. Am. Chem. Soc.* **64**, 121–7 (1942).

Diffraction of Light by Cellulose Acetate Yarn

E. V. Martin

Communication No. 1149 from the Kodak Research Laboratories

SOME experiments now in progress involved winding stretched cellulose acetate yarns (continuous filament) on a small metal frame in such a fashion that many filaments were close together and essentially parallel. When these frames of yarn were immersed in decahydronaphthalene in a glass cell and illuminated with approximately parallel rays of white light, it was noticed that some of the yarns appeared colored by transmitted light when viewed at an angle to the fiber axis from a point in the plane containing the fiber axis and the incident light, and that the color varied with the angle of view. Further investigation showed that this was also true of a single filament mounted on a glass slide under a cover glass. It was necessary to immerse the filaments in a colorless liquid having an index of refraction close to that of the cellulose acetate in order to reduce the general scattering of the white light sufficiently to make the colors visible. The liquid served no other purpose.

Figure 1 illustrates the phenomenon diagrammatically. Filaments illuminated at right angles to the fiber axis with approximately parallel rays of white light appeared colored when viewed at an angle θ, as shown in the figure. The color observed was found to vary with the angle according to the diffraction grating law, $\eta\lambda = d \sin \theta$, where X in the figure is equal to $\eta\lambda$ and d is the distance between adjacent diffracting centers in the filament. In a series of drafted yarns which were available at the time, it was found that the distance d, as measured by the angle of diffraction of a given wave length of light, varied directly with the draft factor, indicating that the diffracting centers either were present in undrafted fibers or appeared early in the drafting process.

The amount of light in the diffracted spectrum was a very small fraction of the total transmitted light, although with several thousand filaments close together on a frame it could be made bright enough to be readily seen when projected on a white screen in a darkened room.

Examination of the filaments with an optical microscope,* under magnification of 1,200 diameters, showed that the diffracting centers were a series of cavities in the interior of the filaments. These cavities were all approximately equal in size and were regularly spaced in one or more rows approximately parallel to the long axis of the filament. Photomicrographs of a longitudinal section and a cross section of one of the yarns are shown in Figure 2. The cavities in the case shown are actually one micron apart, center to center. The cross section shows one cavity, approximately 0.5 micron in diameter.

Two different yarns were used in these experiments, one a 200-denier, 52-filament yarn with a spinning draft of 0.65; the other a 150-denier, 38-

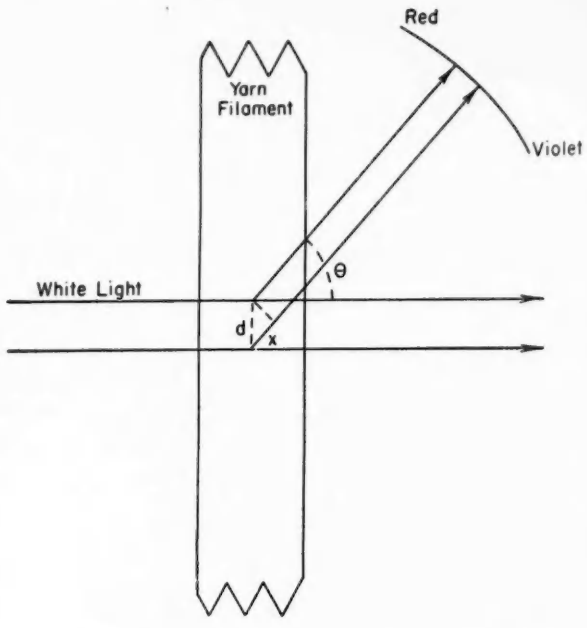

FIG. 1. *Diagrammatic representation of diffraction of visible radiation by a single filament of drafted cellulose acetate yarn.*

* Examination made by Dr. E. E. Jelley, of the Kodak Research Laboratories, Rochester, N. Y.

filament yarn with a spinning draft of 1.4. Table I contains some data obtained from these yarns, including plastic draft factor, tension of yarn during drafting (in hot air), tenacity and extensibility, and measurements of the cavities, including the center-to-center distance between adjacent cavities, the length of each cavity, the length of the bridge of cellulose acetate between adjacent cavities, and the width of the line of cavities. The yarns were drafted different amounts and under different tensions, the tension being varied by changing the temperature of the hot-air drafting chamber. It was found that for all draft factors a tension of about 4 to 5 grams was required to produce the regular rows of cavities. No cavities at all were produced at tensions of less than 0.2 gram, even at high draft factors. As the

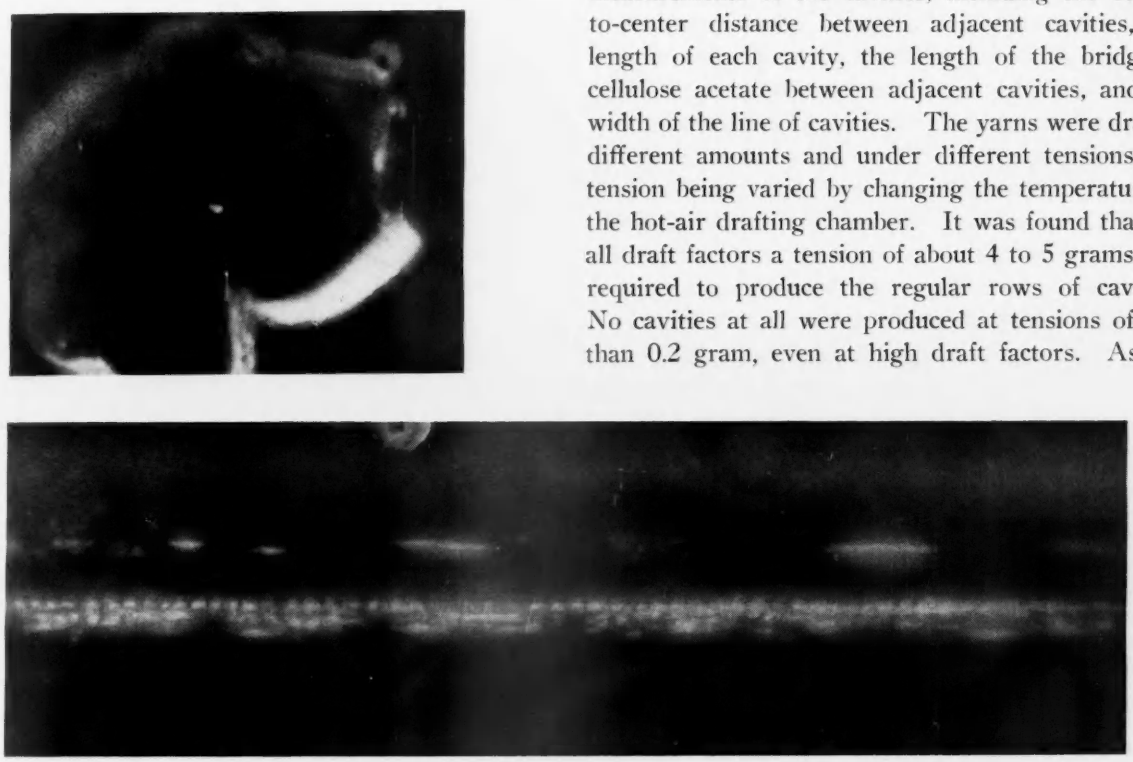

FIG. 2. *Photomicrographs of a cross section (top) and a longitudinal section (bottom) of yarn A drafted by a factor of 5.*

TABLE I. DATA FROM YARNS USED FOR EXPERIMENTS

Yarn	Plastic draft factor	Draft tension (g.)	Tenacity (g./den.)	Extensibility (%)	Cavity spacing (μ)	Cavity length (μ)	Bridge length (μ)	Cavity line width (μ)
A (200/52)	Undrafted		1.31	40.6	No cavities			
Spun draft	1.3	2.0	1.57	28.6	2.2	0.2	2.0	0.6
= 0.65	1.9	3.0	1.78	16.6	Few scattered cavities			
	1.9	3.5	1.85	16.1	3.0	0.4	2.6	0.5
	1.9	4.0	1.96	13.1	0.5	0.25	0.25	0.5
	2.5	4.0	1.96	11.9	0.55	0.3	0.25	0.5
	3.5	4.5	1.97	6.8	0.75	0.5	0.25	0.5
	4.0	5.0	2.05	5.0	0.85	0.5	0.35	0.5
	5.0	5.5	1.99	3.6	1.0	0.6	0.35	0.6
B (150/38)	Undrafted		1.33	26.6	No cavities			
Spun draft	1.5	4	1.41	13.9	0.6	0.35	0.25	0.8
= 1.4	2.25	4	2.03	8.8	0.8	0.45	0.35	0.8
	4.0	<0.2	3.05	5.3	No cavities			
	4.0	1	3.13	3.8	Few scattered cavities			
	4.0	5	2.67	2.7	1.07	0.7	0.4	0.7
	6.0	5	3.28	3.1	1.57	1.1	0.5	0.6
	7.5	5	3.40	3.0	2.06	1.3	0.8	0.7
	10.0	<0.2	3.26	4.4	No cavities			
	10.0	1	3.14	3.6	Few scattered cavities			
	10.0	4	3.38	3.2	2.8	1.7	1.1	0.6

tension was increased to 1 gram, however, a few cavities appeared at irregular intervals along a line parallel to the long axis of the filament. At a little higher tension, cavities appeared at rather regular intervals spaced several microns apart. At still higher tension (about 4 grams), cavities began to appear at even closer intervals. Increasing tension beyond this value did not result in increasing the number of cavities in any particular row, but resulted in more rows of cavities. After two or three regular rows of cavities had appeared, increasing tension resulted in cavities appearing more or less at random over the rest of the filament. At tensions near the breaking value, the filaments usually were so full of cavities that the yarn had a dull, delustered appearance. Cavities could be produced in these yarns by stretching them at room temperature to near the breaking point, but they were not regularly spaced.

Since drafting the yarns under a tension of 4 to 5 grams produced the closest spacing between cavities, the spacing obtained under these conditions was plotted against draft factor, and the resulting curves are shown in Figure 3. Curves A and B correspond to yarns A and B, respectively. Extrapolation of the curves to a draft factor of 1.0 yields an estimate of the cavity spacing at about the point of formation. These values are about 0.3 and 0.4 micron for yarns A and B, respectively. The bridge lengths at draft factors less than 2, given in the table, were estimated by use of the microscope to be approximately 0.25 micron for both yarns. The bridge length under these conditions should be approximately equal to the minimum cavity spacing. The values obtained by the two methods are, however, not in very close agreement, but this is probably due to the low degree of accuracy of measurement with the microscope of distances less than about 0.5 micron.

The two yarns, A and B, are different from each other in two respects, either or both of which may play a role in causing the difference in cavity spacing,

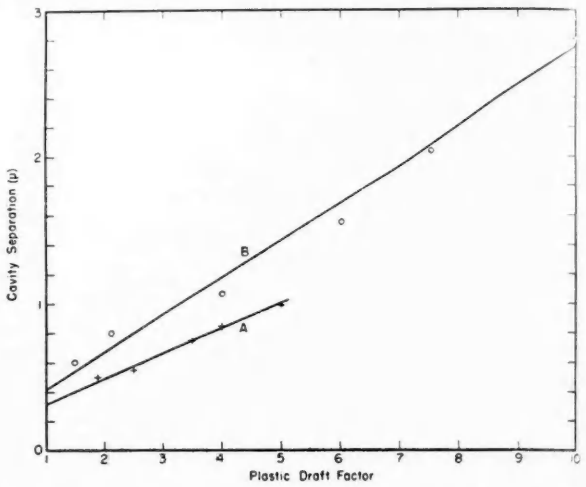

FIG. 3. *Cavity separation in microns as a function of plastic draft factor for yarns A and B.*

as illustrated in Figure 3. Yarn A is made of a polymer of lower average molecular weight than yarn B and also had a lower draft during spinning. The average degrees of polymerization of the two yarn polymers, as determined from measurements of molecular weight by intrinsic viscosity, were 225 for A and 244 for B. This means that the average lengths of the molecules in the two cases were about 0.12 and 0.13 micron, respectively. These lengths are probably higher than they would have been had they been determined from osmotic-pressure measurements instead of from intrinsic viscosity values. Since these values are considerably less than the minimum separation of the cavities, it would seem that the length of the molecules was not a critical factor in determining the points of rupture in the yarn. Possibly the phenomenon is ascribable to some unit in the crystal structure. The fact that these regularly spaced cavities usually occur near a wrinkle in the outer wall of the filament would seem to indicate that the structure of the filament at these points plays a role in the phenomenon, although the mechanism by which it acts is not clear.

ABSTRACTS

SERVICES AVAILABLE

Reprints of the original articles abstracted in TEXTILE RESEARCH JOURNAL *are often available from the publishers. Otherwise, it may be possible to obtain copies of the periodicals. Orders should be sent direct to the publishers.*

Photostat negatives of articles abstracted will be furnished to members of the Institute at a cost of 25 cents per page for pages not exceeding 7 inches in width and 35 cents per page for larger sizes up to 11½ x 14 inches. Photostats of patents are 35 cents a page. Postage will be added.

Microfilm copies and paper enlargements of microfilm may be obtained from: Microfilms Inc., 313 N. First St., Ann Arbor, Mich.; New York Public Library, New York, N. Y.; Yale University Library, New Haven, Conn.; Harvard University Library, Cambridge, Mass.; and Library of Congress, Washington, D. C. Translations may also be obtained from the above sources.

A list of periodicals, the abbreviations used in references to articles, and the addresses of publishers of English language publications is given on page 37 of the January, 1947, issue.

ANALYSIS: TESTING: LABORATORY METHODS

★

Swelling of Cellulose

The swelling of cellulosic textile fibers. A rapid method of determination. Eduardo Blanchard. *Anales fís. y quím.* (Madrid) **42**, 413–22 (1946) (through *Chem. Abstr.* **41**, 4650*f* (July 20, 1947)).

A rapid method includes moistening the fibers, in a small bottle having a bottom opening, with water at 70–80°C, using a little wetting agent, if necessary, allowing it to stand 5 min., centrifuging 10 min. at 2,500 r.p.m., radius of centrifuge 19 cm., weighing rapidly bottle and contents (*a*), drying in a current of air at 110°C 20–30 min., cooling in a $CaCl_2$ desiccator, weighing (*b*), removing the fiber from the container and weighing the fiber (*c*). Swelling is taken as $(a - b)/(b - c) \times 100$. A method involving observation of swelling under a microscope did not give results concordant with the above. Swelling diminishes with increase in drying temperature and is greatest with straw cellulose. Strength and stretch, both moist and dry, suffer considerable diminution, except in the case of "wool-type" fiber. The greatest variation is with straw. Diminution of swelling after drying can be attributed to greater saturation of OH by the lateral walls of the crystallites, which prevents their acting later as acceptors of water molecules. This is important because all fibers which have been dried at elevated temperature lose to a rather great extent their facility to fix water in a moist atmosphere. 6 references.

Text. Research J. Sept. 1947

Fiber Photography

Photography as applied to the study of fibrous material. J. L. Stoves. *Fibers* **8**, 109–12 (Apr. 1947).

Methods of fiber photography are discussed particularly with respect to histology, molecular structure, and properties. 9 references.

J. A. Woodruff

Text. Research J. Sept. 1947

Average Test Results

Methods of averaging physical test results. Use of median. J. M. Buist and O. L. Davies. *India-Rubber J.* **112**, 447–8, 451–2, 454 (1947) (through *Chem. Abstr.* **41**, 4017*h* (July 10, 1947)).

Although testing methods have been prescribed by organizations such as the American Society for Testing Materials and by the British Standards Institute, the problem of averaging has not received enough attention, and the A.S.T.M. specifications, e.g., are open to criticism for their poor methods of averaging results. The present tendency of testing laboratories is to use different

methods of averaging. As a step toward solving the problem of the correct choice of methods, 5 methods were compared: (1) averaging all results within 10% of the highest; (2) averaging all results until the average is within 10% of the highest; (3) averaging the highest 4 results out of 6, or the highest 3 out of 4; (4) taking the median; (5) following the method of Davies and Horrobin (*C.A.* **30**, 8688[3]). Methods (1) and (2) are unacceptable on a logical basis. There is little to choose between methods (3) and (4). The choice for routine testing depends on the simplicity of the method and its freedom from bias. Method (3) introduces a slight bias by always rejecting the low result; hence it is recommended that the median be used, either by averaging the middle 2 out of 4 or by averaging the middle 4 out of 6 results. With 5 test-specimens, take the average of the middle 3, and with 4 specimens, the average of the middle 2. When it is desired to establish the variations from each source, it is preferable to use the more elaborate method (5), which, although not suitable for routine testing, is the most logical of all.

Text. Research J. Sept. 1947

Ultrasonics

Ultrasonics, methods, and applications. C. J. Bradish. *Chem. Products* **10**, 3–9 (1946) (through *Chem. Abstr.* **41**, 4019*d* (July 10, 1947)).

A review of the generation of ultrasonic vibrations, the magnetostriction oscillator, the piezoelectric oscillator, physical applications of ultrasonics, measurement of ultrasonic intensity, cavitation and physical-chemical applications of ultrasonics, and biological applications of ultrasonics. 46 references.

Text. Research J. Sept. 1947

Estimation of Wool Damage

A photoelectric method of estimating wool damage. W. L. Semple. *J. Text. Inst.* **37**, T260–8 (Nov. 1946).

A method of determining the degree of staining of modified wool fibers after treatment with Kiton Red G or Indigo Carmine under arbitrary conditions is described. It is said to eliminate the personal-judgment errors of previous visual classification. The method is based on the micro-projection of the optical images of short pieces of the dyed fibers at a magnification of 300× on a variable slit beneath which is mounted a special color filter and photo-cell. Photographs are shown of the optical equipment and of the Hennings sectioning device which is used to prepare the fiber pieces after they are stained in the form of yarn or sliver. The fiber image is focused sharply on the slit over the photo-cell with the image at right angles across the slit, the transmitted light passing through a selected filter before reaching the photo-cell. The current set up by the caesium-type photo-cell is measured by the deflection of a micro-ammeter. Dividing the difference between the micro-ammeter deflections with and without the image on the slit by the fiber diameter is said to give a value proportional to the amount of modification undergone by the fiber and is called the fiber modification index. Several tables are given showing data obtained by this method which were used on chlorinated wool samples. An appendix on the technique of the Indigo Carmine test by W. S. M. Grieve is given. J. A. Woodruff

Text. Research J. Sept. 1947

CHEMICAL AND PHYSICAL RESEARCH

★

Bacterial Cellulose

Bacterial polysaccharides. T. H. Evans and H. Hibbert. *Advances in Carbohydrate Chem.* **2**, 203–33 (1946).

Includes a brief discussion of bacterial cellulose and its possible industrial significance, as well as a description of the bacterial levans, dextrans, and other polysaccharides, and of a few of the methods used in determination of structure.

Text. Research J. Sept. 1947 W. E. Davis

Cellulose Esters

Cellulose esters of organic acids. C. R. Fordyce. *Advances in Carbohydrate Chem.* **1**, 309–27 (1945).

The growth of the cellulose acetate industry and the raw materials for acetate manufacture are discussed briefly. The basic acetylation procedure is described after which the various modifications of the process used commercially and in the laboratory are discussed. Preparation and properties of higher esters, mixed esters, esters of unsaturated and substituted aliphatic acids, and of aromatic acids, dibasic acids, and sulfonic acids, as well as carbamates, are described briefly. A section on industrial applications discusses production trends and the use of cellulose esters in textiles, protective coatings, films, and molding compositions. W. E. Davis

Text. Research J. Sept. 1947

Cellulose Ethers

Cellulose ethers of industrial significance. J. F. Haskins. *Advances in Carbohydrate Chem.* **2**, 279–94 (1946).

This review describes the raw materials, etherifying agents, and fundamental procedure, then discusses the factors influencing the course of the reaction and modifications of the procedure which would permit better control of the reaction. For discussion of properties and uses, the ethers are classified as organo-soluble (ethyl- and benzylcellulose), water-soluble (methyl-, carboxymethyl-, and hydroxyethylcellulose), and alkali-soluble (ethylcellulose and those mentioned above as water-soluble). Factors affecting solubility are briefly considered in the discussion of water-soluble methylcellulose. W. E. Davis

Text. Research J. Sept. 1947

Emulsions

The study and use of emulsions and emulsifying agents. Jose M. Nolla and Eusebio Díaz. *Afinidad* **21**, 540–9 (1944); **22**, 31–5, 76–81, 168–74, 205–9 (1945); **23**, 541–53 (1946) (through *Chem. Abstr.* **41**, 4322*f* (July 10, 1947)).

A general treatise on the main characteristics of emulsions and suspensions, discussing the theory of the intrasuperficial membrane, general procedures for obtaining emulsions, classification and detailed study of emulsifying agents and saturants, and methods of analyzing them. There is also a résumé of the use and application of these products in the textile, leather, perfume, photographic, and pharmaceutical industries.

Text. Research J. Sept. 1947

Action of Light on Cotton

The action of light on dyed and undyed cotton. G. S. Egerton. *J. Soc. Dyers and Colourists* **63**, 161–7 (June 1947); *Dyer* **97**, 459–60 (May 9, 1947).

A study has been made of the effect of different conditions on the rate of photochemical degradation of cotton, undyed and dyed with different vat dyes varying greatly in their sensitizing action. Sunlight and the high-pressure mercury vapor lamp were used as sources of light energy. The extent of the photochemical degradation of the cotton was measured by the rise in the fluidity of 0.5% solution in a standard cuprammonium solvent and by the fall in its tensile strength. The most important variables were the pressure, composition, and relative humidity of the gaseous atmosphere; the concentration of dye on the cotton (depth of dyeing); the physical state of the dye in so far as it is exemplified by comparisons between pigmented and dyed cotton; and the quality of the light source. Some of these factors are shown to have a great influence, not only on the absolute rate of photochemical degradation but also on the relative rates for different dyeings. In this connection, the effect of the humidity of the atmosphere during exposures in air at atmospheric pressure is of particular importance and of practical interest. The rate of photochemical degradation of dyeings with the strongly sensitizing vat dyes in the yellow and orange shade range is greatly increased by the presence of moisture in the air, and the same is true for undyed cotton. With dyeings of the inactive vat dyes in the green and blue shade range the rate of photochemical degradation is, on the other hand, unaffected, or but slightly affected, by the presence of moisture. A table is given comparing the rate of photochemical degradation of undyed cotton with that of the same cotton dyed with 36 different vat dyes, the samples being exposed to sunlight both in dry and in moisture-saturated air. Author

Text. Research J. Sept. 1947

Pectin

The chemistry of pectic materials. E. L. Hirst and J. K. N. Jones. *Advances in Carbohydrate Chem.* **2**, 235–51 (1946).

The problem of the structure of pectin is broken down into a discussion of the structures of the main constituents: pectic acid, araban, and galactan. The authors consider pectin to be a mechanical mixture of the 3 rather than a complex polysaccharide. W. E. Davis

Text. Research J. Sept. 1947

Synthetic Polyamides

Synthetic fibers. I. Decomposition and synthesis of nylon. Kohei Hoshino. *Bull. Chem. Soc. Japan* **18**, 97–104 (1943); see *C.A.* **36**, 5139[9]. **II. Polycapramide.** Kohei Hoshino and Kisaburo Noissiki. *Ibid.* 105–11; cf. *C.A.* **41**, 3971*f* (through *Chem. Abstr.* **41**, 4313*a* (July 10, 1947)).

A small quantity of water is indispensable for the effective polymerization of ϵ-caprolactam; the optimum amount of water is 1 mol. per mol. of lactam. Data on experimental conditions for the polymerization of ϵ-caprolactam are given, including temperature, period, and the amount of adipic acid as a viscosity stabilizer.

Text. Research J. Sept. 1947

Synthetic polyamides. III. Syntheses of some polyamides. Kohei Hoshino. *Bull. Chem. Soc. Japan* **19**, 153–7 (1944) (through *Chem. Abstr.* **41**, 4313*b* (July 10, 1947)).

The syntheses and properties of polycyclohexylene-1,4-adipamide and polycyclohexylene-5,5-dimethyl-1,3-adipamide and copolymer of hexamethylenediamine with adipic acid ϵ-caprolactam were studied. **IV. Solution viscosity.** *Ibid.* 158–70. Flory's theory on molecular size distribution in linear condensation polymers was applied to linear synthetic polyamides. Viscosities of polyhexamethyleneadipamide or polycapramide in *m*-cresol are expressed by Fickentscher's equation. The application of the Staudinger viscosity relation to polyamide is discussed. The relations between intrinsic viscosity and average molecular weight were established experimentally from Flory's theory and the freezing point depression of phenolic solution. The time dependence of the degree of depolymerization is discussed under the assumption that the rate at which bonds are cut is proportional to the number of uncut bonds in the system.

Text. Research J. Sept. 1947

Polyuronides

A discussion of methods of value in research on plant polyuronides. E. Anderson and L. Sands. *Advances in Carbohydrate Chem.* **1**, 329–44 (1945).

Describes the general properties of polyuronides, their isolation, purification and analysis, their hydrolysis to simple substances and the identification of the units present, and their position in the chain. Results of investigations on pectic acid and pectin, alginic acid, plant gums, and hemicelluloses are discussed briefly.

Text. Research J. Sept. 1947 W. E. Davis

Synthesis of Proteins

Synthesis of protein analogs. R. B. Woodward and C. H. Schramm. *J. Am. Chem. Soc.* **69**, 1551–2 (June 1947).

A report of the first successful synthesis of molecules having, like fibrous proteins, the structure:

$$\mathrm{HOOC{-}CH(R_1){-}NH{-}(COCH(R_i)NH)_n{-}COCH(R_{n+2})NH_2}$$

The monomers are the anhydrides of N-carboxy-α-amino acids and the initiator is water or any substance with an active hydrogen. The reaction proceeds as follows:

1. $\mathrm{H_2O + \overline{COCH(R)NHCOO} \rightarrow HOOCCH(R)NHCOOH}$
2. $\mathrm{HOOCCH(R)NHCOOH \xrightarrow{-CO_2} HOOCCH(R)NH_2}$
3. $\mathrm{HOOCCH(R)NH_2 + \overline{COCH(R)NHCOO} \rightarrow HOOCCH(R)NHCOCH(R)NHCOOH}$

Steps 2 and 3 are then repeated indefinitely. The authors copolymerized N-carboxy-*l*-leucin anhydride and N-carboxy-*dl*-phenylalanine anhydride at room temperature in benzene for 2 weeks and obtained polymers having molecular weights of several million. The reagent-grade benzene used contained sufficient water to initiate the reaction.
Text. Research J. Sept. 1947 A. R. Martin

Sericin

Fixation of sericin of raw silk. VII. Dechromizing action of some chemicals and chemical combinations between sericin and basic chromium complex salt of chrome-fixed cocoon silk fibers. Masami Oku and Shigetoshi Saito. *J. Agr. Chem. Soc. Japan* **17**, 814–21 (1941) (through *Chem. Abstr.* **41**, 4313*e* (July 10, 1947)).

Chrome-fixed cocoon silk fibers were dechromized by boiling in 10% Rochelle salt for 1 hr., or in a 1.0% solution of oxalic acid, H_2SO_4, or HCl for 10 min. However, the fixation-degree of sericin was adversely affected. When boiled in 10% Rochelle salt mixed with 8% HCHO for 1 hr. or in 1.0% $HgSO_4$ mixed with 8% HCHO for 10 min., dechromization was completed without affecting the fixation degree. At room temperature, immersion in 5.0% oxalic acid mixed with 4% HCHO dechromized the fibers in 10 days. Substituting H_2SO_4 or HCl for oxalic acid in the mixture required a longer period. Rochelle salt proved to be an inferior dechromizing agent at room temperature. From the reactions above sericin seems to combine with basic Cr complex salt as $[X_5Cr{-}O{-}H{-}]{-}OC(NHR_1)R$.
Text. Research J. Sept. 1947

Starch Nitrates

Molecular weight and intrinsic viscosity of nitric triesters of corn starches and dextrins. G. V. Caesar, N. S. Gruenhut, and M. L. Cushing. *J. Am. Chem. Soc.* **69**, 617–21 (Mar. 1947).

Three types of corn starch conversion products were nitrated to give the triester and the properties of the ethyl acetate solution examined. One of the types was a wet conversion product; the other two were dry conversions by heat. Intrinsic viscosities were determined by Fenske tubes. Number-average molecular weights were determined by the Barger micro-isopiestic method. The experimental results appear to satisfy Mark's variation of Staudinger's formula. When $\log \bar{M}_n$ is plotted against $\log [\eta]$ 3 linear plots are obtained which intersect at the experimental value of $[\eta]$ for maltose octanitrate. Dry-processed soluble dextrins were found to have a D.P. of less than 7. An apparently more rigid polymer molecule is indicated for the pyrodextrins than for starch. A. R. Macormac
Text. Research J. Sept. 1947

Water Vapor Sorption

The sorption of water vapor by high polymers. Sherman E. Smith. *J. Am. Chem. Soc.* **69**, 646–51 (Mar. 1947).

The sorption of water by high polymer is of two types: (1) that which is bound on the inner or outer surface of the solid adsorbent by forces in excess of the normal forces responsible for condensation of water to the liquid state and (2) that which is normally condensed within the gel. The first will reach a virtual maximum at a vapor pressure well short of saturation while the second will increase progressively towards the saturation vapor pressure. If the sorbent swells, its surface will be a variant. An expression for the bound and unbound water in a non-swelling gel is derived and then modified to apply to a swelling gel upon the assumption that the effective adsorping surface will be proportional to the volume of the adsorbent gel. This gives the expression

$$\bar{w} = \bar{w}_b + \bar{w}_c = \bar{w}_b - \bar{w}' \ln (1 - p/p_0)$$

where w are weight fractions of the sorbate and p are vapor pressures. The application of this equation to cellophane, cotton, wool, and nylon is discussed. It is shown that beyond the point where p/p_0 is 0.4 a straight line is obtained when $\bar{w}$ is plotted against $-\ln (1 - p/p_0)$.
A. R. Macormac
Text. Research J. Sept. 1947

Chemically Modified Wool

Action of sulfites on the cystine disulfide linkages of wool. V. Effect of some chemical modifications of the wool on the magnitude of the bisulfite-reactive fraction (*A*+*B*) and the relative magnitudes of subfractions *A* and *B*. H. Lindley and H. Phillips. *Biochem. J.* **41**, 34–8 (1947); cf. *C.A.* **38**, 5413[1] (through *Chem. Abstr.* **41**, 4651*b* (July 20, 1947)).

About half of the cystine disulfide S reacts with $NaHSO_3$ as follows:

$$\mathrm{R'CH_2SSCH_2R'' + NaHSO_3 \rightleftarrows R'CH_2SH + NaOSO_2SCH_2R''},$$

where R' and R'' represent polypeptide chains. The reactive fraction of the disulfide S is divided into subfraction *A*, which is readily re-

versed to disulfide by rinsing the treated wool with water, and subfraction *B*, which gives thiol and *S*-cysteinesulfonate groups stable to water rinsing. Esterification of the free COOH groups of the combined glutamic and aspartic acids does not increase the bisulfite-reactive fraction (*A* + *B*) but makes the subfraction *A* stable to water rinsing. Hot acetylation and deamination by prolonged treatment with HNO_2 do not alter the magnitude of subfractions *A* and *B*.

Text. Research J. Sept. 1947

Electron Microscopy of Wool

Investigation of wool by the electron microscope. Bertil Olofsson. *Medd. Svenska Textilforskningsinst. Göteborg* **1946**, No. 2, 3–13 (1946) (through *Chem. Abstr.* **41**, 4313*g* (July 10, 1947)).

The main problem is to get the matter to be examined into a state of sufficient dispersion, but yet to avoid uncontrollable destruction of the material. The material was prepared in 4 ways: (1) mechanical methods, (2) fermentative methods, (3) acid treatment of the fiber, and (4) alkaline treatment of the fiber. The electron microscope ought not to be regarded as a decisive, but as a complementary instrument of investigation in the field. Wool keratin can be broken down by "mild" reagents, i.e., trypsin, and concentrated H_2SO_4, which decompose material not very resistant chemically, but leave the peptide, cystine, and other bonds intact. Stronger or longer treatment destroys these bonds too. Acids principally affect the peptide bonds hydrolytically, and at the same time the fiber structure becomes disorientated and "blurred." Alkalies affect principally the cystine bonds; this type of splitting does not seem to react so rapidly on the orientation of the fiber. After some alkaline treatment keratin may be reformed, although in a very degenerate state. In what respect the "easily affected" substance is different from the main part of the keratin seems to be a difficult question. It is possible that the substance sensitive to trypsin is like a net of fine membranes enclosing the fibrils.

Text. Research J. Sept. 1947

BLEACHING: DYEING: FINISHING

★

Continuous Bleaching

Recent developments in the continuous bleaching of textiles. T. E. Bell. *Papers of AATT* **2**, 57–60 (Mar.–May 1947).

A description of the Du Pont type continuous peroxide bleaching installation. J. A. Woodruff

Text. Research J. Sept. 1947

Pad-Steam Dyeing

Continuous pad-steam dyeing. P. L. Meunier. *Papers of AATT* **2**, 61–7 (Mar.–May 1947).

The pad-steam continuous dyeing is compared with older conventional methods. Some modifications of the basic pad-steam process are described. The choice of the pad-steam process over other methods must be made on the basis of specific mill conditions. It is said to facilitate the use of vat colors not only on cotton and viscose but on other fibers in mixed fiber constructions as well. J. A. Woodruff

Text. Research J. Sept. 1947

Re-Dyeing

The re-dyeing of faded woolen garments. G. G. Simpson. *J. Soc. Dyers and Colourists* **63**, 171–5 (June 1947).

A method of obtaining a graded range of "faded" wool pieces suitable for the determination of the fade-covering properties of dyes is described. The fade-covering efficiency of the direct cotton dyes is found to be of first importance, their behavior being broadly linked with dye constitution. In consequence, the union method of dyeing is fully discussed with particular emphasis placed upon the effect of temperature and the pH value of the dye bath with respect to both the dyeing properties of the faded material and the behavior of the dyes used. A specific union method of application is recommended. The influence of salt and dye concentration, time of dyeing, and the preparation of the garments for union dyeing are also discussed. Details of work carried out on the two-bath method of dyeing are also given from which it is shown that although a suitable selection of acid dyes may be made, the subsequent filling-in with direct cotton dyes leads to inferior fade-covering. The results are shown to be linked with the constitution of the dyes used. A comparison is drawn between the fade-covering efficiencies of the two methods.

Text. Research J. Sept. 1947 Authors

Dyeing Viscose

Some experimental work on the dyeing of viscose rayon. C. C. Wilcock. *J. Soc. Dyers and Colourists* **63**, 136–40 (May 1947).

A number of experimental results on the dyeing of viscose rayon are summarized commencing with the methods of classification of even- and uneven-dyeing direct dyes. Methods found for correcting the differences in depth of shade obtained with direct dyes on light and dark dyeing viscose are described under the headings of alkalies and alkaline salt, β-napthol, and pyridine. It is shown that although certain dyeings can be corrected by adding alkali to the dye liquor, others cannot be so treated owing to the ease of reduction of the dyes by the viscose rayon in the presence of hot alkali. An aftertreatment of dyeings with 40% β-napthol and 40% common salt for 30 min. at 90°C is recommended as being commercially useful. The odor of pyridine obviates its apparent usefulness in leveling. Strike tests and leveling tests on 40 weak and 21 strong alkali-type vat dyes are given in a study of dyeing and leveling properties. The results of investigation of restraining agents showed that 6% of a non-restraining-type sulfite cellulose

waste liquor used with 2% Epsom salts becomes a powerful and economical restraining agent. The effect of this combination in restraining dye is greater on the weak dyeings than on heavier dyeings. Tables are given recording the loss in color value of strong alkali-type vat dyes when used with this restrainer. J. A. Woodruff

Text. Research J. Sept. 1947

Pin Tenters

Pin tenters in rayon finishing. K. S. Laurie. *Papers of AATT* **2**, 68–73, (Mar.–May 1947).

The pin tenter developed in England is fully described with special attention to the overfeed, entering roll frame, and hydraulic guider mechanisms. The use of selvage uncurlers, predriers, and automatic moisture control devices are discussed. A full-length pin tenter frame with predrier operating on 36-in. cloth is said to be capable of evaporating about 960 lb. of moisture per hr. The reasons for the use of the pin tenter are given with emphasis on the processes used in dimensional control of spun rayon fabrics. J. A. Woodruff

Text. Research J. Sept. 1947

Rotproofed Sandbags

Hessian sandbags and rotproofed Hessian sandbags. *Brit. Standard* **1214**: 1945 (through *Chem. Abstr.* **41**, 4652*g* (July 20, 1947)).

The materials used for rotproofing are solutions of "cuprammonium," "copper sulfate ammonia," copper naphthenate, creosote, or copper naphthenate in creosote. Specifications for these solutions are given.

Text. Research J. Sept. 1947

FIBERS: YARNS: FABRICS: MECHANICAL PROCESSES

★

Bamboo Pulp

Bamboo pulp: Its possibilities for rayon manufacture. Anon. *Fibers* **8**, 82–4 (Mar. 1947).

A review is given of the processing of bamboo pulp for paper manufacture. A hydrotropic solvent method of obtaining pulp for rayon is discussed. A list of chemical and physical properties compares the bamboo pulp with that of the usual pulps used for rayon manufacture. Bamboo as a source of pulp is said to be easily available in more than adequate amounts. J. A. Woodruff

Text. Research J. Sept. 1947

Fiber Glass Manufacture Flowsheet

Fiber glass production. Anon. *Chem. Eng.* **54**, 130–3 (June 1947).

A flowsheet is given showing the manufacture of Fiberglas continuous filaments and staple fiber.

Text. Research J. Sept. 1947 R. B. Evans

Mechanical Properties of High Polymers

Molecular structure and mechanical properties of fiber forming high polymers. H. F. Mark. *Papers of AATT* **2**, 9–18 (Nov.–Feb. 1946–7).

A nontechnical résumé of the structures and properties considered important in textile fibers.

J. A. Woodruff

Text. Research J. Sept. 1947

Holocellulose

Preparation of holocelluloses from nonwoody plant material. Emmett Bennett. *Anal. Chem.* **19**, 215 (Mar. 1947).

The sodium chlorite method used for the preparation of holocellulose from wood may be adapted for the same use with nonwoody tissue. The older preliminary procedure for this kind of plant tissue involves 2 to 3 days, whereas the one described in this paper seems to yield a product of satisfactory color and furfural content in 2 to 3 hrs. However, when the product is obtained in the manner described, from 30 to 50% of the original nitrogen of the plant material may also be included.

Text. Research J. Sept. 1947 Author

Ramie Cultivation

Field cutting of ramie in Florida. J. M. Dempsey. *Cord Age* **47**, 18, 20 (May 1947); 26, 29 (June 1947).

Peat soils of Everglade, under proper water control, yielded high tonnages of green ramie plants and fiber with strength comparable to that of ramie produced in other countries. Land selection and preparation and methods of planting are discussed. At "cutting maturity," the green plant will contain 3.5 to 4.5% of raw fiber containing 20% gums.

R. B. Evans

Text. Research J. Sept. 1947

Ramie Processing

Ramie. William G. Waldo. Chemurgic Papers 1947 Series No. 3, No. 564. Columbus, Ohio, National Farm Chemurgic Council. 9 pages.

Traditional brittleness of ramie is said to have been due to the fact that gums in imported China grass had hardened, making drastic degumming treatment necessary. This can be avoided by immediately degumming fiber after decortication. Of ramie harvested, only about 3% yield of undegummed fiber is obtained. History of ramie manufacture and prospective markets are discussed. R. B. Evans

Text. Research J. Sept. 1947

Terylene Fiber

Better than nylon? Anon. *Chemical Industries* **60**, 764–5 (May 1947).

A brief description of some of the general properties of terylene fiber. The chief problem appears to be in the dyeing of the material.

A. R. Martin

Text. Research J. Sept. 1947

Fireproofing Fabrics

The fireproofing of fabrics. J. E. Ramsbottom. *Dep. Sci. Ind. Research (Brit.)* **1947**, 121 pp. (Separate); cf. *C.A.* **24**, 3376[3] (through *Chem. Abstr.* **41**, 4652*b* (July 20, 1947)).

Tables and charts show the relative effectiveness of large numbers of soluble and insoluble fireproofing agents (*I*). Single substances and binary, ternary, and quaternary mixtures were investigated with respect to rate of flame propagation, afterglow, and amount of deposit required to prevent flame propagation. The effect of *I* on strength of fabrics during storage and exposure to light and the mechanism of fireproofiing action were investigated. Comparison of vertical, horizontal and oblique test strips showed that the first method gave a more severe test and more concordant results. For large-scale use, the recommended soluble *I* are H_3BO_3, 4.2% plus Na_3PO_4, 2.8% based on the weight of the fabric. No satisfactory waterproofing treatment was found for soluble *I*. For exposed fabrics the best permanent treatments are (1) SnO_2 13.9%, WO_3 15.1%, Fe_2O_3 2% and (2) SnO_2 20.9%, WO_3 8.1%, Fe_2O_3 2%, SiO_2 6%. Treated cotton fabrics are fireproof and glowproof after 70 days exposure or 880 hrs. washing in cold H_2O. Both soluble and insoluble *I* act as catalysts to decompose cellulose below the ignition temperature and form volatile products incapable of sustaining flame. Afterglow is prevented by excluding air from the charred ash or by modifying the *I* during the first-stage reaction so that they no longer act as oxidation catalysts in the second stage. The deposit must be finely dispersed in the fiber walls, and for permanence must not be peptized on washing or exposure. Soluble substances strongly adsorbed by insoluble *I* may appreciably affect their fireproofing action. Kapok is made fireproof and glowproof without impairing its useful properties by treatment with a solution containing 5% Na_2SnO_3, 3% Na_2WO_4, and 3% $NaAlO_2$, precipitating the oxides with 15% $Al_2(SO_4)_3$, then treating with saturated H_3BO_3. No satisfactory fireproofing treatment is known for airplane fabric processed with cellulosic dopes, but fabric proofed with 20% Fe_2O_3 or SnO_2 and doped with chlorinated polyvinyl chloride (60% Cl) does not propagate flame after long weathering. An appendix lists several hundred fireproofing processes.

Text. Research J. Sept. 1947

Rayolanda

Some random thoughts on the use of rayon staple in woven fabrics. R. S. Greenwood. *Papers of AATT* **2**, 89–96 (Mar.–May 1947).

The uses of viscose, Rayolanda, and acetate rayons in England, alone and in combinations with cotton and wool, are discussed. Special attention is given to the uses and properties of Rayolanda.

J. A. Woodruff

Text. Research J. Sept. 1947

Rayon on Flax System

Textile trends in Europe. R. Bouvet. *Papers of AATT* **2**, 80–6 (Mar.–May 1947).

Several European machinery and processing developments are described as worthy of observation. Fabric trends in France are discussed principally from the angle of yarn constructions. Attention is called to an English modified flax machinery method of making yarns of long-staple-length viscose, which yarns are finding use in producing unusual fabrics. J. A. Woodruff

Text. Research J. Sept. 1947

Worsted Yarns on Cotton System

The spinning of worsted yarns on the American system. R. J. McConnell. *Papers of AATT* **2**, 37–43 (Nov.–Feb. 1946–7).

The subject is briefly described under the headings of drawing, roving, work loads, advantages and disadvantages. J. A. Woodruff

Text. Research J. Sept. 1947

MISCELLANEOUS

★

Abaca Prospects in Philippines

Varied factors in effort to bring abaca industry to prewar stamina. C. A. Boonstra. *Cord Age* **47**, 7–8 (Apr. 1947).

Production of abaca in the Philippines totaled 110,000,000 lb. in 1946, a little more than $\frac{1}{4}$ of the prewar level. Production is retarded because (1) Japanese plantations in Davao region were abandoned during the war, (2) new planting had been light for several years preceding war and ceased during war. Approximately 45,000 hectares of new plantings are needed in Davao region to bring acreage up to the prewar total of 70,000 but no steps to accomplish this have been taken. Other abaca-producing regions suffered less during the war than Davao but production is restricted because of higher prices for other crops. In 1948 the total production may reach 150 to 200,000,000 lb. R. B. Evans

Text. Research J. Sept. 1947

British Textile Industry

British textile industries face challenging difficulties. Mary E. Poole. *Foreign Commerce Weekly* **27**, 3–5, 32, 33 (June 28, 1947).

Production and exports of cotton and wool textiles in England are still far below prewar levels but rayon production was 50% greater than the 1938 level at the close of 1946. Labor shortage in the textile industry, traceable to wartime diversion of workers, has been aggravated by official shortening of the work week and by the raising of the compulsory school age to 15 years. Moderniza-

tion of cotton spinning is being subsidized to the extent of 25% under certain conditions. In March, 1947, cotton industry trade-union leaders voted to accept double-shift operations. R. B. Evans

Text. Research J. Sept. 1947

Clothing Production

Indexes of clothing and footwear output for civilians, 1939–47. Lawrence Bridge. *Survey of Current Business* **27**, 17–23 (June 1947).

Forty-four new series of index numbers giving the physical output of various clothing items for civilian use by years from 1939, by quarters for 1943–45, and by months for 1946 and 1947 are given. A new series giving number of production workers and indexes of wage-earner employment and wage-earner payrolls since 1939 is also given. R. B. Evans

Text. Research J. Sept. 1947

Market Research

State publications for market research. Part 1: Industrial directories. Rose L. Vormelker. *Chemical Industries* **60**, 794–6 (May 1947).

A complete index of state industrial directories.

Text. Research J. Sept. 1947

Mothproofing Agents

New chemical weapons spell doom for moths. G. Allen Mail. *Chemical Industries* **60**, 790–2 (May 1947).

In the past 20 yrs. more than 1,000 patents have been issued for mothproofing agents but relatively few of these have been marketed. Probably the largest number of mothproofing products now being sold are aqueous solutions of silicofluorides. Among the trade names identified with the silicofluorides are: "Larvex," "Hex," "Guardex," "Perma-Moth," and "Ya-De." Among the compounds used are magnesium silicofluoride, ethanolamine silicofluoride, sodium aluminum fluosilicate, and lithium fluosilicate. Some commerical compounds contain about 1% sodium arsenite. This chemical has been condemned for the purpose by the American Medical Association and arsenic in any form is considered unsafe for use on clothing. Paradichlorobenzene and napthalene are the two best known and most widely used solid fumigants. Both do a splendid job if properly used. The closest approach to an ideal mothproofing process is said to be the so-called "colorless dyes" of the Eulan type developed in Germany. These and other chlorinated organic compounds are discussed. A. R. Martin

Text. Research J. Sept. 1947

Nylon

Nylon is big business. Anon. *Chemical Industries* **60**, 776–9 (May 1947).

Output of nylon is expected to soar to well over 60,000,000 lb. per yr. by the end of 1948, and will account for about 15% of Du Pont's total sales. As the hosiery industry cannot be expected to absorb more than 20,000,000 lb., this figure indicates other large-scale outlets. One is a staple fiber for blending with wool, cotton, and other fibers. Many problems in carding, spinning, dyeing, and finishing await solution.

Text. Research J. Sept. 1947 A. R. Martin

Rayon Staple Economics

Rayon staple: Its past and its prospects. Clark Lee Allen. *Southern Economic J.* **13**, 146–57 (Oct. 1946).

History of rayon staple with particular reference to the increase in output and improvement in quality is given. Just prior to World War II, 88% of world's supply of rayon staple was produced in Germany, Japan, and Italy. In 1939, the United States imported 46% of the United Kingdom's staple production and 32% of France's production. Unlike cotton and silk prices which are subject to day-to-day fluctuations, rayon prices are relatively stable. If one company changes prices, others usually modify their price lists to conform. Recent history of rayon production has been marked by stability of prices, a tendency toward equality of prices for yarns of same size produced by different processes, and narrowing of price differential between deniers. Continued expansion in rayon production with nonaxis countries increasing in importance is forecast. Most of the rayon expansion thus far has been in fields of use where price as compared with that of cotton is not significant, but if rayon's present price position relative to that of cotton continues, the displacement of cotton by rayon will extend to other fields of use.

Text. Research J. Sept. 1947 R. B. Evans

Steam Economy

Steam economies in wool dyeing and finishing. Anon. *Dyer* **97**, 453–5, 513–14 (May 9, 23, 1947).

The problems of steam economy necessitated by the shortage of coal supplies are listed and suggestions are offered as remedies.

J. A. Woodruff

Text. Research J. Sept. 1947

Wool Manufacturing Prospects in Texas

The utilization of wool and mohair in Texas. Robert E. Pent. Chemurgic Papers 1947 Series No. 3, No. 559. Columbus, Ohio, National Farm Chemurgic Council. 25 pages.

Texas is first in volume of production of wool and mohair, has an excellent all-year climate, a satisfactory fuel in natural gas, and reasonable electricity rates. Water is hard but is abundant and readily softened. Labor is good but the rural population is not accustomed to a continuous work schedule. "Know-how" and craftmanship are said to be major requisites for wool manufacture not now available in Texas. Individuals and organizations participating in wool manufacture in Texas are listed.

Text. Research J. Sept. 1947 R. B. Evans